

Dear Victor,

please find our revised paper on **“Thermal processes of thermokarst lakes in the continuous permafrost zone of northern Siberia – observations and modeling (Lena River Delta, Siberia)”** attached.

During the revision of the paper we made some further corrections to the paper. Thus we have updated our replies to the reviewers and supply the following documents:

- Replies with point-by-point answer to the reviewer comments (based on the replies submitted August 7, 29015). Two additional figures (Figures 10&11 in the current version) have resulted from the comments of reviewer #1
- Manuscript with “tracked changes” as detailed in the replies. Furthermore, it shows the English and technical corrections
- Manuscript with “accepted changes”.

The figures have been revised according to the reviewer’s comments and are imbedded as .png files in the revised manuscript. Please note that we will supply the final figures as .pdf format which will provide the best resolution.

On behalf of the authors,

Julia

**Interactive comment on “Physical processes of thermokarst lakes in the continuous permafrost zone of northern Siberia – observations and modeling (Lena River Delta, Siberia)”**

by J. Boike et al.

Anonymous Referee #1

Received and published: 21 May 2015

**General Comments:**

This paper presents data and analysis of the thermal regimes of five thermokarst lakes located on the Lena River Delta in Siberia over a three year period. This is a worthwhile contribution because 1) there is relatively few studies of lakes in Siberia despite their very high abundance and potentially rapidly changing condition, 2) many such lake studies only collect summer data from single years, whereas year round and multiannual data are presented in this work, and 3) the collection of water level and bathymetry data in addition to thermal data presents additional opportunities to understand these systems.

Many of the observed aspects of thermal regimes such as release heat from the sediment following ice cover development and warming the water column prior to ice out appear correctly interpreted yet are not widely reported in other analyses of lake thermal regimes though I believe these are common processes. Good support for the value of year-round monitoring of lakes. This paper is very descriptive however and it seems there are many opportunities for comparison and analysis the authors elude to but never pursue.

Some examples are comparison of thermal regimes by 1) landscape setting (river terraces vs. Pleistocene Ice Deposit Complex) or source waters (subject to river flooding vs. more isolated), 2) bathymetric characteristic, or 3) interannual variation in relation air temperature, radiation, or wind regimes. I think all of these potential controls on lake thermal regimes are qualitatively addressed to some degree but not analyzed in any meaningful way and thus the paper lacks potential understanding of these relationship that could be use predict changes in lake thermal regimes in time or space. The use of the FLAKE model is somewhat unclear as well. Some

unmeasured parameters were simulated but it is not entirely clear what the value of these are to the analysis and questions of interest.

Additionally the figures are mostly time series plots of different climate, water temperature or heat budget components and not always that insightful. I would simply recommend analyzing the collected data in a way that helps understand how these thermal processes vary in some meaningful way. I think that in addition to the importance of this lake type in this region would make this a valuable paper.

Our reply (marked in blue) is structured the following:

- *Italic indicates that text has been revised or added to paper*
- References are given with full citations when not included in paper already
- Page (pp) and Line (L) numbers refer to revised paper version

#### **Reply to general comments:**

We thank the reviewer for his/her valuable comments. We agree with the reviewer that the data and processes discussed in this paper are not (widely) reported and have, to our knowledge, not been reported for Arctic thermokarst lakes at all. We see the strength and novelty of this paper in presenting data and quantitative analysis of new processes, such as warming of bottom temperatures (following ice cover development) and warming of the lake water during spring under the ice that were speculative in the past. Furthermore, we provide modeled biogeochemical indices that are indices of summer stratification in thermokarst lakes. While commonly reported for non-Arctic lakes, we report and discuss these numbers and processes for the first time for North East Siberian thermokarst lakes.

To address the major comment on the potential controls on the lake thermal regimes in a quantitative way, we have performed additional numerical modeling analysis. In particular, we have explored the relationship between the morphometry (depth) and summer stratification duration as one of the most morphometry-sensitive characteristics of the thermal regime of these northern lakes. Furthermore, we have added quantitative statistics to the model validation that will aid the clarification of the use of the model. Overall, we sharpened the objectives of the paper, including why

we chose the FLake model. We have generally revised the description of the modeling in the aims and method section. Furthermore, we have moved the section 3.3 “Lake Morphometry” to the appendix of the paper.

Please find the specific comments below.

Additions in the abstract:

-pp. 6, L2-5

*Thermokarst lakes are typical features of the northern permafrost ecosystems, and play an important role in the thermal exchange between atmosphere and subsurface. The objective of this study is to describe the main thermal processes of the lakes and to quantify the heat exchange with the underlying sediments.*

-pp. 6, L24-30

*The lake thermal regime was modelled numerically using the FLake model. The model demonstrated good agreement with observations with regard to the mean lake temperature, with a good reproduction of the summer stratification during the ice free period, but poor agreement during the ice covered period. Model sensitivity to lake depth demonstrated that lakes in this climatic zone with mean depths >5 m develop continuous stratification in summer for at least one month.*

Additions and changes to section 1. Introduction:

-pp. 6, L12-20

*Our objectives are ....and (ii) to make use of measured data to validate the freshwater model FLake, as well as estimate water sediment heat exchange. FLake offers a good compromise between computational efficiency and physical reality, and has been coupled to several regional and global climate models (Thiery et al., 2014; Martynov et al., 2010). FLake has been used in various 1 dimensional modeling studies, for a wide range of lakes, including tropical lakes, and in lake model intercomparison projects (LakeMIP; Thiery et al., 2014; Stepanenko et al., 2010). However, it has not been used for Arctic lakes and this study tests the ability of FLake to reproduce the temperature regimes of thermokarst lakes in northern Siberia.*

Removed:

-pp. 10, L23- pp. 11 L31 (Section 3.2 Lake morphometry) and moved to appendix A, pp. 51 L1-25. The method description for bathymetric data is moved to end of method section 3.1 Field instrumentation and ground surveys, pp. 10, L12-21.

Additions to method section 3.3. Modeling of lake thermodynamics:

-pp. 14, L16-32

*The model was used to:*

*- validate the 1-dimensional modeling approach and qualify the main mechanisms governing features of the lake thermal regime, such as summer stratification, water-sediment heat exchange, and ice melt*

*- characterize the water-sediment heat exchange at annual time scales*

*- establish a relationship between the morphometry and summer stratification duration.*

The first two points are addressed in the paper, while the third point has been suggested by the reviewer, and has now been added to this study. We performed a sensitivity study by keeping all model parameters and just changing the morphometry (depth) since this a fundamental parameter for 1 dimensional models. For Sa\_Lake\_1, lake depths were varied for the range of 2-12 m with increments of 0.5 m. From all these results a single characteristics, i.e. the number of days with summer stratification, Sum(Ns) where  $N_s = 1$  if  $(T_s - T_b) > 0.5^\circ\text{C}$  was calculated and put on the line vs. depth (Fig. 10).

Additions to section 5. Discussion:

- pp. 23 L27-31 to pp. 24 L1-11

- pp. 48-49 (figures 10, 11)

*We observed and simulated short stratification periods in summer in the studied lakes (Figures 4 & 5). These stratification events are probably the major physical factor affecting biogeochemical processes in lakes. In particular, the duration of the thermal stratification in summer affects the concentration and vertical distribution of*

dissolved oxygen. Longer summer stratification provokes deep anoxia and favors methanogenesis in the deep water column and upper sediment (Golosov et al., 2012). Under equal climatic forcing, lake depth is the primary factor determining the duration of summer stratification (the second one being the water transparency, Kirillin, 2010). Sensitivity model runs with the lake depth varying in the range 2-12 m using the same meteorological input data from Samoylov demonstrated that lakes in this climatic zone with mean depths >5 m should have dimictic stratification regimes, i.e. develop continuous stratification in summer with a duration of 1 month or longer (Figure 10). This also supports the observation of summer stratification in deeper (> 6 m) Alaskan thermokarst lakes (Sepulveda-Jáuregui et al., 2015). In lakes of about 8 m depth or more, the summer stratification duration significantly increases since high thermal inertia prevents vertical mixing during the autumn cooling in August-September (Figure 11).

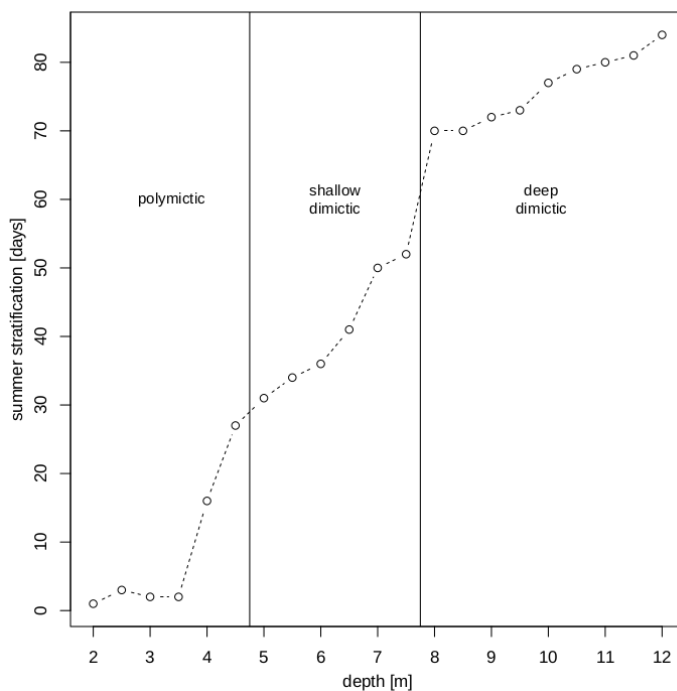


Figure 10. Total number of days with summer stratification in lakes of varying depths modeled with FLake driven by the meteorological data from the Samoylov observatory station for 2010. Existence of stratification was determined by the criterion  $(T_s - T_b) > 0.5^\circ\text{C}$ , where  $T_s$  and  $T_b$  are the modeled temperatures at lake surface and lake bottom, respectively.

While the majority of thermokarst lakes are shallow, our results suggest that stratification events can be sufficiently long in lakes with depths > ~ 5 m with corresponding effects on biogeochemical processes within the water column and on the lake-atmosphere exchange of dissolved gases. Hence, relatively deep lakes might play the role of ‘hot spots’ in the tundra landscape, where methane production due to anaerobic decomposition of organic matter in the deep water column and in the upper sediment is accelerated by the isolation from the atmospheric oxygen.

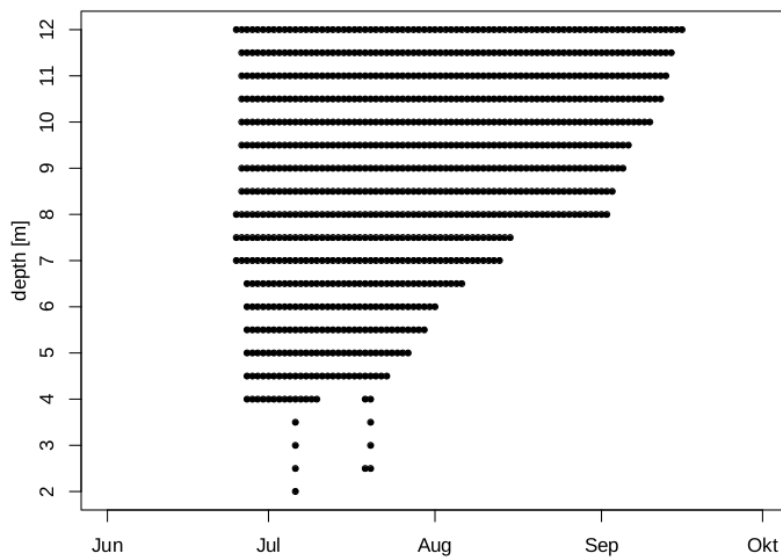


Figure 11. Summer stratification duration in lakes of varying depth (see Fig. 10 for definitions).

Added to references, pp. 28 ff:

Sepulveda-Jauregui, A., Walter Anthony, K. M., Martinez-Cruz, K., Greene, S., and F. Thalasso (2015). Methane and carbon dioxide emissions from 40 lakes along a north–south latitudinal transect in Alaska, *Biogeosciences*, 12, 3197-3223, doi:10.5194/bg-12-3197-2015.

### Reply to specific comments:

Title: I would replace “Physical Processes” with either “Thermal Processes or Regimes” because it doesn’t seem like other physical processes were analyzed or considered.

Changed, pp. L1

Abstract: 6639 L16 – might just say what Wedderburn number mean as many readers might not be familiar with this term.

Added, pp. 2, L21-22

*..., a quantitative measure of the balance between wind mixing and stratification that is important for describing the biogeochemical cycles of lakes.*

6639 L19-20 – Not sure naming the model is necessary

Removed, pp. 2, L30

6640 L30 – Seem abstract should follow with some treatment of ideas in the Summary and Conclusions section.

We assume that the reviewer refers to the abstract (page 6640, L1-3, since Line 30 does not exists on this page)?

We have revised the abstract by including the results of the new modeling results, as well as further details from the summary and conclusion section. Please find details above.

Introduction 6641 L12 – Toolik Lake is a Long Term Ecological Research (LTER) station, not a Long Term Experimental (LTE) site (though the latter might be more fitting). Also, if there are long-term data from this site that are truly exceptional they should be noted here.

Corrected, pp. 5, L 4

We assume that the reviewer refers to long-term data collected from lakes at this site. Initial limnological work at the Arctic LTER began at Toolik Lake in 1975, but time-series of temperature data have been collected routinely in Toolik Lake starting in 1998 (<http://ecosystems.mbl.edu/ARC/>). This data record is already noted in the paper (pp. 5, L20).

Last paragraph on aims; ii) doesn't appear to have been done, but it is a very good idea, and iii) it is unclear to what end this modeling part is for.

We assume that the reviewer refers to i) and ii) of aims (page 6642)?



i) thermal processes have been addressed qualitatively in sections 4.6.1-4.6.3 of the manuscript. ii) validation of FLake has been addressed in section 4.6.

The results of the new statistical analysis have been added to section 4.6 Modeled seasonal lake thermal dynamics:

-pp. 19 L20-30 to pp. 20 L1-10

*To quantify the model performance for thermokarst lakes we applied standard measures (e.g. Thiery et al. 2014) of the model's ability to reproduce the observed mean temperature ( $T_m$ ), the standard deviation ratio ( $SD_{model}/SD_{obs}$ ), the centered root mean squared error (RMSEc), and the Pearson correlation coefficient ( $r$ ). In contrast to other lake model evaluations using surface temperature  $T_s$  (for example, from African and West European lakes), we used  $T_m$  since no temperature probes were installed at the surface due to the seasonal ice cover. FLake demonstrated good performance with regard to the mean lake temperature. The statistics—Pearson correlation coefficient  $r = 0.97$ ,  $SD_{model}/SD_{obs}$  1.28, RMSE 1.49 °C are slightly worse than those reported previously for temperate lakes ( $r = 0.988$ ; Stepanenko et al., 2010) and better than FLake performance on deep tropical lakes ( $r = 0.78$ ,  $SD_{model}/SD_{obs}$  1.25, RMSE 0.75 °C; Thiery et al., 2014). The model reproduced summer stratification during the ice free period ( $r = 0.93$ ,  $SD_{model}/SD_{obs}$  1.25, RMSE 1.82 °C). Solar heating of the water below the ice is not included in the model and thus the agreement between model and observations is lower during the ice-covered period ( $r = -0.42$ ,  $SD_{model}/SD_{obs}$  0.37, RMSE 0.66 °C). The resulting uncertainties in the ice break up prediction affect also the model performance with regard to the lake heat content at the beginning of the open water period in early summer (Figure 8). As thermal dynamics under the ice cover are crudely reproduced by the majority of 1-dimensional lake models used in coupled climate modeling systems (Stepanenko et al., 2010), estimation of the role played by thermokarst lakes in regional climate requires integration of a cost-effective and physically sound sub-model of winter lake thermodynamics into lake parameterization schemes for climate models (e.g. Oveisy and Boegman 2014).*

Added to references, pp. 28 ff

Thiery, W., V. M. Stepanenko, X. Fang, K. D. Jöhnk, Z. Li, A. Martynov, M. Perroud, Z. M. Subin, F. Darchambeau, D. Mironov and N. P. M. van Lipzig (2014). *LakeMIP Kivu: evaluating the representation of a large, deep tropical lake by a set of one-dimensional lake models. Tellus A*, 66. 10.3402/tellusa.v66.21390.

Stepanenko, V. M., Goyette, S., Martynov, A., Perroud, M., Fang, X., and D. Mironov (2010). *First steps of a lake model intercomparison Project: lakemiP. Boreal environment research*, 15, 191-202.

Oveisy, A. and L. Boegman, (2014). *One-dimensional simulation of lake and ice dynamics during winter. Journal of Limnology* 73, no. 3.

### **Site Description:**

6644 L13-15 This statement that lake source water is ground ice has a reference, but this seems unlikely. More likely its snow-water which has a similar isotopic signature to ground ice (suggest removing this).

The statement is taken from the article by Abnizova et al. (2012) who conducted water balance measurements, as well as detailed analysis of stable isotopic signatures of waters at this site. In addition, ongoing research at this site confirms thawed ground ice as one main source of lake water with potential mixing with precipitation. The isotopic compositions of snow and ice wedges are isotopically much “colder” compared to lakes and ponds. The isotopic composition of ice wedges ranges between  $\delta^{18}\text{O}$  -27 und -21 ‰, with slopes close to the Global Meteoric Water Line (Meyer et al. 2015). Snow shows a large spread in its isotopic composition ( $\delta^{18}\text{O}$  36.1 to -16.1 ‰), with an average of about  $\delta^{18}\text{O}$  -27.5 ‰ and with slopes close to the Global Meteoric Water Line (pers. Communication T. Opel). The slopes of the lake water and ground ice are both about 6 (Figure 4 in Abnizova et al. 2012), which further supports the observation of ground ice as an important source for the lakes.

Other publications of Siberian thermokarst lakes also point to ground ice as an important source for thermokarst lake water, for example by Fedorov et al. (2014).

Added, pp. 8, L12

The stable isotopic ratios indicate that the thermokarst lake water is sourced mainly from thawed ground ice *mixed with precipitation* and the water in shallow ponds is sourced mainly from summer precipitation (Abnizova et al., 2012).

Meyer, H., Opel, T., Laepple, T., Dereviagin, A. Y., Hoffmann, K., and Werner, M.: Long-term winter warming trend in the Siberian Arctic during the mid- to late Holocene, *Nature Geosci*, 8, 122-125, 10.1038/ngeo2349

Fedorov, A.N., Gavriliev, P., Konstantinov, P., Hiyama, T., Iijima, Y., and Iwahana, G., 2014. Estimating the water balance of a thermokarst lake in the middle of the Lena River basin, eastern Siberia, *Ecohydrology*, 7, 188-196.

Methods 6645 L25 – 6646 L6 – How were the buoys relocated and retrieved if they are located well below the water surface? Just curious as this seems challenging.

The reviewer recognizes the difficulties since only sometimes the yellow buoys are visible through the upper m of the water column! We have established a system of land based markers that together with GPS coordinates, as well as “catch method” by rowing in circles around the GPS position with a rope on the bottom sediment.

6648 L7 – This section is interesting, but seems more rational is needed as to why this is a good way to present lake thermal data.

Added to section 3.2, pp. 12, L2-5

*The ability of lakes to store and redistribute additional heat at seasonal time scales may affect the heat budget of adjacent permafrost areas at the landscape spatial scale. For this reason, we observe the thermal regime of tundra lakes to make inferences about their effect on heat exchange processes. The..*

6648 L19-20 – Since latent heat of freezing and thawing aren't the same, why should this necessarily be the case.

To our best knowledge the latent heat of fusion and freezing for freshwater is essentially the same and both terms are interchangeable. For some high Arctic lakes, however, the ice cover does not thaw completely during some years and thus multiyear ice cover can form (though rare, for example on Color Lake on Axel Heiberg Island, Nunavut, Canada; Adams et al., 1989).

Adams, W. P., Doran, P. T., Ecclestone, M., Kingsbury, C. M and C. J. Allan (1989).  
A Rare Second Year-Lake Ice Cover in the Canadian High Arctic, Arctic,  
42(4), 299-306.

6649 – L19-21 – How certain are you that lakes are snow- free most winters? Have multiple lakes been observed throughout multiple winters? Are there other studies or observations to back this up?

We have field observations for several spring field seasons in 2009, 2011 and 2013 for a number of lakes on both islands (Samoylov and surrounding island, such as Kurungnakh). The larger lakes had almost no snow cover, only isolated patches along ice cracks show snow accumulation. These field observations are also supported by optical satellite images. Likely, the (little) snow is blown away by high winter winds. On the smaller lakes (ponds), with slight topographic depression, a snow cover exists and varies between years.

### **Results:**

6657 L16-22 – This lake sediment data is very interesting, but not from this study so why is it in the results.

We prefer to keep these in results as they are directly related to model application for estimating the typical ranges of the water-sediment heat fluxes in seasonal cycle.

For clarification, we have moved and added further information on this data set in the method section 3.3. Modeling of lake thermal dynamics

- pp. 13, L 27 to pp. 14, L2

*Two temperature profiles were obtained in June 1984 for one shallow (1 m) and one deep (5 m) lake, down to a sediment depth of 16 and 21 m below the lake bed, respectively. These temperature profiles are used as input for the model experiments since the assumption of thermal equilibrium does not necessarily exist for the lakes in the permafrost landscape.*

Furthermore, the following information was added to section 1. Introduction:

- pp. 6, L13-20

*(ii) to make use of measured data to validate the freshwater model FLake, as well as estimate water sediment heat exchange. FLake offers a good compromise between computational efficiency and physical reality, and has been coupled to several regional and global climate models (Thiery et al. 2014; Martynov et al. 2010) and has been tested for a wide range of lakes, including tropical lakes in lake model intercomparison projects. However, it has not been used for Arctic lakes and thus, for the first time, the ability of FLake is tested to reproduce the temperature regimes of thermokarst lakes in northern Siberia.*

## **Discussion:**

6659 L2 – What is CALON?

We explain CALON on pp. 5, L20:

CALON is a new Circum-Arctic Lakes Observation Network initiative, see also (<http://www.arcticlakes.org/calon-lakes.html>)

6659 L10 – I believe that (lake depth > winter ice cover depth) should be (lake depth > maximum ice thickness)

Changed, pp. 23, L16

6660 L22-27 – Not sure I follow the comparison of fall and spring thermal dynamics here.

For clarification, we revised and added in section 5. Discussion:

- pp. 25, L7-20

*The warming of lake-bottom temperatures with the onset of ice cover was initially attributed by Brewer (1958) to heating by shortwave solar radiation and by Mortimer and Mackereth (1958) to the heat release from the lake sediment. Our observed near-bottom temperatures increased beneath the ice cover and the modeling experiments suggested this warming was solely due to heat flow from the sediment, with typical rates of  $< 10 \text{ W m}^{-2}$ . However, the heat flux from the sediment in tundra lakes appears to decay within less than one month, which is much faster than in ice-covered lakes of the temperate and boreal climates (cf. Rizk et al. 2014), and is followed by a gradual decrease of the deep water temperatures. The latter is not reproduced by the parameterized sediment module of FLake.*

- pp. 25, L25-29

*Lake temperatures increase, starting in spring 1-2 months before ice-off, apparently by radiative solar heating. This temperature increase suggests that radiation can make a significant direct contribution to sediment heating in shallow and clear-water thermokarst lakes – a contribution that is usually neglected in lake models.*

Added to references, pp. 28 ff:

*Mortimer, C. and F. Mackereth (1958). Convection and its consequences in ice-covered lakes. Verh Int Ver Limnol 13:923–932.*

*Rizk, W., Kirillin, G., and M. Lepparanta (2014). Basin-scale circulation and heat fluxes in ice-covered lakes. Limnol. Oceanogr. 59: 445–464.  
doi:10.4319/lo.2014.59.2.0445.*

6661 – L19-23 – I didn't see data presented to support this statement (may have missed it) but would be interesting to see this and focus more on such question with data presented in results (and figures) and discussed. All time series figures should have y-axis title in addition to units and x-axis dates are hard to read.

Flooding of river water and the effect on the thermal regimes of the lakes was discussed in section 4.3 (pp.17, L8). To clarify and highlight the river flooding events, we have added arrows in the revised figures 4, 5 and 7, pp.42, 43 and 45.

Furthermore, all figures were redrawn with a reformatted x-axis and titles were added to the y-axes, please see pp. 41-43, 45-46, 57-59.

#### Figure 6 – Which months are which and why the interannual variation?

Starting with colder mean bottom temperature in July after ice break up, gradual warming creates warmest mean bottom temperatures in the deepest lake Sam\_Lake\_4 always in August and in the shallowest lake Sam\_Lake\_3 in July. For all other lakes, maximum bottom temperatures occur either in July or August, depending on the lakes's seasonal energy balance. Maximum air temperature usually during July, but net radiation can be quiet variable (Fig. 3 c). Interannual variations are mostly due to the differences in timing of ice cover break up which is determined by a combination of factors (thickness of ice, wind forces that break up the ice, surface energy balance, turbidity of the water influencing the light transmission and absorption). As listed in Table 1, the start of ice cover break up and complete melt can range over several weeks in its length and annual variability.

We added the following information to the section results 4.4:

- pp. 18, L12-16

*Starting with colder mean bottom temperature in July, gradual warming creates warmest mean bottom temperatures in the deepest lake (Sa\_Lake\_4) in August and in the shallowest lake (Sa\_Lake\_3) in July. For all other lakes, maximum bottom temperatures occur either in July or August, depending on the timing of ice break up and the lake's seasonal energy balance.*

A summary data table on monthly air and bottom lake temperatures is also supplied in the supplementary material of this paper (description on pp. 60), since the figure would otherwise be too crowded.

Lake bathymetry figures – Can you show where sensors were located in each?

The lake bathymetry figures have been revised and now include the location of the sensors (pp. 52-56).



**Interactive comment on “Physical processes of thermokarst lakes in the continuous permafrost zone of northern Siberia – observations and modeling (Lena River Delta, Siberia)” by J. Boike et al.**

**Anonymous Referee #2** Received and published: 26 June 2015

General comments:

In general, the paper seems worth publishing. Lakes are frequent phenomena in arctic landscapes, yet still not many studies have been published on their thermal behaviour, namely for multiannual periods including cold seasons. The purpose of observing them but also designing a model and evaluating it with the observed data is important. It is well pointed out that albeit similar studies are around on lakes in these landscapes, a lack of data is addressed with the present study located in northern Eurasia. However, while the study specifically investigates a small number of lakes in the Lena delta in northern Siberia, I somewhat miss a statement on how applicable the results are for Siberia in general, or how specific the lakes in this study are. It was not so clear to me why specifically the FLake model was used. This could be motivated actually when hinting to the possibility of implementing/coupling it (in)to regional or global climate models, as in fact these large scale models often still very much simplify lake physics, in contrast to what is stated in the introduction (see specific comments). Is there any conclusion on the usability of the FLake model for such a purpose? I would also recommend some statement on the applicability of the FLake concept of self-similarity for such complex systems, and/or e.g. where reasons might be for the disagreement between model and observations during winter time. An advantage of the study is that the measurements of the lake, e.g. water depth, ice break up, and temperatures, are related to data from the surroundings, as river flooding events and river temperatures; the description of the observed phenomena in the lakes is conducted in context with these supplementary observations.

Our reply (marked in blue) is structured the following:

- *Italic indicates that text has been revised or added to paper*
- References are given with full citations when not included in paper already
- Page (pp) and Line (L) numbers refer to revised paper version

## Reply to general comments:

We thank the reviewer for the valuable comments. As outlined in our response to reviewer #1, we have sharpened/tightened the manuscript by performing additional model runs with FLake. Overall, we sharpened the objectives of the paper, including why we use the FLake model, we have generally revised the description of the modeling in the aims and method section. In particular, we have refined the description of the modeling section in the aims and methods and the applicability of the FLake is addressed in the discussion/conclusion section.

Please find our answers to the specific comments below.

### Why was the FLake model used?

We added an explanation why we used the FLake model at the end of the introduction section 1, pp 6, L13-20:

*FLake offers a good compromise between computational efficiency and physical reality, and has been coupled to several regional and global climate models (Thiery et al., 2014; Martynov et al., 2010). FLake has been used in various 1 dimensional modeling studies, for a wide range of lakes, including tropical lakes, and in lake model intercomparison projects (LakeMIP; Thiery et al., 2014; Stepanenko et al., 2010). However, it has not been used for Arctic lakes and this study tests the ability of FLake to reproduce the temperature regimes of thermokarst lakes in northern Siberia.*

How applicable are the results for Siberia in general, or how specific are the lakes in this study?

The lakes presented in this paper are of thermokarst origin which is common for the lowland tundra permafrost areas of North East Siberia. These areas were not ice-covered during the latest glacial period (70,000-10,000 years ago) and are characterized by high to moderate ground ice content and thick sediment cover. Arctic lowlands with similar landscape characteristics and lake distributions can be found in Central and East Siberia, Interior and Northern Alaska as well as Northwest Canada (Grosse et al., 2013).

Added to section 2 “Site description”:

- pp. 7, L24-29

*The lakes presented in this paper are of thermokarst origin which is common for the lowland tundra permafrost areas of North East Siberia. These areas were not ice-covered during the latest glacial period (70,000-10,000 years ago) and are characterized by high to moderate ground ice content and thick sediment cover. Arctic lowlands with similar landscape characteristics and lake distributions can be found in Central and East Siberia, Interior and Northern Alaska as well as Northwest Canada (Grosse et al., 2013).*

Added to section 6 “Summary and conclusion”:

- pp. 27, L8-10

*The investigated thermokarst lakes are representative of Arctic tundra lowlands characterized by thermokarst processes that are common for large regions in Central and East Siberia, Interior and Northern Alaska as well as Northwest Canada.*

Is there any conclusion on the usability of the FLake model for such a purpose? I would also recommend some statement on the applicability of the FLake concept of self-similarity for such complex systems, and/or e.g. where reasons might be for the disagreement between model and observations during winter time.

We revised the paper and added to the discussion on the model performance as this was also requested by reviewer #1. Please find a detailed response to this in the “Reply to general comments” to reviewer #1, pp. 2-6.

Furthermore, we added the following text to address the applicability of the FLake concept of self-similarity for the complex thermokarst lake system in section 5.

Discussion:

- pp. 25, L 25-31 to pp. 26, L1-2

*The concept of self-similarity cannot account for the permafrost-talik specific lake processes, such as (i) warming of bottom waters immediately following onset of ice formation and (ii) phase change in the lake's frozen sediment, i.e. annual freeze thaw processes and thawing at the talik-permafrost boundary.*

**Specific comments:**

**Abstract:** Why the FLake model? Is it necessary to mention here the specific model?

We would like to mention FLake once in the abstract, but remove the additional ones.

We added an explanation why we used the FLake model at the end of the introduction section 1, pp 6, L13-20:

*FLake offers a good compromise between computational efficiency and physical reality, and has been coupled to several regional and global climate models (Thiery et al., 2014; Martynov et al., 2010). FLake has been used in various 1 dimensional modeling studies, for a wide range of lakes, including tropical lakes, and in lake model intercomparison projects (LakeMIP; Thiery et al., 2014; Stepanenko et al., 2010). However, it has not been used for Arctic lakes and this study tests the ability of FLake to reproduce the temperature regimes of thermokarst lakes in northern Siberia.*

**'Wedderburn number'**: if mentioned, please shortly explain it.

Added, pp. 2, L21-22

*..., a quantitative measure of the balance between wind mixing and stratification that is important for describing the biogeochemical cycles of lakes.*

**Introduction:** Caution: 'thermal dynamics [of lakes] are often incorporated in RCMs and GCMs' is not fully true, as still the representation of lakes is rather simple in large scale models. –

Changed, pp. 4, L5-7

*...but their thermal dynamic represented in RCMs and GCMs is rather simple, and does not include all physical processes that are necessary for reproducing atmosphere-lake interaction (...)*

**3.2 Lake morphometry:** P6647 L 8-10: if not treated here, why mentioned?

– many details on the morphometry, but are these related later to the results?

The section is shortened and moved to the appendix A, pp. 51.

**3.4 Modelling of lake thermodynamics:** P 6649, L 13-15: Golosov and Kirilin and Mironov et al. applied this concept to observations? Not clear to me whether this was also modelling or observations.

Golosov and Kirillin developed the sediment model, Mironov et al. developed the ice model. Both references contain model comparisons to observations.

**4.4 Summer:** interesting points with the Wd number: 'monthly bottom Ts for some lakes were also warmer than the corresponding monthly air Ts' reasoning given is that radiative heating as well as mixing is at work.

To highlight this point, we added the following in section 6. Summary and conclusion:

-pp. 26, L23

The lakes were shown to receive substantial energy for warming from net shortwave radiation *during the summer*. Warming also occurs during the ice cover period in spring, resulting in convective mixing...

**4.5 Lake heat content:** P 6655, L 11: annually, the energy fluxes should be more or less balanced - I had problems with approaching the energy balance by summing up all terms into an 'annual heat budget [...] up to 1 GJ/m<sup>2</sup>', in other words neglecting the sign of a term. Latent heat of fusion, e.g., is consumed in spring/summer, yet

released in fall and winter. Is the interesting point in that as to how strong the consumption of incoming energy through these lakes is (the sales, so to say)?

We calculated the lake heat content (described in 3.2 Heat content, equation 1, pp.12 L 5-11) following Wetzel (2001). Following this method, the heat content is divided for the periods of summer, winter, and annually. Though the latent heat of fusion of the formation/thawing of the ice equals out on an annual basis (in case of a complete thawing of lake ice cover), this amount is included in the annual heat content in this method (Wetzel, 2001). This allows also direct comparison with the heat content numbers given for a worldwide variety of lakes (Wetzel, 2001, Table 6-2). We compare our heat content numbers with numbers given by previous calculations in section 5. Discussion (pp. 24, L12-19).

For clarification we added the following text in the method section 3.2 Heat content:

-pp. 12, L2-5

*The annual heat budget is the total amount of heat necessary to raise the water from the minimum temperature to maximum summer temperature. The winter heat income and the annual heat budget must include the latent heat of fusion for the ice cover, especially for high latitude lakes (Wetzel, 2001).*

The “sales point” here is that these lakes process much larger amounts of energy compared to lakes in temperate environments. Furthermore, their heat storage is much larger compared to their frozen environment (please also see reply to the following comment).

#### **4.6.3 Thermal properties of the lake sediments and water-sediment heat flux:**

really interesting: how much warmer these lakes are than both the underlying ground and the atmosphere.

The „thermal offset“, i.e. difference between the mean annual temperature of permafrost and air is a result of the thermal influence of snow cover and active layer, As a result, the permafrost soil is several degrees warmer than the mean annual air temperature (MAAT) at this site of about -12.5°C. The lake with mean annual positive

water temperatures is significantly warmer than MAAT, and with a higher thermal capacity resulting in a much higher annual energy density.

The energy densities for measured mean annual temperatures for a lake (3°C) and permafrost soil at 2 m depth (-7°C) were calculated using the respective volumetric heat capacities for water ( $c_w = 4.2 \text{ MJ/m}^3\text{K}$ ) and frozen soil ( $c_s = 1.8 \text{ MJ/m}^3\text{K}$ ; Langer et al., 2011b) and a MAAT of -12.5°C. The calculated energy density for the lake is  $65.1 \text{ MJ/m}^3$ , thus more than six times compared to the amount for the permafrost soil of  $9.9 \text{ MJ/m}^3$ .

We added to Section 4.6.3, Thermal properties of the lake sediments and water sediment heat flux:

-pp. 22, L18-22

*Overall, the calculated energy density for the lake with mean annual water temperature of 3°C is about  $65 \text{ MJ m}^{-3}$ , thus more than six times the amount for the permafrost soil of about  $10 \text{ MJ m}^{-3}$ . Lakes are therefore effective for energy storage compared to the frozen landscape, and the fraction of landscape covered by thermokarst lakes has the potential to significantly affect the land-atmosphere energy exchange.*

**5. Discussion:** P 6660, L 9: where does this specific number come from, and for which region/landscape?

This number is the measured reported maximum thaw depth of active layer from the polygonal tundra landscape of this area using a 150 point grid (Boike et al. 2013).

Added, pp. 24, L24-26

In contrast, progressive deepening of the seasonally thawing upper layer of permafrost (the active layer) *of the polygonal tundra landscape at this site* takes several months and only reaches a maximum thaw depth of about 0.6 m (Boike et al., 2013).

– Is it possible to state that the effect of lakes on PF below is still somewhat unclear, that is, whether a talik necessarily thaws the PF below?

Below the talik permafrost will degrade as long the vertical heat flux is not balanced by the lateral heat flux which depends on lake size and the thermal state of the surrounding soil.

We would like to point out that the bottom lake temperatures are highly relevant for talik development underneath; a difference in mean annual bottom lake temperature of 2°C would change the heat flux by a factor of two. Thus, our data aid constraining future numerical modeling experiments for talik development. For example, the numerical study of talik development for shallow lakes on the Alaskan Arctic Coastal Plain (Ling and Zhang, 2003) uses a range between 1-3°C, and thus about twofold modeled talik thickness.

Added to section 5. Discussion

- pp. 23, L13-15

*Mean bottom lake temperatures, which ranged between 2.7 and 4 °C in this study, depend on lake depth and are important for constraining future numerical modeling experiments on talik development.*

P 6660, L 15-21: If a still downward directed heat flux at the lake bottom during winter really implies PF degradation/warming can only be stated if heat fluxes during warm periods are also mainly downwards. Couldn't it be that lakes, through their much larger heat capacity as they freeze and melt, exert a larger phase lag on temperature variations of the ground as the surroundings? –

The average bottom temperature is always larger than the freezing point which is the temperature at lower boundary of the talik. Thus, there is on an annual average a net downward ground heat flux no matter of the annual air temperature variations. However, this heat flux linear decreases with talik depth and will equilibrate at a certain point with lateral heat fluxes resulting from heat budget differences to the surrounding soils.

P 6661, L 6-8: Is it really the case that heat transfer to the atmosphere is of minor importance during winter? Ice has a large thermal conductivity, and the temperature



gradient between ice (/water below) and atmosphere is large. Are there any references for that?

The reviewer is absolutely right. The heat flux from lakes to the atmosphere is much higher than the heat flux from snow covered soils (for example, shown by Langer et al. 2011b for ponds and Jeffries et al. 1999 for Alaskan lakes; both cited in this paper). In particular during winter the subsurface heat flux becomes an essential component in the surface energy balance due to the lag of incoming short wave radiation. The sub surface heat flux balances up to 90% of the radiative losses. Thus, lakes could play an important role in the atmosphere heat budget during winter.

**Technical:**

P 6646, L 3: 'were reinstalled'

Corrected, pp. 9, L25

P 6647, L 8: 'obtained for additional ...'

Corrected, pp.10, L17

- generally, visibility in Fig.s 4b, 5b, 8c may be improved

We supply higher resolution figures (pdfs) with the final manuscript version.

P 6652, L 21: replace 'with a light extinction of ...' with 'assuming light extinction to be ...'

Corrected, pp. 16, L20

P 6652, L 23: 'radiative' instead of 'radiation'

Corrected, pp. 16 L22

P 6658, L 2: 'release of heat'

Corrected, pp. 22, L3

P 6659, L 10-11: 'ice cover thickness'

Corrected, pp. 23, L16

P 6661, L 11: '...such as thawing.'

Corrected, pp. 26, L9

1 **Physical–Thermal processes of thermokarst lakes in the**  
2 **continuous permafrost zone of northern Siberia -**  
3 **observations and modeling (Lena River Delta, Siberia)**

4  
5 **J. Boike<sup>1</sup>, C. Georgi<sup>1</sup>, G. Kirilin<sup>2</sup>, S. Muster<sup>1</sup>, K. Abramova<sup>3</sup>, I. Fedorova<sup>4,5,6</sup>, A.**  
6 **Chetverova<sup>4,5</sup>, M. Grigoriev,<sup>7</sup> N. Bornemann<sup>1</sup> and M. Langer<sup>1,8</sup>**

7 [1] Alfred Wegener Institute Helmholtz Center for Polar and Marine Research,  
8 Telegrafenberg A43, 14473 Potsdam, Germany

9 [2] Leibniz-Institute of Freshwater Ecology and Inland Fisheries (IGB), Mueggelseedamm  
10 310, 12587 Berlin, Germany

11 [3] Lena Delta Nature Reserve, Ak. Fedorova 28, 678400 Tiksi, Sakha Republic, Russia

12 [4] Institute of Earth Science, Saint-Petersburg State University, 10th line of Vasiljevsky  
13 Island, 33-35. 199178 Saint-Petersburg, Russia

14 [5] Arctic and Antarctic Research Institute, 38, Beringa str., St. Petersburg, 199397, Russia

15 [6] Kazan Federal University, 18, Kremlyovskaya str., Kazan, Russia

16 [7] Melnikov Permafrost Institute, Siberian Branch, Russian Academy of Sciences, Yakutsk,  
17 Russia

18 [8] Laboratoire de Glaciologie et Géophysique de l'Environnement (LGGE), 38402 St Martin  
19 d'Hères Cedex, France

20  
21 Correspondence to: J. Boike (Julia.Boike@awi.de)

## 1 Abstract

2 Thermokarst lakes are typical features of the northern permafrost ecosystems, and play an  
3 important role in the thermal exchange between atmosphere and subsurface. The objective of  
4 this study is to describe the main thermal processes of the lakes and to quantify the heat  
5 exchange with the underlying sediments. The thermal regimes of five lakes located within the  
6 continuous permafrost zone of northern Siberia (Lena River Delta) ~~have been~~ were  
7 investigated using hourly water temperature and water level records covering a three year  
8 period (2009-2012), together with bathymetric survey data. The lakes included thermokarst  
9 lakes located on Holocene river terraces that may be connected to Lena River water during  
10 spring flooding, and a thermokarst lake located on deposits of the Pleistocene Ice Complex.  
11 ~~The data were used for numerical modeling with FLake software, and also to determine the~~  
12 ~~physical indices of the lakes. The lakes vary in area, depths and volumes. The winter thermal~~  
13 ~~regime is characterized by an-~~ Lakes were covered by ice cover up to 2 m thick that survives  
14 persisted for more than 7 months of the year, from October until about mid-June. Lake-  
15 bottom temperatures increased at the start of the ice-covered period due to upward-directed  
16 heat flux from the underlying thawed sediment. ~~The effects of solar radiation return p~~ Prior to  
17 ice break-up, solar radiation effectively warmed the water beneath the ice cover and  
18 induced convective mixing. Ice break-up started at the beginning of June and lasted ~~takes~~  
19 until the middle or end of June ~~for completion~~. Mixing occurs within the entire water  
20 column from the start of ice break-up and continues during the ice-free periods, as confirmed  
21 by the Wedderburn numbers, a quantitative measure of the balance between wind mixing and  
22 stratification that is important for describing the biogeochemical cycles of lakes. Some of the  
23 ~~lakes located closest to the Lena River are subjected to varying levels of spring flooding with~~  
24 ~~river water, on an annual basis. The lake thermal regime was modelled numerically using the~~  
25 FLake model. The model demonstrated good agreement with observations with regard to the  
26 mean lake temperature, with a good reproduction of the summer stratification during the ice  
27 free period, but poor agreement during the ice covered period. Model sensitivity to lake depth  
28 demonstrated that lakes in this climatic zone with mean depths >5 m develop continuous  
29 stratification in summer for at least one month. Numerical modeling using FLake software  
30 ~~indicates that -~~ The modeled vertical heat flux across the bottom sediment tends towards an  
31 annual mean of zero, with maximum downward fluxes of about  $5 \text{ W m}^{-2}$  in summer and with

1 heat released back into the water column at a rate of less than  $1 \text{ W m}^{-2}$  during the ice-covered  
2 period.

3 The lakes are shown to be efficient heat absorbers and effectively distribute the heat through  
4 mixing. Monthly bottom water temperatures during the ice-free period range up to  $15^{\circ}\text{C}$  and  
5 are therefore higher than the associated monthly air or ground temperatures in the surrounding  
6 frozen permafrost landscape. The investigated lakes remain unfrozen at depth, with mean  
7 annual lake –bottom temperatures of between  $2.7$  and  $4^{\circ}\text{C}$ .

8 The data are available in the supplementary material for this paper and through the  
9 PANGAEA website (<http://doi.pangaea.de/10.1594/PANGAEA.846525>).

# 1 1 Introduction

2 Lakes can be interpreted as sensitive climatic indicators that respond to a range of different  
3 influences affecting the world's climate. They can also exert an important influence on the  
4 local, regional, and global climate and hydrology by regulating heat and water fluxes, ~~and~~  
5 ~~their thermal dynamics are often incorporated into regional and global climate models but~~  
6 ~~their thermal dynamic represented in RCMs and GCMs is rather simple, and does not include~~  
7 ~~all physical processes that are necessary for reproducing atmosphere-lake interaction~~ (Walsh  
8 et al., 1998; Martynov et al., 2012). Lakes are often typical features of northern hemisphere  
9 ecosystems (Figure 1). In permafrost areas, which occupy about 25% of the world's landmass,  
10 lakes influence not only the thermal regime of the surrounding and underlying permafrost, but  
11 also the atmospheric heat and water fluxes, due to their large thermal heat reservoirs and heat  
12 capacities. The winter heat flux into the atmosphere through the ice cover from deep lakes  
13 that remain unfrozen at depth is several times greater than that from the surrounding tundra  
14 (Jeffries et al., 1999). Even smaller polygonal water bodies (thermokarst ponds), which freeze  
15 to the bottom every winter, have heat fluxes that are an order of magnitude greater than those  
16 from the surrounding permafrost (Langer et al., 2011b). The large thermal heat reservoir in  
17 lakes prevents the sediment beneath those lakes with a water depth greater than about 2 or 3  
18 meters from freezing, thus allowing a talik to develop (Lachenbruch, 1962). However, little  
19 data exists on the thermal conditions of lakes in north and central Yakutia, or the taliks  
20 beneath them (Grigoriev, 1960, 1966; Are, 1974; Pavlov et al., 1981). These unfrozen layers  
21 of lake sediment can enhance mobilization of the carbon reservoir by enabling year-round  
22 microbial decomposition in otherwise frozen surroundings, and water bodies can thus be  
23 hotspots for CO<sub>2</sub> and CH<sub>4</sub> emissions (Langer et al., 2015; Schneider von Deimling et al.,  
24 2014; Walter et al., 2006; Abnizova et al., 2012; Laurion et al., 2010). Water bodies are also  
25 important because they provide habitats for zooplankton, fish, and migratory birds (Vincent  
26 and Hobbie, 2000; Alerstam et al., 2001), and are a source of drinking water for northern  
27 communities, of water for irrigation, and of water for industry, exploration, and ice-road  
28 construction in winter (Vincent et al., 2013).

29 Measuring the water temperatures in lakes over both short and long terms is therefore  
30 important, not only for modeling the development of the subsurface thermal regime, but also  
31 for understanding and modeling ecological and physical dynamics. Few investigations have,

1 however, been carried out into the physical and thermal characteristics of Arctic water bodies,  
2 especially over the long term, and there is a particular shortage of data from northern Siberia.  
3 A notable exception is the long term biological, physical and chemical lake study initiated in  
4 | 1975 at the Toolik Lake Long Term ~~Experimental~~ Ecological Research (LTER) site in  
5 Alaska. The lakes studied are located on the North Slope of Alaska, in the foothills of the  
6 Brooks Range, and are classified as low Arctic lakes (Hobbie and Kling, 2014). Toolik Lake  
7 and most of the other lakes in this area are “kettle lakes” that formed as a result of glaciation;  
8 their lake morphometries (surface areas, depths) are a result of the glaciation history and the  
9 age of the landscape. Water depths can range up to 25 m, as is the case in Toolik Lake  
10 (Hobbie and Kling, 2014). The thermal stratification varies considerably between lakes  
11 (depending on the lake’s morphometry), as well as between years (Luecke et al., 2014). Also  
12 in northern Alaska, Arp et al. (2010) made use of an original method that combined short term  
13 (for example, over one year) measured lake surface temperatures (from depths of 0.5 m and  
14 1.0 m) with meteorological and remote sensing data on lake surface temperatures and ice  
15 thicknesses. The latter variables were compared with measured temperatures and ice  
16 thicknesses, and with modeled results (Arp et al., 2010). The advantage of this approach is  
17 that, following successful calibration, a monitoring network can be established that is based  
18 purely on remote sensing data. Monitoring in some of these lakes on the Alaskan Coastal  
19 Plain has continued since 2010 as part of the new Circum-Arctic Lakes Observation Network  
20 (CALON) initiative (<http://www.arcticlakes.org/calon-lakes.html>; Hinkel et al., 2012). An  
21 initial series of data for vertical temperature profiles from the summer of 2010 has been  
22 provided for a number of lakes, together with time series of hourly temperature data, in order  
23 to demonstrate the seasonal and temporal variability (Hinkel et al., 2012).

24 Sporadic measurements of lake temperatures have been obtained in conjunction with  
25 limnological studies (for example, by Keatley et al., 2007, or Pienitz et al., 1997),  
26 paleolimnological investigations (such as in the 172 m deep El’gygytgyn Lake of north-  
27 eastern Siberia, a meteoritic impact crater; Nolan and Brigham-Grette, 2006), and physical  
28 experiments (such as dye tracing under the ice cover in a small Arctic lake; Welch and  
29 Bergmann, 1985). Vincent et al. (2008) measured temperatures and salinity in a high Arctic,  
30 125 m deep, perennially ice-covered lake on Ellesmere Island in Nunavut, Canada. The  
31 authors then successfully modeled the lake’s temperature regime using a one-dimensional

1 heat diffusion equation and including heat transfer by radiation through ice and water. For  
2 lakes within the Mackenzie Delta (Northwest Territories of Canada), Burn (2002, 2005)  
3 demonstrated that the temperatures in the deep central pool of a thermokarst lake on Richards  
4 Island remained positive throughout the winter, with a mean annual temperature of 3.5°C,  
5 whereas freezing occurred in the shallow littoral terrace of the lake (mean annual temperature  
6 -3.7°C).

7 This paper aims to quantify the seasonal thermal dynamics of lakes in the Eurasian north,  
8 where monitoring observatories have recently been established in the central part of the Lena  
9 River Delta. Our objectives are (i) to describe the thermal patterns and processes in both  
10 thermokarst lakes and “perched” lakes (which can have seasonal connections to river water),  
11 and (ii) to make use of measured data to validate the ~~FLake numerical model—a freshwater~~  
12 ~~lake model that has been used for climate modeling and weather prediction—freshwater model~~  
13 FLake, as well as estimate water sediment heat exchange. FLake offers a good compromise  
14 between computational efficiency and physical reality, and has been coupled to several  
15 regional and global climate models (Thiery et al., 2014; Martynov et al., 2010). FLake has  
16 been used in various 1 dimensional modeling studies, for a wide range of lakes, including  
17 tropical lakes, and in lake model intercomparison projects (LakeMIP; Thiery et al., 2014;  
18 Stepanenko et al., 2010). However, it has not been used for Arctic lakes and this study tests  
19 the ability of FLake to reproduce the temperature regimes of thermokarst lakes in northern  
20 Siberia.

21

22

## 23 **2 Site description**

24 The Lena River Delta in northern Yakutia is one of the largest deltas in the Arctic and has one  
25 of the largest catchment areas (2,430,000 km<sup>2</sup>) in the whole of Eurasia (Costard and Gautier,  
26 2007). The Lena River discharges about 525 km<sup>3</sup> of water through the delta into the Arctic  
27 Ocean every year, with an average annual discharge rate of 16,800 m<sup>3</sup> s<sup>-1</sup> (Gordeev and  
28 Sidorov, 1993). This discharge rate has been reported to be increasing (Fedorova et al., 2015;  
29 Rawlins et al., 2009). As it passes through its estuarine area, the main flow of the Lena River



1 splits into numerous arms and transverse branches to form the most extensive delta in the  
2 Russian Arctic, covering 25,000 km<sup>2</sup> and including about 1,500 islands and 60,000 lakes.

3 Continuous cold permafrost (with a mean annual temperature of -10°C at 10 m depth)  
4 underlies the study area to between about 400 and 600 m below the surface. Since  
5 observations started in 2006, the permafrost at 10.7 m depth has warmed by > 1.5°C (Boike et  
6 al., 2013; <http://gtnpdatabase.org/boreholes/view/53/>).

7 The main features of the annual energy balance for these sites with continuous permafrost in  
8 the subsurface typically include low net radiation, higher atmospheric latent heat flux than  
9 sensible heat flux, and a large proportion of soil heat flux (Boike et al., 2008; Langer et al.,  
10 2011a, 2011b). Previous publications have reported that shallow (< 1 m deep) ponds freeze  
11 completely in winter, but that the timing of freeze-back can vary by up to 2 months between  
12 years, depending on the surface energy balance (Langer et al., 2011b; Langer et al., 2015).

13 The study areas are located on the islands of Samoylov and Kurungnakh, within the central  
14 part of the Lena River Delta (Figure 1). Samoylov Island (72°22'N, 126°28'E) lies within one  
15 of the main river channels in the southern part of the delta and is relatively young, with an age  
16 of between 4 and 2 ka BP (Schwamborn et al., 2002), which is also the estimated maximum  
17 age of the investigated lakes on the island. In contrast, Kurungnakh Island forms part of the  
18 third terrace of the Lena Delta and is an erosional remnant of a late-Pleistocene accumulation  
19 plain. It consists of fluvial sands overlain by Yedoma-type ice complex deposits, which  
20 accumulated between 100 and 50 ka BP and since 50 ka BP, respectively, and a Holocene  
21 cover (8 to 3 ka BP) (Schwamborn et al., 2002; Wetterich et al., 2008). Large thermokarst  
22 lakes and basins are major components of the ice-rich permafrost landscape of Kurungnakh  
23 Island; they have formed since 13 to 12 ka BP (Morgenstern et al., 2011, 2013).

24 The lakes presented in this paper are of thermokarst origin which is common for the lowland  
25 tundra permafrost areas of North East Siberia. These areas were not ice-covered during the  
26 latest glacial period (70,000-10,000 years ago) and are characterized by high to moderate  
27 ground ice content and thick sediment cover. Arctic lowlands with similar landscape  
28 characteristics and lake distributions can be found in Central and East Siberia, Interior and  
29 Northern Alaska as well as Northwest Canada (Grosse et al., 2013).

1 The landscape on both of these islands, and in the delta as a whole, has generally been shaped  
2 by water through erosion and sedimentation (Fedorova et al., 2015), and by thermokarst  
3 processes (Morgenstern et al., 2013). The proportion of the total land surface of the delta  
4 covered by surface water can amount to more than 25% (Muster et al., 2012). Up to 50% of  
5 the total surface water area in permafrost landscapes is attributed to small lakes and ponds  
6 with surface areas of less than  $10^5$  m<sup>2</sup>, which have the potential to grow into large thermokarst  
7 lakes (Muster et al., 2012). Water budget modeling for the tundra landscape has shown a  
8 small positive balance since 1953, which has been confirmed by satellite observations (since  
9 1964) of the surface areas of water bodies (Boike et al., 2013). The chemical and isotopic  
10 signals from the water in lakes on Samoylov Island generally indicate low levels of  
11 mineralization (Table 1). The stable isotopic ratios indicate that the thermokarst lake water is  
12 sourced mainly from thawed ground ice mixed with precipitation and the water in shallow  
13 ponds is sourced mainly from summer precipitation (Abnizova et al., 2012).

14 Small ponds and lakes emit more CO<sub>2</sub> and CH<sub>4</sub> per square meter than the surrounding tundra,  
15 and greenhouse gas production continues during winter in those lakes that do not freeze to the  
16 bottom (Langer et al., 2015). Modeling studies have demonstrated that an unfrozen layer of  
17 lake sediment is maintained throughout the year beneath thermokarst lakes (Yi et al., 2014).  
18 During high spring floods some of the lakes on the first terrace are flooded with Lena River  
19 water. Observations in 2014 on Samoylov Island, for example, confirmed the flooding of a  
20 large part of the first terrace on the island, including most of the lakes.

21 Additional detailed information concerning the climate, permafrost, land cover, vegetation,  
22 and soil characteristics of these islands in the Lena River Delta can be found in Boike et al.  
23 (2013) and Morgenstern et al. (2013).

24

## 25 **3 Methods**

### 26 **3.1 Field instrumentation and ground surveys**

27 In July 2009, water level and temperature sensors (HOBO Temp Pro v2, HOBO U20, Onset,  
28  $\pm 0.2^\circ\text{C}$  across a temperature range from  $0^\circ\text{C}$  to  $70^\circ\text{C}$ , and  $\pm 0.4^\circ\text{C}$  across a temperature range  
29 from  $-40^\circ\text{C}$  to  $0^\circ\text{C}$ ) were installed within the water columns of the investigated lakes on

1 Samoylov and Kurungnakh Island. Figure 1 shows the locations of the lakes (labelled  
2 Sa\_Lake\_1-4 for Samoylov and Ku\_Lake\_1 for Kurungnakh) and the location of the long  
3 term weather station. Gaps in the climate data record (air temperature, radiation, humidity,  
4 wind speed and direction, and snow depth) were filled whenever possible with data from  
5 temporary climate and eddy covariance stations located in close proximity to the weather  
6 station (Boike et al., 2013). Temperature and water depth sensors were placed directly above  
7 the sediment-water interface and then temperature sensors at 2 m intervals up to 2 m below  
8 the water surface (Figure 2). The sensors were suspended in the water column from a buoy  
9 and anchored in the sediment below. The sensor at the bottom of the lake (just above the  
10 sediment) was labelled as “0 m”, the sensor 2 m above the sediment as “2 m”, and so on. The  
11 uppermost sensors were usually about 2 m below the water surface since we were concerned  
12 about the formation of ice and the potential drift of sensors with the shifting of ice cover. End-  
13 of-winter ice thickness (obtained by drilling) was measured in 2014; it ranged between 1.9  
14 and 2 m in lakes Sa\_Lake\_1-4 on Samoylov Island. During some winters the uppermost  
15 sensors became enclosed within the ice cover (for example, Sa\_Lake\_1 in 2012), but they  
16 were not moved out of position. One sensor was installed in the Lena River during August  
17 2009 (Figure 1) and recorded data from July 2009 to August 2010 but was lost during the  
18 following year.

19 Sensors were usually retrieved once a year (in August) and then re-launched in approximately  
20 the same position. The temperature record was therefore briefly interrupted during the period  
21 when the sensors were retrieved and read. The water depth (“sensor depth”) recorded by the  
22 bottom sensor sometimes changed following retrieval due to a change in the sensor position,  
23 although the actual water level of the lake remained the same. For example, for Sa\_Lake\_4 (a  
24 perched lake), sensors that were deployed at a water depth of about 8.5 m in 2009 were ~~and~~  
25 re-installed at a depth of about 9.5 m in August 2010. Water level variations due to water  
26 balance changes (when the sensor position had not changed), for example during the summer  
27 period, were usually less than 0.5 m.

28 Data is only available over a one-year period for the lake on Kurungnakh Island (2009-2010)  
29 as the loggers were subsequently displaced, presumably during ice break-up. For the lakes on  
30 Samoylov Island, however we obtained continuous temperature and water level data over a  
31 period of 3 years from 2009 to 2012. All data and metadata are provided in the supplementary

1 material for this publication and through the PANGAEA website  
2 (<http://doi.pangaea.de/10.1594/PANGAEA.846525>).

3 Bathymetric surveys were carried out in 2009 and 2010 on all of the investigated thermokarst  
4 lakes, using a GPSMAP 178 C echo sounder, a GPSMAP 421S plotter and a GPS 60  
5 navigator, all from Garmin. The shorelines were mapped either by GPS field survey or by  
6 manually digitizing the shoreline from high resolution aerial images. The accuracy of the echo  
7 sounder equipment was about 0.1 m and was regularly checked using manual profiling. Depth  
8 measurements were taken along the longest lake axis as well as along a zigzag track in order  
9 to cover most of the lake surface and to locate any local “holes” that might exist as a result of  
10 thermokarst processes. ~~Bathymetric data and metadata can again be found in the  
11 supplementary material for this publication, as well as through the PANGAEA website  
12 (<http://doi.pangaea.de/10.1594/PANGAEA.846525>).~~ Surface areas, mean and maximum depths,  
13 volumes, and hypsographic (depth/area) curves were calculated for the five lakes investigated  
14 using linear distance nearest neighbor interpolation in ArcGIS software (v.10.1) (Table 1). A  
15 description of the morphometry, including two-dimensional contour plots and cross sectional  
16 profiles of the lakes can be found in the appendix of this paper (Figures A1 to A5).  
17 Bathymetric records were also obtained for eight additional lakes (Chetverova et al., 2013)  
18 but are not included herein since temperature sensors were not installed. Bathymetric data,  
19 metadata and morphometric descriptions can be found in the appendix material for this  
20 publication, as well as through the PANGAEA website  
21 (<http://doi.pangaea.de/10.1594/PANGAEA.846525>).

22

### 23 **~~3.2 Lake morphometry~~**

24 ~~A lake's morphometric parameters such as its area ( $A$ ), depth ( $z$ ), and volume ( $V$ ), influence~~  
25 ~~the boundary fluxes (heat and water exchanges) between sediment and water and between~~  
26 ~~water and atmosphere, as well as the dynamics of physical processes (such as mixing). For~~  
27 ~~example, in winter shallow water depths ( $< 2$  m) usually experience freezing of the entire~~  
28 ~~water column and hence the sediment beneath the lake floor also freezes. In summer, a strong~~  
29 ~~thermal stratification of lake waters in deeper lakes (with temperatures of  $4^{\circ}\text{C}$  at the bottom of~~

1 ~~the lake) prevents warming of lake sediments even though the lake's surface temperatures~~  
2 ~~may be higher.~~

3 ~~Surface areas, mean and maximum depths, volumes, and hypsographic (depth/area) curves~~  
4 ~~were calculated for the five lakes investigated using linear distance nearest neighbor~~  
5 ~~interpolation in ArcGIS software (v.10.1) (Table 1). Two dimensional contour plots and cross~~  
6 ~~sectional profiles of the lakes can be found in the Appendix of this paper (Figures A1 to A5).~~  
7 ~~Bathymetric records were also obtained for an additional eight lakes (Chetverova et al., 2013)~~  
8 ~~but are not included herein since temperature sensors were not installed.~~

9 ~~The topographic slope on the polygonal tundra (first terrace) is very low ( $< 5^\circ$ ). Aerial images~~  
10 ~~of Sa\_Lake\_2 and Sa\_Lake\_3 show submerged polygons beneath the water surface,~~  
11 ~~indicating that these lakes are likely to have been formed by the thawing of ground ice and ice~~  
12 ~~wedges and the subsequent merging of polygonal ponds. The shorelines adjacent to shallow~~  
13 ~~parts of these younger thermokarst lakes (with depths of 0–3 m) are very irregular and feature~~  
14 ~~protrusions of different shapes and sizes (Figures A1–A4). Where deeper sections ( $> 3$  m)~~  
15 ~~occur close to the shore the shorelines are smooth and the lakes tend to have an oval shape.~~  
16 ~~The profiles of thermokarst lakes tend to be V-shaped rather than flat-bottomed and the~~  
17 ~~thermokarst lakes investigated were up to 6.4 m deep. The deepest lake on this island, with up~~  
18 ~~to 11.6 m water depth, is Sa\_Lake\_4. It has an elongated shape and is one of three~~  
19 ~~interconnected lakes that occur in an abandoned channel of the Lena River (“oxbow” or~~  
20 ~~“perched” lakes; Figure A4). The largest monitored lake in this series of lakes was~~  
21 ~~Ku\_Lake\_1, located on sediments of the Pleistocene Ice Complex, which have a high ice~~  
22 ~~content. This lake is the largest of three residual lakes located within an alas that is more than~~  
23 ~~20 m deep. This thermokarst basin evolved in two phases (Morgenstern et al., 2013): in the~~  
24 ~~first phase the original large lake covering the entire basin drained abruptly through a~~  
25 ~~thermo-erosional valley at about 5.7 ka BP, leaving the  $> 20$  m deep alas with residual lakes;~~  
26 ~~this was then followed by thermokarst processes of varying intensity during the second phase~~  
27 ~~(5.7 ka BP to the present). This lake is an order of magnitude larger in surface area than the~~  
28 ~~other four thermokarst lakes investigated and, in contrast to those lakes on Samoylov Island,~~  
29 ~~has a regular oval shape, occurs within a basin with steep sides and has a smooth, flat~~  
30 ~~shoreline. The maximum water depth is about 3.6 m and the profile is flat-bottomed (Figure~~  
31 ~~A5).~~

### 3.3.2 Heat content

The ability of lakes to store and redistribute additional heat at seasonal time scales may affect the heat budget of adjacent permafrost areas at the landscape spatial scale. For this reason, we observe the thermal regime of tundra lakes to make inferences about their effect on heat exchange processes. Therefore, the heat content of each lake ( $H_l$ ) was calculated at hourly time steps from the thermal energy stored in a water column from the lake's surface to its maximum depth ( $z_{\max}$ ):

$$H_l = c_w \rho_w \int_0^{z_{\max}} T(z, t) dz \quad (1)$$

where  $c_w$  is the specific heat capacity of water,  $\rho_w$  is the freshwater density, and  $T$  is the temperature. The calculated heat budgets were divided into different time periods, as proposed by Wetzel (2001). The summer heat income is defined as the amount of heat required to raise the temperature of the lake from isothermal conditions at 4°C to the maximum observed depth-averaged summer temperature (summer heat content). The winter heat income is the amount of heat required to raise the temperature from the minimum temperatures to 4°C. The annual heat budget is the total amount of heat necessary to raise the water from the minimum temperature to maximum summer temperature. The winter heat income and the annual heat budget must include the latent heat of fusion for the ice cover, especially for high latitude lakes (Wetzel, 2001). The ice cover thickness was measured during May 2014 and varied slightly from 2 m (Sa\_Lake\_1, Sa\_Lake\_2) to 1.9 m (Sa\_Lake\_4). The ice cover in these lakes melts completely every summer so that freezing and melting energies usually balance out over a year. The timing of spring ice break-up extends from the first ice melt, through moat formation and drifting of the ice cover, to the complete disappearance of ice. It is defined herein as the time at which the temperatures from all sensors indicate isothermal conditions, with temperature differences from the bottom to the top of the water column of  $< 0.1^\circ\text{C}$  following the period of stratification that occurs during ice cover, i.e. the time at which the lake water becomes completely mixed. The ice formation in fall is defined by the start of stratification in lake temperatures, i.e. when temperature differences from bottom to top exceed  $0.1^\circ\text{C}$ . The uncertainties in these determined times are estimated to be  $\pm 5$  days and are based on comparison with (infrequently available) satellite data (Table 1).

1

### 2 **3.43.3 Modeling of lake thermodynamics**

3 FLake is a freshwater lake model (Mironov, 2005) aimed at predicting the vertical thermal  
4 structure and mixing conditions in lakes over periods ranging from a few hours to a few years.  
5 The model is based on a two-layer parametric representation of the evolving temperature  
6 profile in the water column and on the integrated heat and kinetic energy budgets. The upper  
7 mixed layer is treated as thermally homogeneous, while the structure of the stratified layer  
8 between the upper mixed layer and the bottom of the basin (the lake thermocline) is described  
9 using the concept of self-similarity (or assumed shape) of the temperature-depth curve. The  
10 same self-similarity concept is used to describe the temperature structure of the thermally  
11 active upper layer of bottom sediments (Golosov and Kirillin, 2010) and of the ice (Mironov  
12 et al., 2012). It should be noted that no change in water depth as a result of winter ice  
13 formation is included in the computation, and the water depth is therefore assumed to be  
14 constant. Precipitation is also not included as an input into the model and snow accumulation  
15 is therefore not computed. Visual observations confirm that the lakes are usually snow free  
16 due to the generally low snowfall (although a few areas with snow and hardened wind crusts  
17 occur locally), combined with high wind speeds blowing the snow away.

18 The following input data and settings were used for the lakes investigated in this study and  
19 tested with data for Sa\_Lake\_1, i.e. a lake depth of 4 m (93% of this lake has a water depth of  
20 not more than 4 m), a water optical light extinction coefficient of  $0.5 \text{ m}^{-1}$ , a 6 m thickness for  
21 the thermally active sediment layer beneath the lake, and a temperature at the bottom of the  
22 thermally active sediment layer of  $4.5^\circ\text{C}$ . Due to their very low contents of organic material  
23 and low levels of biological productivity the lakes are usually very clear: in shallow lakes (for  
24 example, Sa\_Lake\_3) the lake bottom is visible even at 2 m water depths. The thermal  
25 characteristics of the sediment are based on sediment temperatures measured beneath two  
26 lakes in the Lena River Delta (on the Bykovsky Peninsula; Grigoriev, 1993) and are discussed  
27 in the Sects. 4 and 5. Two temperature profiles were obtained in June 1984 for one shallow (1  
28 m) and one deep (5 m) lake, down to a sediment depth of 16 and 21 m below the lake bed,  
29 respectively. These temperature profiles are used as input for the model experiments since the

1 assumption of thermal equilibrium does not necessarily exist for the lakes in the permafrost  
2 landscape.

3 Two meteorological datasets were used to drive the model: (1) hourly data from the on-site  
4 weather station (air temperature at 2 m height, wind speed, humidity, and radiation  
5 components), and (2) 6-hourly NCEP/NCAR reanalysis data provided by the  
6 NOAA/OAR/ESRL PSD, Boulder, Colorado, USA (<http://www.esrl.noaa.gov/psd/>; Kalnay  
7 et al., 1996). The two driving datasets were compared and were found to be in good  
8 agreement with each other, having some discrepancies in the short wave radiation  
9 components (Figure 3). The modeled lake temperatures were nearly identical in both  
10 datasets (not shown), indicating that reanalysis data sets perform well for lake modeling in  
11 these remote areas, where on-site meteorological information is often limited. For further  
12 analysis we used the measured on-site meteorological dataset, which can be found in the  
13 supplementary material for this publication. The FLake model output parameters (water  
14 temperatures, ice cover thickness, bottom sediment heat flux) for one of the lakes  
15 (Sa\_Lake\_1) are compared for the time period 9 July 2009 to 29 July 2011 with the measured  
16 parameters in Sect. 4. The model was used to:

17 - validate the 1-dimensional modeling approach and qualify the main mechanisms governing  
18 features of the lake thermal regime, such as summer stratification, water-sediment heat  
19 exchange, and ice melt

20 - characterize the water-sediment heat exchange at annual time scales

21 - establish a relationship between the morphometry and summer stratification duration.

22  
23 The “Lake Analyzer” numerical tool (<http://lakeanalyzer.gleon.org/>; Read et al., 2011) was  
24 used to determine the dimensionless Wedderburn number (Wd), a quantitative measure of the  
25 balance between wind mixing and stratification that is important for describing the  
26 biogeochemical cycles of lakes (Spigel and Imberger 1980). A Wd number of 1 indicates a  
27 threshold value at which the wind shear brings the thermocline to the lake's surface along the  
28 upwind shoreline. For large Wedderburn numbers ( $\gg 1$ ) the buoyancy force is much greater  
29 than the wind stress suggesting strong vertical stratification. For small Wedderburn numbers  
30 ( $\ll 1$ ) the wind stress is much greater than the buoyancy force suggesting destruction of the



1 vertical thermal stratification in the lake. On-site weather data from hourly time series of  
2 water temperature, wind speed, and bathymetric data were used as model inputs for the  
3 calculation of  $W_d$ .

4

5

## 6 **4 Results**

### 7 **4.1 Lake thermal dynamics based on observations**

8 The following analyses were based on temperature and sensor depth (water depth) data  
9 collected over the course of three years (2009-2012) from the investigated lakes, covering a  
10 range of morphometric characteristics and located on two geomorphologically different  
11 terraces (consisting of sediments of the Pleistocene Ice Complex on Kurungnakh and a  
12 Holocene flood plain on Samoylov). The seasonal thermal dynamics are only discussed in  
13 detail for two of these lakes: Sa\_Lake\_1 which is a thermokarst lake, and Sa\_Lake\_4 which is  
14 a perched/oxbow lake (Figures 4 and 5; an animation of the daily temperatures of Sa\_Lake\_1  
15 is also provided in the supplement). These lakes were selected as they have the best data  
16 records, taking into account the temporal coverage and the total number of sensors in each  
17 lake profile. The seasonal temperature dynamics of the other lakes (Sa\_Lake\_2, Sa\_Lake\_3,  
18 and Ku\_Lake\_1) are illustrated in the Appendix of this paper (Figures A6-A8).

### 19 **4.2 Fall & winter**

20 During fall, cooling and complete mixing occurs at about the end of September resulting in  
21 isothermal conditions at 0°C immediately prior to ice cover formation (Figures 4 & 5). The  
22 ice cover growth can be briefly interrupted due to short-lived warming events during the fall  
23 (as was observed, for example, in late September and early October of 2008) but the ice cover  
24 then persists from October through to June (Figures 4b & 5c; Table 1). The water column  
25 becomes stratified following the formation of the ice cover and the initial isothermal  
26 conditions change so that lake-bottom temperatures are consistently warmer than those higher  
27 up in the water column (towards the water/ice interface). This bottom temperature  
28 development under ice, which involves rapid warming immediately after ice-cover formation  
29 followed by subsequent gradual cooling, takes place in all lakes but the rates of warming and

1 cooling vary (Figures 4b, 5c, A6-8). In Sa\_Lake\_1 the maximum vertical temperature  
2 gradient was less than  $1^{\circ}\text{C m}^{-1}$  (with a maximum of  $1^{\circ}\text{C m}^{-1}$ ) in the winter of 2010/2011 and  
3 decreased over the course of the winter (Figure 4b). In Sa\_Lake\_4, the maximum temperature  
4 gradient was less than  $0.2^{\circ}\text{C m}^{-1}$  and, in contrast, increased over the course of the winter  
5 (Figure 5c). The waters in both lakes remained stratified during the winter, with gradual  
6 overall cooling of the stratified profile continuing until the end of winter.

### 7 **4.3 Spring**

8 The snow cover on the tundra landscape was usually very thin during the winter ( $< 0.5$  m) and  
9 had usually thawed by the end of May or early June. Field observations during a number of  
10 spring field campaigns showed that the frozen surfaces of the lakes were normally kept snow-  
11 free by wind action. It is interesting to note that the under-ice warming of the water column  
12 (Figures 4b, 5c) started as early as the beginning of March (e.g., in 2012), when air  
13 temperatures were still well below  $0^{\circ}\text{C}$ , as a result of strong solar radiation input through the  
14 ice. A temperature increase of about  $4^{\circ}\text{C}$  over the 6 week period prior to ice break-up is equal  
15 to an energy input of about  $30\text{ W m}^{-2}$ . With solar radiation returning after the polar night, the  
16 shortwave net radiation on the ice surface is about  $50\text{ W m}^{-2}$  in March and increases to about  
17  $300\text{ W m}^{-2}$  by the end of May or the beginning of June (Figure 3b). The net shortwave  
18 radiation penetrating to the water column is thus reduced by about 15-20% as a result of  
19 transmission through the ice cover. Radiation can penetrate to great water depths depending  
20 on the optical properties of the lake water: ~~Assuming with a~~ light extinction in the water  
21 column ~~of to be~~  $0.5\text{ m}^{-1}$ , about 13% of the radiation penetrating the ice cover (or  $\sim 4\text{ W m}^{-2}$ )  
22 will reach the lake floor beneath 4 m of water. The solar ~~radiation-radiative~~ heating of the  
23 water (still below its maximum density at  $4^{\circ}\text{C}$ ) and subsequent convective mixing effectively  
24 reduced the temperature gradient beneath the ice cover to less than  $0.5^{\circ}\text{C m}^{-1}$  for Sa\_Lake\_1  
25 and less than  $0.1^{\circ}\text{C m}^{-1}$  for Sa\_Lake\_4 (Figures 4b & 5c), this being a well-known  
26 mechanism in ice-covered fresh water lakes during spring (Mironov et al., 2002; Kirillin et  
27 al., 2012). Continued solar radiation and air temperature warming induce lake ice melt, which  
28 can also be accelerated by high wind speeds. For example, in 2009 the ice cover on  
29 Sa\_Lake\_1 was observed to drift, break-up, shrink, and then disappear, over the course of just  
30 a few days due to strong, warm winds. Satellite radar observations from 2011 show that the  
31 ice cover break-up occurred over a period of about 10 days from the beginning of June,

1 starting with the formation of a moat. On 10<sup>th</sup> June all lakes had an ice cover with a moat (i.e.  
2 an unfrozen ring close to the shoreline); on 21<sup>st</sup> June, Sa\_Lakes 1, 2, and 3 were ice free but  
3 the largest and deepest lakes (Ku\_Lake\_1 and Sa\_Lake\_4) still had 40-50% ice cover (Table  
4 1). Complete mixing of the water, as indicated by the first isothermal conditions after the  
5 winter stratification (Table 1), had already occurred during the early part of ice break-up  
6 (Table 1; Figures 4b, 5c). The lakes were usually ice free by the middle or end of June (Table  
7 1).

8 Seasonal flooding by the Lena River was an additional process that had an important effect on  
9 the water temperatures in Sa\_Lake\_4 (which was formed in a former river channel) and  
10 Sa\_Lake\_1. River ice break-up and flooding took place at the end of May in all three years,  
11 when the lakes were still ice covered (Table 1). Lena River temperatures recorded over a  
12 complete year (2009-2010) showed that the river temperatures remained around 0°C during  
13 the winter, warmed up briefly for about 2 days to a peak temperature of 1.1°C (31 May 2010)  
14 and then cooled again to 0°C before steadily increasing thereafter to reach a maximum of  
15 19.4°C on 20 July 2010 (Figure 5a). Radiative under-ice warming and convection in  
16 Sa\_Lake\_4 continued until lake ice break-up in 2010, but this spring under-ice warming was  
17 interrupted in both 2011 and 2012 by intense flooding with cold Lena River water, as  
18 indicated by both the temperature profiles and the water depth data (Figure 5b). The water  
19 level in this lake rose by about 1 m over the course of a few hours (28-29 May 2011 & 27-28  
20 May 2012), returning to the original level within 4-5 days. Concomitant with water level rise  
21 in Sa\_Lake\_4, the water temperatures fell to 0°C in the upper sensors (immediately beneath  
22 the ice). Lake\_Sa\_1 was also connected to the river during the flood events, as can be  
23 recognized by the slight increase in water depth at the end of May in 2010 and 2011 (no water  
24 depth data are available for 2012), but the increase was less than in Sa\_Lake\_4 (< 10 cm  
25 variation; Figure 4a).

#### 26 **4.4 Summer**

27 During the summer months positive air temperatures and continuous heat input from solar  
28 radiation steadily raised the water temperatures of the lakes at all depths, until September.  
29 Heat input from net shortwave radiation supplied about 150 W m<sup>-2</sup> in mid-July (Figure 3).  
30 Maximum air temperatures occurred over very short (daytime) periods, reaching up to more

1 than 25°C. The highest air temperatures were recorded in July 2010, reaching a maximum of  
2 31.9°C on 5<sup>th</sup> July.

3 All of the lakes experienced short periods of thermal stratification during the summer, which  
4 varied both between the lakes and between the summers; the highest temperature gradient  
5 reached was about 5°C m<sup>-1</sup> in the deepest lake, Sa\_Lake\_4 (Figure 5). Maximum water  
6 temperatures of around 20°C were usually reached in mid-July, with up to 22°C recorded for  
7 the shallow lake (Sa\_Lake\_3). Mean monthly bottom temperatures during periods with no ice  
8 cover ranged between 4°C and 15°C (Figure 6), and can therefore be considerable higher  
9 during the summer than their annual means (Table 1).

10 The monthly bottom temperatures for some lakes were also warmer than the corresponding  
11 monthly air temperatures (Figure 6), confirming that radiation input is an important additional  
12 energy source, as well as effective mixing of the lake waters. Starting with colder mean  
13 bottom temperature in July, gradual warming creates warmest mean bottom temperatures in  
14 the deepest lake (Sa\_Lake\_4) in August and in the shallowest lake (Sa\_Lake\_3) in July. For  
15 all other lakes, maximum bottom temperatures occur either in July or August, depending on  
16 the timing of ice break up and the lake's seasonal energy balance.

17 The Wedderburn numbers are in agreement with the observed short periods of weak  
18 stratification during the ice-free period (Figures 4c, 5d). Remarkably, Wd remain rather low  
19 throughout the whole summer (between 1 and 8 for Sa\_Lake\_1 and Sa\_Lake\_4) and there are  
20 even short periods with Wd < 1. These Wd values indicate that buoyancy and wind stress  
21 were almost in equilibrium, suggesting favorable conditions for occasional upwelling of the  
22 thermocline along the upwind shorelines of the lakes, which would make an additional  
23 contribution to the mixing of water in the lakes and to the heat/mass exchange between the  
24 lakes and the atmosphere. During short periods with Wd < 1 the wind stress is much greater  
25 than the buoyancy, effectively destroying the thermal stratification.

#### 26 **4.5 Lake heat content**

27 The heat content in the investigated lakes at times varied by up to +/- 50 MJ m<sup>-2</sup> over just a  
28 few days (Figure 7), with the maximum heat content being reached at the end of July or in  
29 early August. The summer heat income of the lakes was of the order of 100 to 400 MJ m<sup>-2</sup> and  
30 had a linear relationship with their depths (see Equation 1). The winter heat income of the

1 lake water beneath the ice cover varied between 50 and 150 MJ m<sup>-2</sup>, not including the heat  
2 transfer associated with the formation of the ice cover. However, if a 2 m thick ice cover is  
3 taken into account (which is especially important for Arctic lakes; Wetzel, 2001), the annual  
4 heat budget can reach up to about 1 GJ m<sup>-2</sup> (Table 1).

5 Sa\_Lake\_4, which can be subjected to substantial seasonal flooding during spring, showed a  
6 reduction in heat content of about 100 MJ m<sup>-2</sup> (in 2010 and 2011) within a few hours, thus  
7 suppressing the ongoing radiative warming of the lake water. Although the Lena River carries  
8 a substantial amount of heat into its delta every year ( $\sim 0.49 * 10^{12}$  J s<sup>-1</sup>; Alekseevsky, 2007)  
9 due to very warm summer temperatures, the flooding of the lakes occurs when its  
10 temperatures are at their coldest.

#### 11 **4.6 Modeled seasonal lake thermal dynamics**

12 A comparative analysis of the modeling results and observational data has revealed the  
13 capabilities of, and flaws in, the use of one-dimensional modeling to reproduce the thermal  
14 dynamics of lakes formed on permafrost, as well as providing additional quantitative insights  
15 into the major mechanisms governing the seasonal thermal dynamics of Siberian lakes. The  
16 FLake model results for the Sa\_Lake\_1 over a period of 2 years (2009-2011) have been in  
17 overall good agreement with on-site observations with regard to seasonal variations in lake  
18 temperatures, the mean and maximum temperatures in winter and summer, and the durations  
19 of the open water and ice cover seasons (Figure 8a-c).

20 To quantify the model performance for thermokarst lakes we applied standard measures (e.g.  
21 Thiery et al., 2014) of the model's ability to reproduce the observed mean temperature ( $T_m$ ),  
22 the standard deviation ratio ( $SD_{model}/SD_{obs}$ ), the centered root mean squared error (RMSEc),  
23 and the Pearson correlation coefficient ( $r$ ). In contrast to other lake model evaluations using  
24 surface temperature  $T_s$  (for example, from African and West European lakes), we used  $T_m$   
25 since no temperature probes were installed at the surface due to the seasonal ice cover. FLake  
26 demonstrated good performance with regard to the mean lake temperature. The statistics—  
27 Pearson correlation coefficient  $r = 0.97$ ,  $SD_{model}/SD_{obs}$  1.28, RMSE 1.49 °C are slightly worse  
28 than those reported previously for temperate lakes ( $r = 0.988$ ; Stepanenko et al., 2010) and  
29 better than FLake performance on deep tropical lakes ( $r = 0.78$ ,  $SD_{model}/SD_{obs}$  1.25, RMSE  
30 0.75 °C; Thiery et al., 2014). The model reproduced summer stratification during the ice free

1 period ( $r = 0.93$ ,  $SD_{\text{model}}/SD_{\text{obs}} 1.25$ ,  $RMSE 1.82$  °C). Solar heating of the water below the ice  
2 is not included in the model and thus the agreement between model and observations is lower  
3 during the ice-covered period ( $r = -0.42$ ,  $SD_{\text{model}}/SD_{\text{obs}} 0.37$ ,  $RMSE 0.66$  °C). The resulting  
4 uncertainties in the ice break up prediction affect also the model performance with regard to  
5 the lake heat content at the beginning of the open water period in early summer (Figure 8). As  
6 thermal dynamics under the ice cover are crudely reproduced by the majority of 1-  
7 dimensional lake models used in coupled climate modeling systems (Stepanenko et al., 2010),  
8 estimation of the role played by thermokarst lakes in regional climate requires integration of a  
9 cost-effective and physically sound sub-model of winter lake thermodynamics into lake  
10 parameterization schemes for climate models (e.g. Oveisy and Boegman 2014).

#### 12 **4.6.1 Open water period and summer stratification**

13 The duration of the warming and cooling periods, as well as the mean water temperatures  
14 during the autumn cooling, are well simulated by the model suggesting that the model  
15 adequately captures the net heat storage of the lakes. The model was also able to reproduce  
16 the development of weak thermal stratification in summer (i.e. the short periods during which  
17 the bottom temperatures differed from the mean temperatures of the lakes in June and July,  
18 2010 and 2011: Figure 8c). The largest discrepancies in the water temperatures produced by  
19 the model occurred during the period of spring warming, with maximum deviations of about  
20 6°C from the measured mean temperatures (Figure 8). These deviations can be explained by  
21 the ice break-up being modeled too early, with subsequent early warming of the lake. Lake  
22 temperatures were consequently consistently overestimated during the warming period in  
23 2010.

#### 24 **4.6.2 Ice duration and thickness, and water temperatures beneath the ice** 25 **cover**

26 The mean rate of ice growth modeled with FLake was about  $0.92 \text{ cm day}^{-1}$  for 2010  
27 (minimum  $0.021 \text{ cm day}^{-1}$ , maximum  $8 \text{ cm day}^{-1}$ ) and  $0.89 \text{ cm day}^{-1}$  for 2011 (minimum  
28  $0.026 \text{ cm day}^{-1}$ , maximum  $4.6 \text{ cm day}^{-1}$ ), with the maximum thickness of ice cover remaining  
29 below 2 m. The modeled ice thickness of no more than 2 m agrees well with the temperature  
30 data from the sensor located 4 m above the sediment (approximately 2 m from the lake

1 surface) in Sa\_Lake\_1 (Figure 4b). This sensor did not record any freezing in 2010 or 2011,  
2 but in 2012 the sensor froze into the lake ice (Figure 4b), recording sub-zero temperatures and  
3 thus indicating thicker ice ( $> 2$  m) in 2012.

4 The modeled melting of the ice cover in spring and subsequent warming of lake temperatures  
5 is, in general, well reproduced by the model. The measured development of under-ice bottom  
6 temperatures (with warming following the onset of ice cover formation, followed by a later  
7 winter cooling) is only partly reproduced in the modeled results due to rather simplified  
8 parameterization of the under-ice thermodynamics in the FLake model, with a linear vertical  
9 temperature profile in the ice-covered water column and no solar radiation penetrating the ice  
10 cover.

### 11 **4.6.3 Thermal properties of the lake sediments and water-sediment heat flux**

12 Heat conduction from a lake's water column to the underlying sediment is a key  
13 thermodynamic process for understanding the role of lakes in the permafrost landscape. The  
14 Flake model incorporates simulation of seasonal temperature variations within the thermally  
15 active sediment layer, based on an assumption of thermal equilibrium in the sediment over  
16 longer-than-seasonal time scales (i.e. a constant temperature beneath the seasonally thermally  
17 active sediment layer, ensuring zero mean annual flux across the water-sediment boundary;  
18 Golosov and Kirillin, 2010). Since this thermal equilibrium does not necessarily exist in lakes  
19 on permafrost, we performed two separate model experiments with different thermal  
20 conditions beneath the lakes, based on temperature profiles measured in lake sediments at  
21 comparable sites in the Lena River Delta (Grigoriev 1993; Figure 9). ~~Two temperature  
22 profiles were obtained in June 1984 for one shallow (1 m) and one deeper (5 m) lake, down to  
23 a sediment depth of up to 20 m.~~ While the sediment temperature beneath the shallow lake fell  
24 to below  $0^{\circ}\text{C}$  at about 2 m depth and reached  $-6^{\circ}\text{C}$  at 15 m depth, the temperatures beneath  
25 the deeper lake indicated an unfrozen layer to about 25 m depth, with a maximum temperature  
26 of about  $4.5^{\circ}\text{C}$  at a depth of about 3 m beneath the lake floor (Figure 9 a, b). The reported  
27 temperatures at depth, where seasonal variations were minimal, ranged from  $-6^{\circ}\text{C}$  beneath the  
28 1 m deep lake to  $4^{\circ}\text{C}$  beneath the 5 m deep lake. Using the measured temperature profile  
29 below the 5 m deep lake, the thickness of the sediment layer with appreciable seasonal  
30 variations in temperature was estimated to be  $\sim 6$  m (Figure 9 b). The FLake modeled heat flux  
31 at the lake-sediment boundary for different ground temperatures revealed two characteristic

1 seasonal patterns of lake-permafrost heat exchange: the flux across the frozen sediment  
2 beneath the shallow lake was directed downwards during the summer, with a magnitude of up  
3 to  $4 \text{ W m}^{-2}$ , the fast release of ~~the~~ heat from the sediment during autumn cooling, and the  
4 water-sediment heat flux of  $\sim 0 \text{ W m}^{-2}$  during the entire ice-covered period (Figure 9 c). This  
5 seasonal pattern suggests an annually positive heat budget of the under-lake ground and  
6 thawing of the permafrost, which is continuously heated by the lake above. For a lake with  
7 deep temperatures approaching  $4^\circ\text{C}$ , the annual mean flux across the sediment tended towards  
8 zero, with maximum downward fluxes in summer of  $3 \text{ W m}^{-2}$ , a maximum of  $7 \text{ W m}^{-2}$  heat  
9 released back into the water column during early freeze back, and a continuous low rate of  $< 1$   
10  $\text{W m}^{-2}$  during the ice-covered winter (Figure 9 d). In the absence of any additional  
11 information available on the ground temperatures under Sa\_Lake\_1, the latter case was  
12 adopted for the longer model run (Figures 8b, c), with an “equilibrium state” suggesting little  
13 or no permafrost thawing beneath the lake. The maximum modeled heat flux at the sediment-  
14 water interface was about  $4 \text{ W m}^{-2}$  into the sediment (in summer) and about  $7 \text{ W m}^{-2}$  (to  
15 almost zero) from the sediment into the water column during the ice-covered period. The  
16 rapidly changing (negative) hourly heat fluxes during the fall cooling period were due to rapid  
17 cooling of the water column, which could not be reproduced by the model.

18 Overall, the calculated energy density for the lake with mean annual water temperature of  $3^\circ\text{C}$   
19 is about  $65 \text{ MJ m}^{-3}$ , thus more than six times the amount for the permafrost soil of about  $10$   
20  $\text{MJ m}^{-3}$ . Lakes are therefore effective for energy storage compared to the frozen landscape,  
21 and the fraction of landscape covered by thermokarst lakes has the potential to significantly  
22 affect the land-atmosphere energy exchange.

23

24

## 25 **5 Discussion**

26 Lakes can be considered to represent “hot spots” in the permafrost landscape. This study has  
27 demonstrated that the investigated lakes remain unfrozen throughout the winter and have  
28 mean bottom water temperatures (between  $2.7$  to  $4.0^\circ\text{C}$ ) that are significantly warmer than the  
29 mean annual air temperature ( $\sim -13^\circ\text{C}$ ) or the permafrost temperature ( $-9.2^\circ\text{C}$  at  $10.7 \text{ m}$   
30 depth). This is in agreement with observations made by Jorgenson et al. (2010) who reported



1 thermokarst lake-bottom temperatures in Alaska that were up to 10°C warmer than the mean  
2 annual air temperatures. Harris (2002) attributed the anomalously high mean annual  
3 temperature in a shallow lake in western Canada to convective heat exchange and the  
4 absorption of radiation through the water column. Mean annual lake-bottom temperatures in  
5 northern Alaska also showed a similar range of values (Arp et al. 2012; CALON), and this  
6 range has therefore been used in previous modeling studies to estimate the development of  
7 talik (Burn, 2002; Ling and Zhang, 2003). Differences in heat content are related to  
8 morphometric parameters, particularly to water depth. Burn (2002) found mean annual lake-  
9 bottom temperatures of between 1.5°C and 4.8°C for the deeper pools in tundra lakes on  
10 Richards Island (north-western Canada). Ensom et al. (2012) reported mean annual bottom  
11 temperatures of between 3.4°C and 5.5°C from a number of lakes and channels in the  
12 Mackenzie Delta (Canada) and computed that 60% of the lakes maintained taliks.

13 Mean bottom lake temperatures, which ranged between 2.7 and 4 °C in this study, depend on  
14 lake depth and are important for constraining future numerical modeling experiments on talik  
15 development. -Our study also confirms previous findings that there is a “critical lake depth”  
16 (lake depth > winter ice cover ~~depth~~ thickness) for water to remain unfrozen beneath the ice  
17 cover (Arp et al., 2012; Burn, 2002). All lakes in this study had a depth > 3 m, which exceeds  
18 the maximum ice thickness of about 2 m.

19 The bottom temperatures in the lakes varied significantly between summer and winter but  
20 their annual mean temperatures and temperature dynamics were similar despite the range of  
21 morphometric and geomorphological characteristics. The Wd numbers indicated that the lakes  
22 were all well-mixed during the summer periods, and it can therefore be assumed that both  
23 heat and dissolved gases, in particular, oxygen, are effectively transported through the water  
24 column. This assumption is supported by the measured oxygen concentrations in these lakes,  
25 which ranged between 8 and 10 mg l<sup>-1</sup>, and the lack of any detected vertical stratification (R.  
26 Osudar, personal communication, 2015).

27 We observed and simulated short stratification periods in summer in the studied lakes  
28 (Figures 4 & 5). These stratification events are probably the major physical factor affecting  
29 biogeochemical processes in lakes. In particular, the duration of the thermal stratification in  
30 summer affects the concentration and vertical distribution of dissolved oxygen. Longer  
31 summer stratification provokes deep anoxia and favors methanogenesis in the deep water

1 [column and upper sediment \(Golosov et al., 2012\). Under equal climatic forcing, lake depth is](#)  
2 [the primary factor determining the duration of summer stratification \(the second one being the](#)  
3 [water transparency, Kirillin, 2010\). Sensitivity model runs with the lake depth varying in the](#)  
4 [range 2-12 m using the same meteorological input data from Samoylov demonstrated that](#)  
5 [lakes in this climatic zone with mean depths >5 m should have dimictic stratification regimes,](#)  
6 [i.e. develop continuous stratification in summer with a duration of 1 month or longer \(Figure](#)  
7 [10\). This also supports the observation of summer stratification in deeper \(> 6 m\) Alaskan](#)  
8 [thermokarst lakes \(Sepulveda-Jáuregui et al., 2015\). In lakes of about 8 m depth or more, the](#)  
9 [summer stratification duration significantly increases since high thermal inertia prevents](#)  
10 [vertical mixing during the autumn cooling in August-September \(Figure 11\).](#)

11 The summer heat budgets of Arctic lakes are much smaller than those of low-latitude lakes.  
12 The only previously reported summer heat budget for an Arctic lake (Chandler Lake, Alaska)  
13 was  $240 \text{ MJ m}^{-2}$ , which lies in the same range as the heat budgets in this study (Wetzel, 2001).  
14 In contrast, the summer heat budget for a large lake such as Lake Superior on the Canada-  
15 USA border is much larger at about  $1.3 \text{ GJ m}^{-2}$ . In comparison, the annual heat budget of  
16 Lake Baikal in Siberia is estimated to be about  $2.7 \text{ GJ m}^{-2}$  (Wetzel, 2001). The total annual  
17 heat budget for all of the investigated lakes (including the latent heat of the ice cover)  
18 amounts up to about  $1 \text{ GJ m}^{-2}$  (Table 1). In view of the large proportion of land covered by  
19 water bodies in this landscape (25%) and the volumes of water that they contain, their energy  
20 storage and turnover within the permafrost landscape are of considerable significance.  
21 Furthermore, changes in the heat content of lakes occur much more rapidly than changes in  
22 the heat content of the surrounding permafrost soils as a result of efficient energy absorption  
23 and effective mixing. In contrast, progressive deepening of the seasonally thawing upper layer  
24 of permafrost (the active layer) [of the polygonal tundra landscape at this site](#) takes several  
25 months and only reaches a maximum thaw depth of about 0.6 m (Boike et al., 2013). Lakes  
26 also have an important effect on the subsurface thermal conditions beneath the lake and  
27 potentially also in the surrounding permafrost. Our results show that, during the summer, heat  
28 is continuously transferred from lake water into the bottom sediment. The importance of  
29 summer heat gain and its dissipation into the water body and the underlying sediment was  
30 first discussed by Vtyurina (1960), using data from a 12 m deep lake in Siberia. Her findings  
31 showed heat fluxes directed into the sediments during winter (Figure 5 in Vtyurina, 1960; also

1 reported in Grosse et al., 2013) which, according to our findings, is an indicator of permafrost  
2 thaw. Our modeling results, however, suggest that the temperature increase associated with  
3 permafrost thaw eventually results in a net annual heat equilibrium between deeper lakes and  
4 the underlying sediments, characterized by a continuous negative heat flux (i.e. heat loss from  
5 the sediment into the water column) during the long ice-covered winter and heat gain by the  
6 sediment during the open water summer period. The warming of lake-bottom temperatures  
7 with the onset of ice cover was initially attributed by Brewer (1958) to heating by shortwave  
8 solar radiation ~~warming and by Mortimer and Mackereth (1958) to the heat release from the~~  
9 ~~lake sediment. Our results support an important contribution from solar heating in the heat~~  
10 ~~budget of the water column under ice, especially in spring, and suggest that radiation can also~~  
11 ~~make a significant direct contribution to sediment heating in shallow and clear water~~  
12 ~~thermokarst lakes—a contribution that is usually neglected in lake models.~~

13 Our observed near-bottom temperatures increased beneath the ice cover and the modeling  
14 experiments suggested this warming was solely due to heat flow from the sediment, with  
15 typical rates of  $< 10 \text{ W m}^{-2}$ . However, the heat flux from the sediment in tundra lakes appears  
16 to decay within less than one month, which is much faster than in ice-covered lakes of the  
17 temperate and boreal climates (cf. Rizk et al. 2014), and is followed by a gradual decrease of  
18 the deep water temperatures. The latter is not reproduced by the parameterized sediment  
19 module of FLake.

20  
21 Our numerical modeling of the thermal dynamics of lakes has shown that the basic processes  
22 can be accurately reproduced for the summer. However, the model parameters that yielded the  
23 best fit for the seasonal heat budget and ice cover duration resulted in less accurate predictions  
24 of the bottom temperature under ice.— Lake temperatures increase, starting in spring 1-2  
25 months before ice-off, apparently by radiative solar heating. This temperature increase  
26 suggests that radiation can make a significant direct contribution to sediment heating in  
27 shallow and clear-water thermokarst lakes – a contribution that is usually neglected in lake  
28 models. The warming of the bottom water in fall during ice cover formation and the  
29 subsequent cooling were not accurately reproduced. The concept of self-similarity cannot  
30 account for the permafrost-talik specific lake processes, such as (i) warming of bottom waters  
31 immediately following onset of ice formation and (ii) phase change in the lake's frozen

1 | sediment, i.e. annual freeze thaw processes and thawing at the talik-permafrost boundary.

2 | While the short period of warming of bottom water is due to heat flux from the sediment into  
3 | the water body, the cooling in winter from mid-winter onwards suggests a loss of heat. This  
4 | heat loss may occur through transmission into both the sediment and the atmosphere, the  
5 | latter being of minor importance due to isolation of the water column by the ice cover. Further  
6 | investigations into these processes of warming and subsequent gradual cooling under the ice  
7 | cover would require a more advanced lake model that is able to take into account deep,  
8 | continuously frozen sediments and characteristic processes such as thawing.

## 10 | **6 Summary and conclusions**

11 | We have measured and modeled the thermal dynamics of lakes in the Lena River Delta of  
12 | northern Siberia over a three year period (2009-2012), with the objective of understanding  
13 | and quantifying the important thermal processes that operate in this permafrost environment.  
14 | The investigated lakes were situated in two different geomorphologic settings (sediments of  
15 | the Pleistocene Ice Complex and on a younger river terrace) with a range of morphometric  
16 | characteristics. Some of the lakes were seasonally connected to the Lena River through high  
17 | floods that occurred during spring. Such annual flooding of these lakes by cold river water  
18 | results in a significant reduction in the ongoing warming (and thus sensible heat storage),  
19 | depending on the magnitude of the flooding. A schematic summary of our results is provided  
20 | in Figure 120.

21 | The lakes were shown to receive substantial energy for warming from net shortwave radiation  
22 | during the summer,; such warming-Warming also occurs during the ice cover period in spring,  
23 | resulting in convective mixing beneath the ice cover. Mixing also occurs following ice break-  
24 | up, during the summer, and during the fall cooling, resulting in efficient heat transfer to  
25 | bottom waters and across the sediment-water interface. Numerical modeling suggests that the  
26 | annual mean net heat flux across the bottom sediment boundary is approximately zero, with  
27 | positive summer downward fluxes during the ice-free period (4 months) and heat-release back  
28 | into the water column at much lower rates during the ice-covered period (8 months). Overall,  
29 | the ice formation and thaw together account for most of the annual variations in a lake's heat  
30 | content. Furthermore, their timing and durations determine the magnitude and direction of  
31 | bottom sediment heat fluxes and the timing of water column mixing. Future warming may

1 result in changes to the ice cover but may also produce more pronounced summer  
2 stratification, thus potentially reducing the heat input into the sediment layers.

3 In view of the large area covered by water bodies in permafrost landscapes (25% of the land  
4 surface) and their efficiency at energy absorption and mixing, these water bodies are clearly  
5 of considerable importance with respect to energy storage and turnover, atmospheric fluxes,  
6 and sediment heat fluxes in permafrost landscapes.

7 The investigated thermokarst lakes are representative of Arctic tundra lowlands characterized  
8 by thermokarst processes that are common for large regions in Central and East Siberia,  
9 Interior and Northern Alaska as well as Northwest Canada. –Despite their importance,  
10 however, lakes are not yet included in earth system models. Future work should therefore  
11 include lakes in these models and test their sensitivity to possible future changes in climate.

12

13 Author contributions: J. Boike designed the research and led the discussions, supported by G.  
14 Kirilin and M.Langer. The FLake modeling was carried out by G. Kirilin and C. Georgi. The  
15 paper was written by J.Boike, with comments from all authors.

16

17 Acknowledgements: The logistical support provided by the Russian Research station on  
18 Samoylov Island is gratefully acknowledged. Field support, including data collection, was  
19 provided by Grigoriy Soloviev, Waldemar Schneider, Günther Stoof, and Karoline  
20 Wischnewski. Elizabeth Miller, Max Heikenfeld, Wil Lieberman-Cribbin and Stephan Lange  
21 assisted with the data analysis and helpful discussions. The authors acknowledge the financial  
22 support provided through the European Union's FP7-ENV PAGE21 project under contract  
23 number GA282700, and through the Feodor Lynen grant from the Alexander-von-Humboldt  
24 Foundation awarded to Moritz Langer. The research was carried out under the Russian  
25 government's Program of Competitive Growth, Kazan Federal University.

## 1 **References**

- 2 Alekseevsky, N. I. (Ed.): Geocological state of Russian Arctic coast and their safety of  
3 nature management (in Russian), GEOS Publ., Moscow, Russia, 586 pp., 2007.
- 4 Abnizova, A., Siemens, J., Langer, M., and Boike, J.: Small ponds with major impact: The  
5 relevance of ponds and lakes in permafrost landscapes to carbon dioxide emissions, *Global*  
6 *Biogeochem. Cycles*, 26, GB2041, doi: 10.1029/2011gb004237, 2012.
- 7 Alerstam, T., Gudmundsson, G. A., Green, M., and Hedenström, A.: Migration along  
8 orthodromic sun compass routes by arctic birds, *Science*, 291, 300-303, 2001.
- 9 Are F. E.: Thermal regime of small thermokarst lakes in the Siberian Taiga zone (for example  
10 of Central Yakutia) (in Russian), Collection of papers "Lakes of Cryolithozone of Siberia",  
11 edited by: Are F.E., Nauka, Siberian brunch, 98-116, 1974.
- 12 Arp, C. D., Jones, B. M., Whitman, M., Larsen, A., and Urban, F. E.: Lake Temperature and  
13 Ice Cover Regimes in the Alaskan Subarctic and Arctic: Integrated Monitoring, Remote  
14 Sensing, and Modeling, *J. Am. Water Resour. Assoc.*, 46, 777-791, doi: 15, 10.1111/j.1752-  
15 1688.2010.00451.x, 2010.
- 16 Arp, C. D., Jones, B. M., Lu, Z., and Whitman, M. S.: Shifting balance of thermokarst lake  
17 ice regimes across the Arctic Coastal Plain of northern Alaska, *Geophys. Res. Lett.*, 39, doi:  
18 10.1029/2012gl052518, 2012.
- 19 Boike, J., Wille, C., and Abnizova, A.: Climatology and summer energy and water balance of  
20 polygonal tundra in the Lena River Delta, Siberia, *J. Geophys. Res.*, 113, G03025,  
21 doi:10.1029/2007JG000540, 2008.
- 22 Boike, J., Kattenstroth, B., Abramova, K., Bornemann, N., Chetverova, A., Fedorova, I.,  
23 Fröb, K., Grigoriev, M., Grüber, M., Kutzbach, L., Langer, M., Minke, M., Muster, S., Piel,  
24 K., Pfeiffer, E. M., Stoof, G., Westermann, S., Wischnewski, K., Wille, C., and Hubberten, H.  
25 W.: Baseline characteristics of climate, permafrost and land cover from a new permafrost  
26 observatory in the Lena River Delta, Siberia (1998-2011), *Biogeosciences*, 10, 2105-2128,  
27 doi: 10.5194/bg-10-2105-2013, 2013.
- 28 Burn, C. R.: Tundra Lakes and Permafrost, Richards Island, Western Arctic Coast, Canada,  
29 *Canadian Journal Earth Science*, 39, 1281-1298, doi:10.1139/E02-035, 2002.

1 Burn, C. R.: Lake-bottom Thermal Regimes, Western Arctic Coast, Canada, Permafr.  
2 Periglac. Proc., 16, 355–367, doi: 10.1002/PPP.542, 2005.

3 Brewer, M. C.: The thermal regime of an arctic lake, EOS Transactions ,American  
4 Geophysical Union, 39, 2, 278-284, doi: 10.1029/TR039i002p00278, 1958: Costard, F., and  
5 Gautier, E.: The Lena River: Hydromorphodynamic Features in a Deep Permafrost Zone, in:  
6 Large Rivers: Geomorphology and Management, edited by: Gupta, A., John Wiley & Sons,  
7 Ltd, West Sussex, England, 225-233, 2007.

8 Chetverova, A., Fedorova, I., Potapova, T., Boike, J.: Hydrological and geochemical features  
9 of lakes of Samoylov Island of the Lena River Delta./ Proceedings of AARI, № 1 (95), 97-  
10 110, 2013 (in Russian).

11 Ensom, T. P., Burn, C. R., and Kokelj, S. V.: Lake- and channel-bottom temperatures in the  
12 Mackenzie Delta, Northwest Territories, Can. J. Earth Sci., 49, 16, 963-978, doi:  
13 10.1139/e2012-001, 2012.

14 Fedorova, I., Chetverova, A., Bolshiyarov, D., Makarov, A., Boike, J., Heim, B.,  
15 Morgenstern, A., Overduin, P. P., Wegner, C., Kashina, V., Eulenburg, A., Dobrotina, E., and  
16 Sidorina, I.: Lena Delta hydrology and geochemistry: long-term hydrological data and recent  
17 field observations, Biogeosciences, 12, 345-363, doi: 10.5194/bg-12-345-2015, 2015.

18 Golosov, S., and Kirillin, G.: A parameterized model of heat storage by lake sediments,  
19 Environ. Model. Software, 25, 793-801, doi: 10.1016/j.envsoft.2010.01.002, 2010.

20 ~~Golosov, S., Terzhevik, A., Zverev, I., Kirillin, G. and Engelhardt, C.: Climate change~~  
21 ~~impact on thermal and oxygen regime of shallow lakes. Tellus A, 64, 17264, doi:~~  
22 ~~10.3402/tellusa.v64i0.17264, 2012.~~

23 Gordeev, V. V., and Sidorov, I. S.: Concentrations of major elements and their outflow into  
24 the Laptev Sea by the Lena River, Marine Chemistry, 43, 33-45, 1993.

25 Grigoriev, M.: Cryomorphogenesis of the Lena River mouth area (in Russian), Siberian  
26 Branch, USSR Academy of Sciences, Yakutsk, 176 pp., 1993.

27 Grigoriev, N. F.: The temperature of permafrost in the Lena delta basin–deposit conditions  
28 and properties of the permafrost in Yakutia (in Russian), Yakutsk, 2, 97-101, 1960.

1 Grigoriev, N. F. Perennially frozen rocks of the maritime lowlands of Yakutia (in Russian),  
2 Moscow, Nauka, 80, pp, 1966.

3 Grosse, G., Jones, B., and Arp, C. D.: Thermokarst Lakes, Drainage, and Drained Basins, in:  
4 Treatise on Geomorphology, edited by Giardino, R. & Harbor, J., 8 Glacial and Periglacial  
5 Geomorphology, 29, 325-353, Academic Press, San Diego, CA, doi: 10.1016/B978-0-12-  
6 374739-6.00216-5, 2013.

7 Harris, S. A.: Causes and consequences of rapid thermokarst development in permafrost or  
8 glacial terrain, *Permafr. Periglac. Proc.*, 13, 237-242, doi: 10.1002/ppp.419, 2002.

9 Hinkel, K. M., Lenters, J. D., Sheng, Y., Lyons, E. A., Beck, R. A., Eisner, W. R., Maurer, E.  
10 F., Wang, J., and Potter, B. L.: Thermokarst Lakes on the Arctic Coastal Plain of Alaska:  
11 Spatial and Temporal Variability in Summer Water Temperature, *Permafr. Periglac. Proc.*, 23,  
12 207-217, doi: 10.1002/ppp.1743, 2012.

13 Hobbie, J. E., and Kling, G. W.: Alaska's changing Arctic: Ecological consequences for  
14 tundra, streams, and lakes, Oxford University Press, 352 pp., 2014.

15 Jeffries, M. O., Zhang, T., Frey, K., and Kozlenko, N.: Estimating Late-Winter Heat Flow to  
16 the Atmosphere from the Lake-Dominated Alaskan North Slope, *Journal Glaciology*, 45, 315-  
17 347, 1999.

18 Jorgenson, M. T., Romanovsky, V., Harden, J., Shur, Y., O'Donnell, J., Schuur, E. A. G.,  
19 Kanevskiy, M., and Marchenko, S.: Resilience and vulnerability of permafrost to climate  
20 change, *Canadian Journal of Forest Research*, 40, 1219-1236, doi: 10.1139/x10-060, 2010.

21 Kalnay, E., Kanamitsu, M., Kistler, R., Collins, W., Deaven, D., Gandin, L., Iredell, M., Saha,  
22 S., White, G., Woollen, J., Zhu, Y., Leetmaa, A., Reynolds, R., Chelliah, M., Ebisuzaki, W.,  
23 Higgins, W., Janowiak, J., Mo, K. C., Ropelewski, C., Wang, J., Jenne, R., and Joseph, D.:  
24 The NCEP/NCAR 40-Year Reanalysis Project, *Bull. Am. Meteorol. Soc.*, 77, 437-471, 1996.

25 Keatley, B. E., Douglas, M. S. V., and Smol, J. P.: Physical and chemical limnological  
26 characteristics of lakes and ponds across environmental gradients on Melville Island,  
27 Nunavut/N.W.T., High Arctic Canada, *Fundamental and Applied Limnology - Archiv für*  
28 *Hydrobiologie*, 168, 355–376, doi: 10.1127/1863-9135/2007/0168-0355, 2007.



- 1 [Kirillin, G.: Modeling the impact of global warming on water temperature and seasonal](#)  
2 [mixing regimes in small temperate lakes. \*Boreal Environ. Res.\*, 15, 279-293, 2010.](#)  
3
- 4 Kirillin, G., Leppäranta, M., Terzhevik, A., Granin, N., Bernhardt, J., Engelhardt, C.,  
5 Efremova, T., Golosov, S., Palshin, N., and Sherstyankin, P.: Physics of seasonally ice-  
6 covered lakes: a review, *Aquat. Sci.*, 74, 659-682, 2012.
- 7 Lachenbruch, A. H.: Mechanics of thermal contraction cracks and ice-wedge polygons in  
8 permafrost, *Special papers*, 70, Geological Society of America, New York, 69 pp., 1962.
- 9 Langer, M., Westermann, S., Muster, S., Piel, K., and Boike, J.: The surface energy balance  
10 of a polygonal tundra site in northern Siberia Part 1: Spring to fall, *The Cryosphere*, 5, 151-  
11 171, doi: 10.5194/tc-5-151-2011, 2011a.
- 12 Langer, M., Westermann, S., Muster, S., Piel, K., and Boike, J.: The surface energy balance  
13 of a polygonal tundra site in northern Siberia - Part 2: Winter, *The Cryosphere*, 5, 509-524,  
14 doi: 10.5194/tc-5-509-2011, 2011b.
- 15 Langer, M., Westermann, S., Heikenfeld, M., Dorn, W., and Boike, J.: Satellite-based  
16 modeling of permafrost temperatures in a tundra lowland landscape, *Remote Sensing of*  
17 *Environment*, 135, 12-24, doi: 10.1016/j.rse.2013.03.011, 2013.
- 18 Langer, M., Westermann, S., Walter Anthony, K., Wischnewski, K., and Boike, J.: Frozen  
19 ponds: production and storage of methane during the Arctic winter in a lowland tundra  
20 landscape in northern Siberia, Lena River delta, *Biogeosciences*, 12, 977-990, doi:  
21 10.5194/bg-12-977-2015, 2015.
- 22 Laurion, I., Vincent, W.F., Retamal, L., Dupont, C., Francus, P., MacIntyre, S. & Pienitz, R.:  
23 Variability in greenhouse gas emissions from permafrost thaw ponds. *Limnology and*  
24 *Oceanography* 55, 115-133, 2010.
- 25 Lehner, B., and Döll, P.: Development and validation of a global database of lakes, reservoirs  
26 and wetlands, *Journal of Hydrology*, 296, 1-22, 2004.
- 27 Ling, F., and Zhang, T.: Numerical simulation of permafrost thermal regime and talik  
28 development under shallow thaw lakes on the Alaskan Arctic Coastal Plain, *J. Geophys. Res.*,  
29 108, 4511, doi: 10.1029/2002JD003014, 2003.

1 Luecke, C., Giblin, A. E., Bettez, N. D., Burkart, G. A., Crump, B. C., Evans, M. A., Gettel,  
2 G., McIntyre, S., O'Brien, W. J., Rublee, P. A., and King, G. W.: The response of lakes near  
3 the Arctic LTER to environmental change, in: Alaska's changing Arctic: ecological  
4 consequences for tundra, streams, and lakes, edited by: Hobbie, J., and Kling, G. W., Oxford  
5 University Press, New York, 238-286, 2014.

6 [Martynov, A., Sushama, L. and Laprise, R.: Simulation of temperate freezing lakes by one-](#)  
7 [dimensional lake models: performance assessment for interactive coupling with regional](#)  
8 [climate models. Boreal Environ. Res., 15\(2\), 143-164, 2010.](#)

9 Martynov, A., Sushama, L., Laprise, R., Winger, K., and Dugas, B.: Interactive lakes in the  
10 Canadian Regional Climate Model, version 5: the role of lakes in the regional climate of  
11 North America, Tellus A, 64, 16226, doi: 10.3402/tellusa.v64i0.16226, 2012.

12 Mironov, D. V., Terzhevik, A., Kirillin, G., Jonas, T., Malm, J., and Farmer, D.: Radiatively  
13 driven convection in ice-covered lakes: Observations, scaling, and a mixed layer model,  
14 Journal of Geophysical Research: Oceans, 107, 7, 1-16, doi: 10.1029/2001JC000892, 2002.

15 Mironov, D. V.: Parameterization of lakes in numerical weather prediction. Description of a  
16 lake model, COSMO technical report, 2005.

17 Mironov, D., B. Ritter, J.-P. Schulz, M. Buchhold, M. Lange, and E. Machulskaya:  
18 Parameterization of sea and lake ice in numerical weather prediction models of the German  
19 Weather Service. Tellus A, 64, 17330. doi: 10.3402/tellusa.v64i0.17330, 2012 Morgenstern,  
20 A., Grosse, G., Günther, F., Fedorova, I., and Schirrmeister, L.: Spatial analyses of  
21 thermokarst lakes and basins in Yedoma landscapes of the Lena Delta, The Cryosphere, 5,  
22 849-867, 10.5194/tc-5-849-2011, 2011.

23 Morgenstern, A., Grosse, G., Günther, F., Fedorova, I., and Schirrmeister, L.: Spatial analyses  
24 of thermokarst lakes and basins in Yedoma landscapes of the Lena Delta, The Cryosphere, 5,  
25 849-867, doi:10.5194/tc-5-849-2011, 2011.

26 Morgenstern, A., Ulrich, M., Günther, F., Roessler, S., Fedorova, I. V., Rudaya, N. A.,  
27 Wetterich, S., Boike, J., and Schirrmeister, L.: Evolution of thermokarst in East Siberian ice-  
28 rich permafrost: A case study, Geomorphology, 201, 363-379, doi:  
29 10.1016/j.geomorph.2013.07.011, 2013.

- 1 [Mortimer, C. and Mackereth F: Convection and its consequences in ice-covered lakes. Verh](#)  
2 [Int Ver Limnol, 13, 923–932, 1958.](#)  
3
- 4 Muster, S., Langer, M., Heim, B., Westermann, S., and Boike, J.: Subpixel heterogeneity of  
5 ice-wedge polygonal tundra: a multi-scale analysis of land cover and evapotranspiration in the  
6 Lena River Delta, Siberia, *Tellus B*, 64, 17301, doi: 10.3402/tellusb.v64i0.17301, 2012.
- 7 Nolan, M., and Brigham-Grette, J.: Basic hydrology, limnology, and meteorology of modern  
8 Lake El'gygytgyn, Siberia, *J. Paleolimnol.*, 37, 17-35, doi: 10.1007/s10933-006-9020-y,  
9 2006.
- 10 [Oveisy, A. and Boegman, L.: One-dimensional simulation of lake and ice dynamics during](#)  
11 [winter. J. Limnol., 73, doi: 10.4081/jlimnol.2014.903, 2014.](#)
- 12 Pavlov A.V., Tishin M.I.: Heat balance of a large lake and surrounding area in central Yakutia  
13 (in Russian), Collection of papers "Structure and thermal regime of frozen rocks", edited by:  
14 Katasonova E.G., Pavlov A.V., Nauka, Siberian branch, 53-62 1981.
- 15 Pienitz, R., Smol, J. P., and Lean, D. R. S.: Physical and Chemical limnology of 59 lakes  
16 located between the southern Yukon and the Tuktoyaktuk Peninsula, Northwest Territories  
17 (Canada), *Can. J. Fish. Aquat. Sci.*, 54, 330-346, 1997.
- 18 Rawlins, M. A., Serreze, M. C., Schroeder, R., Zhang, X., and McDonald, K. C.: Diagnosis of  
19 the record discharge of Arctic-draining Eurasian rivers in 2007, *Environmental Research*  
20 *Letters*, 4, 1-8, 2009.
- 21 Read, J. S., Hamilton, D. P., Jones, I. D., Muraoka, K., Winslow, L. A., Kroiss, R., Wu, C. H.,  
22 and Gaiser, E.: Derivation of lake mixing and stratification indices from high-resolution lake  
23 buoy data, *Environ. Model. Software*, 26, 1325-1336, doi: 10.1016/j.envsoft.2011.05.006,  
24 2011.
- 25 [Rizk, W., Kirillin, G. and Leppäranta, M.: Basin-scale circulation and heat fluxes in ice-](#)  
26 [covered lakes. Limnol. Oceanogr., 59, 445-464, 2014.](#)
- 27 [Sepulveda-Jauregui, A., Walter Anthony, K. M., Martinez-Cruz, K., Greene, S., and](#)  
28 [Thalasso, F.: Methane and carbon dioxide emissions from 40 lakes along a north–south](#)

- 1 [latitudinal transect in Alaska, \*Biogeosciences\*, 12, 3197-3223, doi:10.5194/bg-12-3197-2015,](#)  
2 [2015.](#)
- 3 Schertzer, W. M.: Freshwater Lakes, in: Surface climates of Canada, edited by: Bailey, W. G.,  
4 Oke, T. R., and Rouse, W. R., McGill-Queens University Press, Montreal, 124-148, 1997.
- 5 Schneider von Deimling, T., Grosse, G., Strauss, J., Schirrmeister, L., Morgenstern, A.,  
6 Schaphoff, S., Meinshausen, M., and Boike, J.: Observation-based modelling of permafrost  
7 carbon fluxes with accounting for deep carbon deposits and thermokarst activity, *Biogeosci.*  
8 *Disc.*, 11, 16599-16643, doi: 10.5194/bgd-11-16599-2014, 2014.
- 9 Schwamborn, G., Rachold, V., and Grigoriev, M. N.: Late Quaternary sedimentation history  
10 of the Lena Delta, *Quat. Int.*, 89, 119-134, doi: 10.1016/S1040-6182(01)00084-2, 2002.
- 11 Sobiech, J., Boike, J., and Dierking, W.: Observation of melt onset in an Arctic Tundra  
12 landscape using high resolution TerraSAR-X and RADARSAT-2 data, IGARSS, Munich,  
13 Germany, 3552–3555, 2012.
- 14 Spigel, R. H., and Imberger, J. The classification of mixed-layer dynamics of lakes of small  
15 to medium size. *Journal of physical oceanography*, 10(7), 1104-1121, 1980.
- 16 Stefan, J.: Über die Theorie der Eisbildung, insbesondere über die Eisbildung im Polarmeere,  
17 *Annalen der Physik*, 278, 269-286, 1891.
- 18 [Stepanenko, V.M., Goyette, S., Martynov, A., Perroud, M., Fang, X. and Mironov, D.: First](#)  
19 [steps of a lake model intercomparison Project: LakeMIP. \*Bor. Environ. Res.\*, 15, 191-202,](#)  
20 [2010.](#)
- 21 [Thiery, W., Stepanenko, V. M., Fang, X., Jöhnk, K. D., Li, Z., Martynov, A., Perroud, M.,](#)  
22 [Subin, Z. M., Darchambeau, F., Mironov, D., and van Lipzig, N. P. M.: LakeMIP Kivu:](#)  
23 [evaluating the representation of a large, deep tropical lake by a set of one-dimensional lake](#)  
24 [models, 2014, doi: 10.3402/tellusa.v66.21390, 2014.](#)
- 25 Vincent, A. C., Mueller, D. R., and Vincent, W. F.: Simulated heat storage in a perennially  
26 ice-covered high Arctic lake: Sensitivity to climate change, *J. Geophys. Res.*, 113, C04036,  
27 doi: 10.1029/2007JC004360, 2008.
- 28 Vincent, W.F., Pienitz, R., Laurion, I. and Walter Anthony, K.: Climate impacts on Arctic  
29 lakes. In: Goldman, C.R., Kumagai, M. and Robarts, R.D. (eds). *Climatic Change and Global*

- 1 Warming of Inland Waters: Impacts and Mitigation for Ecosystems and Societies, John Wiley  
2 & Sons, Ltd, Chichester, U.K., 27-42, 2013.
- 3 Vtyurina, E. A.: Temperature regime of the Lake Glubokoe Trudy institute merzlotovedeniya  
4 im. V.A. Obrucheva. AN SSSR, Moscow, 132-140, 1960 (in Russian).
- 5 Walsh, S. E., Vavrus, S. J., Foley, J. A., Fisher, V. A., Wynne, R. H., and Lenters, J. D.:  
6 Global Patterns of Lake Ice Phenology and Climate: Model Simulation and Observation, J.  
7 Geophys. Res., 103, 28, 825-828, 1998.
- 8 Walter, K. M., Zimov, S. A., Chanton, J. P., Verbyla, D., and Chapin III, F. S.: Methane  
9 bubbling from Siberian thaw lakes as a positive feedback to climate warming, Nature, 443,  
10 71-75, doi: 10.1038/nature05040, 2006.
- 11 Welch, H. E., and Bergmann, M. A.: Water circulation in small arctic lakes in winter, Can. J.  
12 Fish. Aquat. Sci., 42, 506-520, 1985.
- 13 Wetterich, S., Schirrmeister, L., Meyer, H., Andreas, F. A., and Mackensen, A.: Arctic  
14 freshwater ostracods from modern periglacial environments in the Lena River Delta (Siberian  
15 Arctic, Russia): geochemical applications for palaeoenvironmental reconstructions, J.  
16 Paleolimnol., 39, 427-449, doi: 10.1007/s10933-007-9122-1, 2008.
- 17 Wetzel, R. G.: Limnology: lake and river ecosystems, 3rd ed., Gulf Professional Publishing,  
18 Orlando, 1006 pp., 2001.
- 19 Yi, S., Wischnewski, K., Langer, M., Muster, S., and Boike, J.: Freeze/thaw processes in  
20 complex permafrost landscapes of northern Siberia simulated using the TEM ecosystem  
21 model: impact of thermokarst ponds and lakes, Geoscientific Model Development, 7, 1671-  
22 1689, doi: 10.5194/gmd-7-1671-2014, 2014.
- 23

1 Table 1. Physical and chemical characteristics of the studied lakes in the Lena River Delta,  
 2 Siberia

	Sa_Lake_1	Sa_Lake_2	Sa_Lake_3	Sa_Lake_4	Ku_Lake_1
Area [m <sup>2</sup> ]	39,541	39,991	23,066	47,620	1,730,000 <sup>a</sup>
Max. depth [m]	6.4	5.7	3.4	11.6	3.6 <sup>a</sup>
Mean depth [m]	3	3.1	1.2	4.5	2.4
Volume [m <sup>3</sup> ]	106,500	103,600	18,800	175,121	3,321,000
Volume/Area [m]	2.7	2.6	0.8	3.7	1.8
Perimeter [m]	1,931	1,471	1,760	1,474	5,170 <sup>a</sup>
Period of data collection	04 July 2009 - 07 Aug. 2012	10 July 2009 - 07 Aug. 2012	13 July 2009 - 14 Aug. 2012	06 July 2009 - 06 Aug. 2012	24 July 2009 - 29 July 2010
Location	126.486 E, 72.373 N	126.496 E, 72.378 N	126.511 E, 72.374 N	126.505 E, 72.369 N	126.177 E, 72.328 N
Start of ice cover formation (temp. diff. from bottom to top > 0.1°C)	05 Oct. 2009 01 Oct. 2010 02 Oct. 2011	1 Oct. 2009 28 Sep. 2010 05 Oct. 2011	04 Oct. 2009 30 Sep. 2010 26 Sep. 2011	04 Oct. 2009 28 Sep. 2010 4 Oct. 2011	04 Oct. 2009 02 Oct. 2010
Start of ice cover break-up (temp.	04 July 2009 14 June 2010	12 July 2009 23 June 2010	24 June 2009 14 June 2010	07 July 2009 20 June 2010	24 July 2009 20 June 2010

diff. from bottom to top > 0.1°C)	08 June 2011	16 June 2011	10 June 2011	20 June 2011	
	15 June 2012	15 June 2012	10 June 2012	21 June 2012	
% ice cover (satellite radar data <sup>b)</sup> 2011	5 June:100%	5 June: 100%	5 June: 100%	5 June: 95%	5 June: 95%
	10 June: 95%	10 June: 100%	10 June: 90%	10 June: 95%	10 June: 95%
	16 June: 85%	16 June: 90%	16 June: ice free	16 June: 85%	16 June: 90%
	21 June: ice free	21 June: ice free		21 June: 50%	21 June: 40%
					27 June: ice free
2012	27 June: ice free	27 June: ice free	27 June: ice free	27 June: ice free	05 June: 90%
					27 June: ice free
Mean annual bottom temperature [°C] (2010-2011)	3.7	3.6	2.7	2.9	4.0
Winter lake water heat budget [MJ m <sup>-2</sup> ]	93	66	44	145	61
Summer lake water heat budget [MJ m <sup>-2</sup> ]	140	206	161	340	112
Annual lake heat budget	[233]	[272]	[205]	[485]	[173]
	838	877	810	1090	778

[MJ m<sup>-2</sup>]

(2010-2011)

c, d

Residence time [years] <sup>e</sup>	14	14	4	24	9
Electrical conductivity [μS cm <sup>-1</sup> ]	140 <sup>f</sup>	127 <sup>f</sup>	64 <sup>i</sup>	185 <sup>f</sup> 59 <sup>g</sup> 80 <sup>h</sup>	30 <sup>i</sup>
pH-value <sup>f</sup>	6.99 <sup>f</sup>	6.82 <sup>f</sup>	7.3 <sup>i</sup>	6.95 <sup>f</sup> 7.36 <sup>g</sup> 7.28 <sup>h</sup>	7.64 <sup>i</sup>

---

1

2 <sup>a</sup> data provided in Morgenstern et al. (2011, 2013) and <http://doi.pangaea.de/10.1594/PANGAEA.848485>

3 <sup>b</sup> Sobiech et al. (2012) & TerraSar-X data (copyright: DLR, 2011) where available with sufficiently high  
4 resolution

5 <sup>c</sup> numbers in brackets represent the total annual lake water budget (sensible heat), without taking into account the  
6 latent heat of ice cover formation

7 <sup>d</sup> includes latent heat for the formation of a 2 m ice cover (605 MJ m<sup>-2</sup>)

8 <sup>e</sup> residence time  $F = V/E$ ; roughly approximated by the ratio of the lakes's volume ( $V$ ) divided by the sum of  
9 evapotranspiration ( $E$ ) and runoff  $R$  ( $F = V/(E-R)$ ; Schertzer 1997). Within the study area, the annual  
10 evapotranspiration is about ~190 mm and runoff is to be negligible within the overall water balance (Boike et al.,  
11 2013)

12 <sup>f</sup> mean value for ice-covered period (April – May 2014)

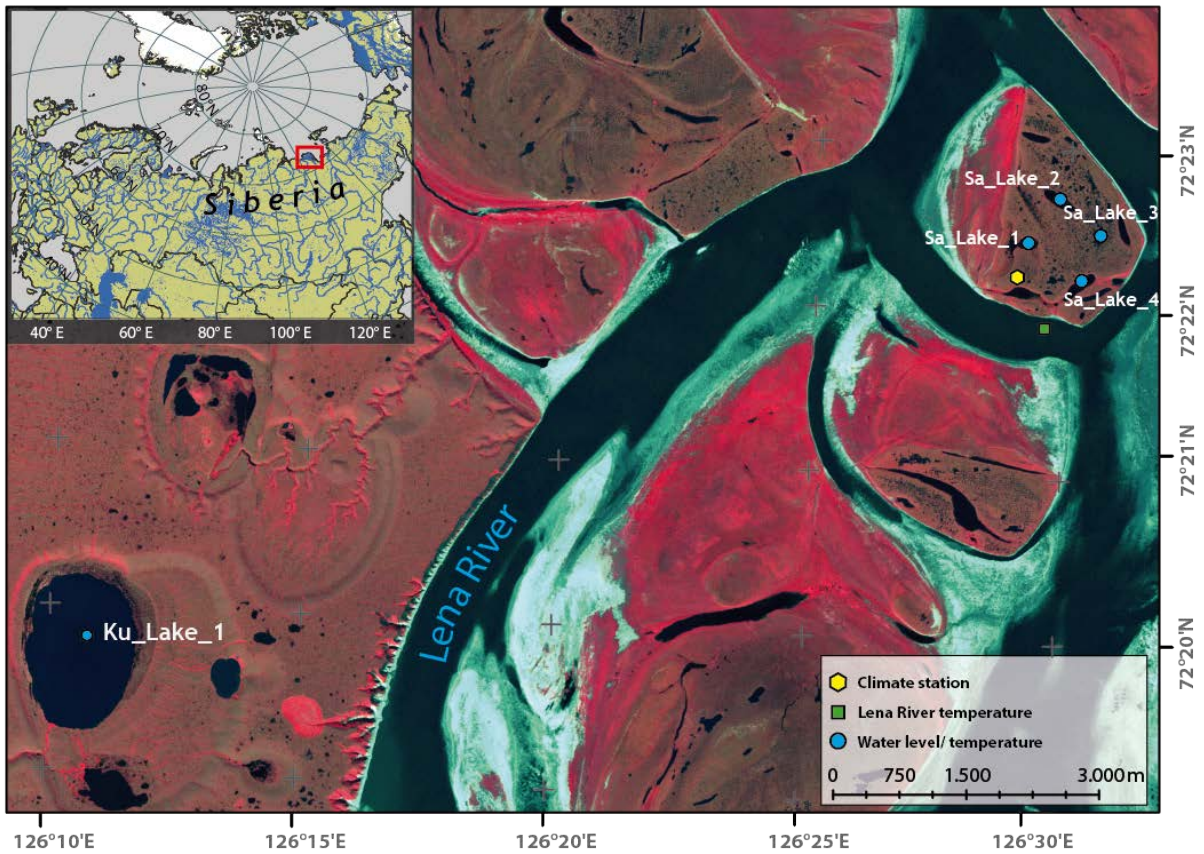
13 <sup>g</sup> mean value for the Lena River flood period (May – June 2014)

14 <sup>h</sup> mean value for summer period (July – August 2014)

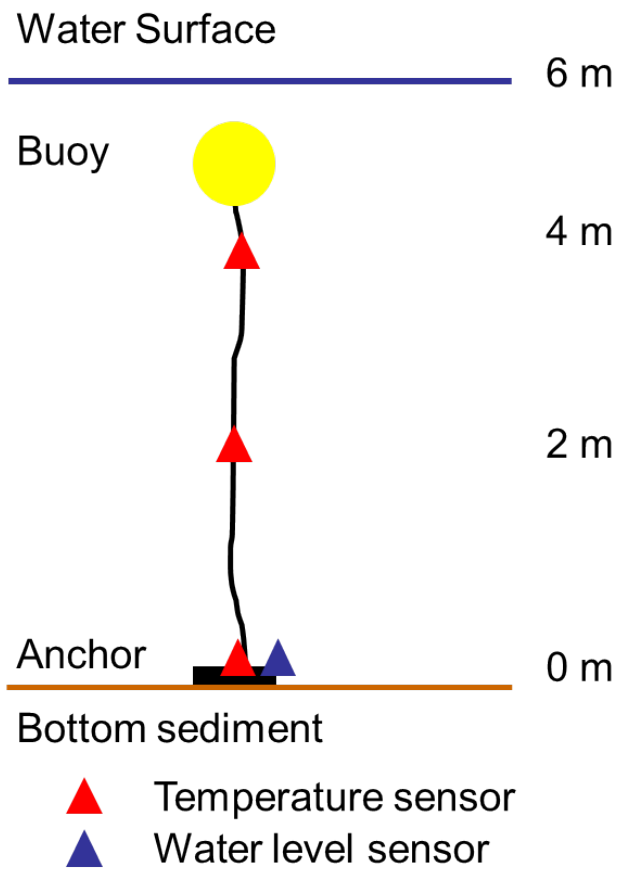
15 <sup>i</sup> mean value for summer period (measured in July 2009)

16



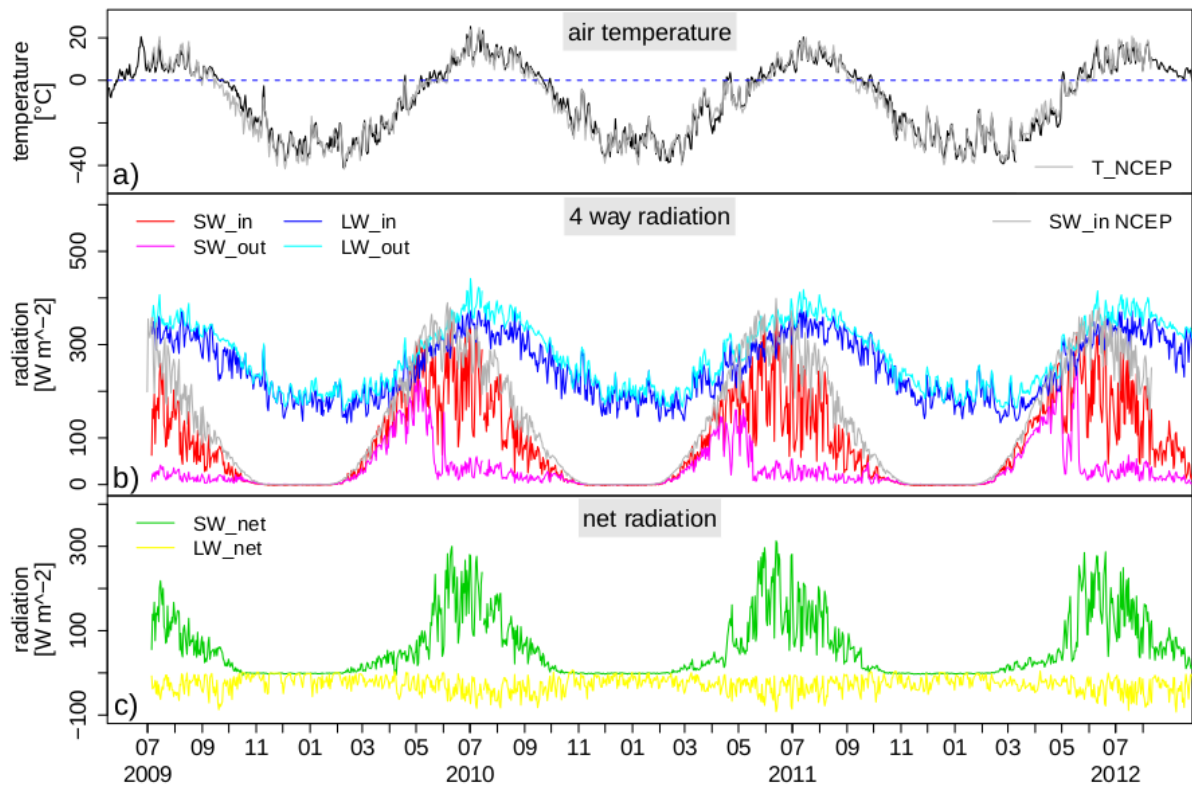


1 126°10'E 126°15'E 126°20'E 126°25'E 126°30'E  
 2 Figure 1. Location of the study sites in the Lena River Delta of eastern Siberia; sites are  
 3 within the zone of continuous permafrost on the islands of Kurungnakh (Ku\_Lake\_1), and  
 4 Samoylov (Sa\_Lakes\_1-4). [The insert map](#) shows the location of the Lena River Delta in  
 5 northern Eurasia and the distribution of lakes (Global lakes and wetland map; Lehner and  
 6 Döll, 2004).



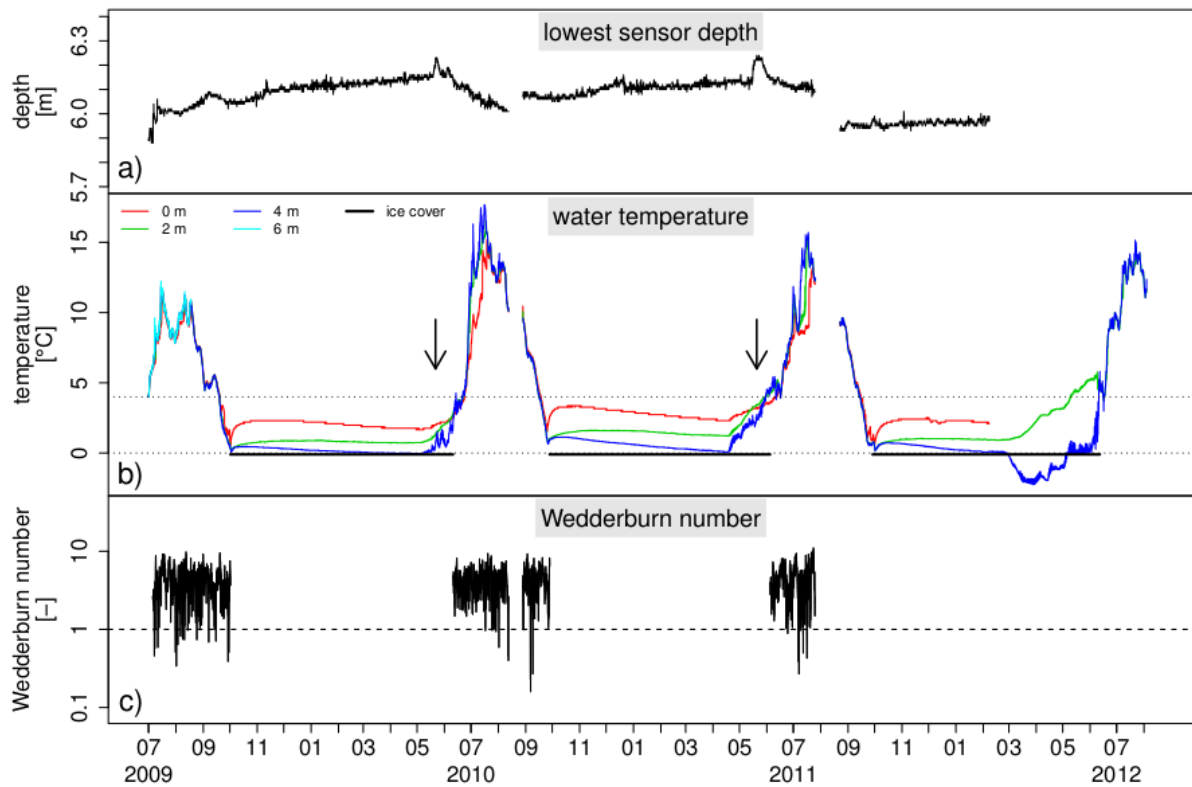
1

2 Figure 2. Schematic diagram showing the positions of sensors within the water column. To  
 3 prevent freezing of the buoy within the ice cover (maximum 2 m thick), sensors were  
 4 deployed 2 m below the water surface in most lakes. The water level sensor was located just  
 5 above the bottom sensor, referred to in Figures 4 & 5 as the “lowest sensor depth”.



1

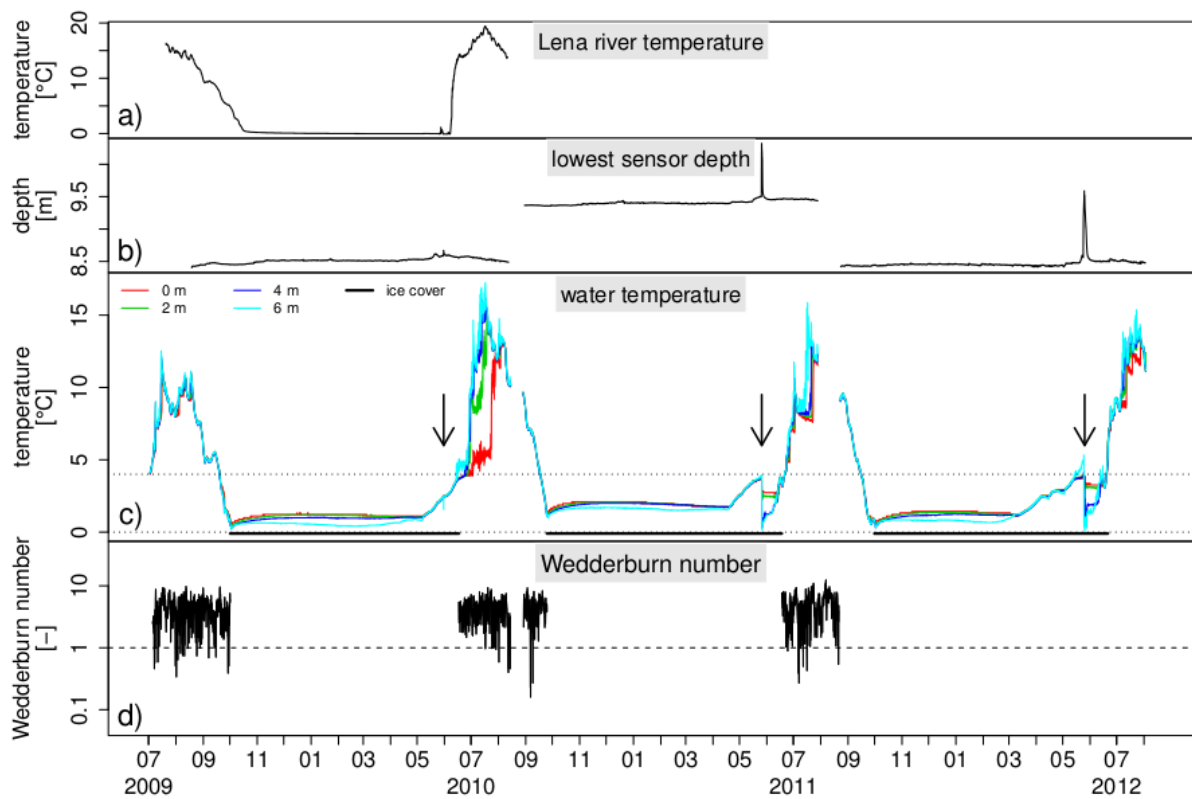
2 Figure 3. a) Mean daily air temperature at 2 m above ground level from Samoylov and NCEP;  
 3 b) radiation balance (Samoylov) and shortwave incoming radiation (NCEP); c) net shortwave  
 4 and longwave radiation (Samoylov) and radiation balance measured at the Samoylov climate  
 5 station July 2009 - August 2012.



1

2 Figure 4. Hourly physical characteristics for Sa\_Lake\_1, July 2009 - August 2012. a) depth of  
 3 bottom lake sensor as an indicator of water level changes; b) water temperatures and ice cover  
 4 duration; c) Wedderburn number (dimensionless), calculated for the ice free period only.

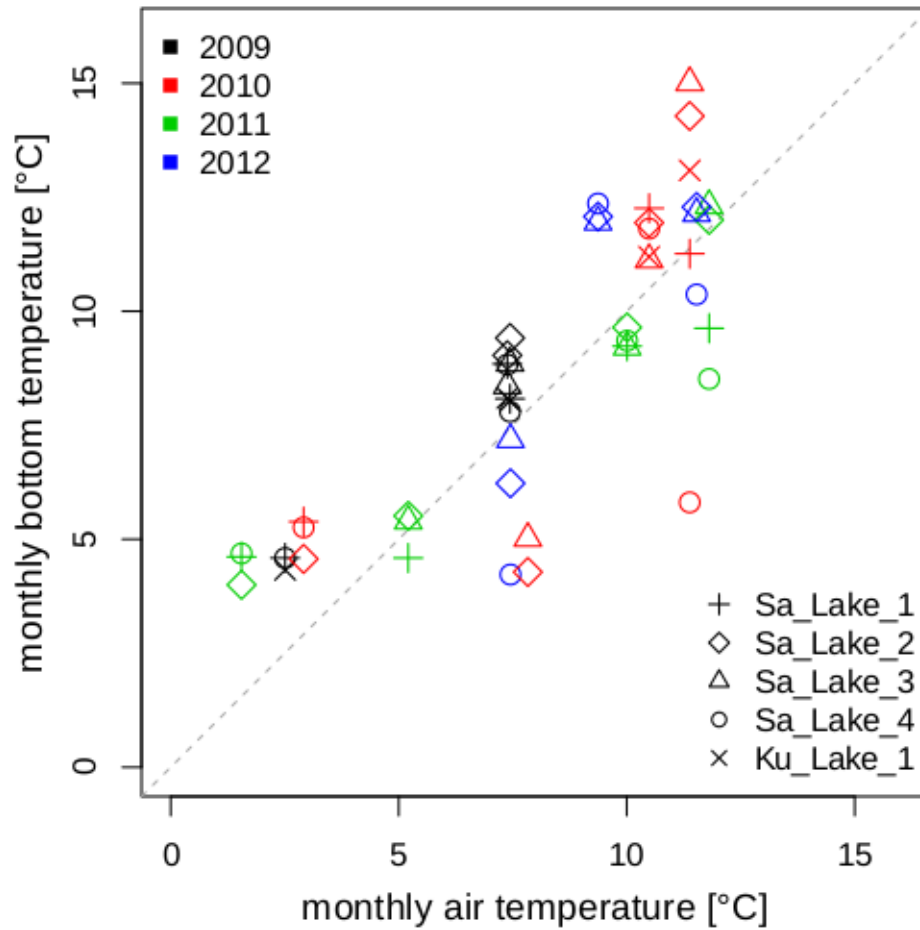
5 | Arrows indicate the timing of the lake's seasonal flooding by Lena river water.



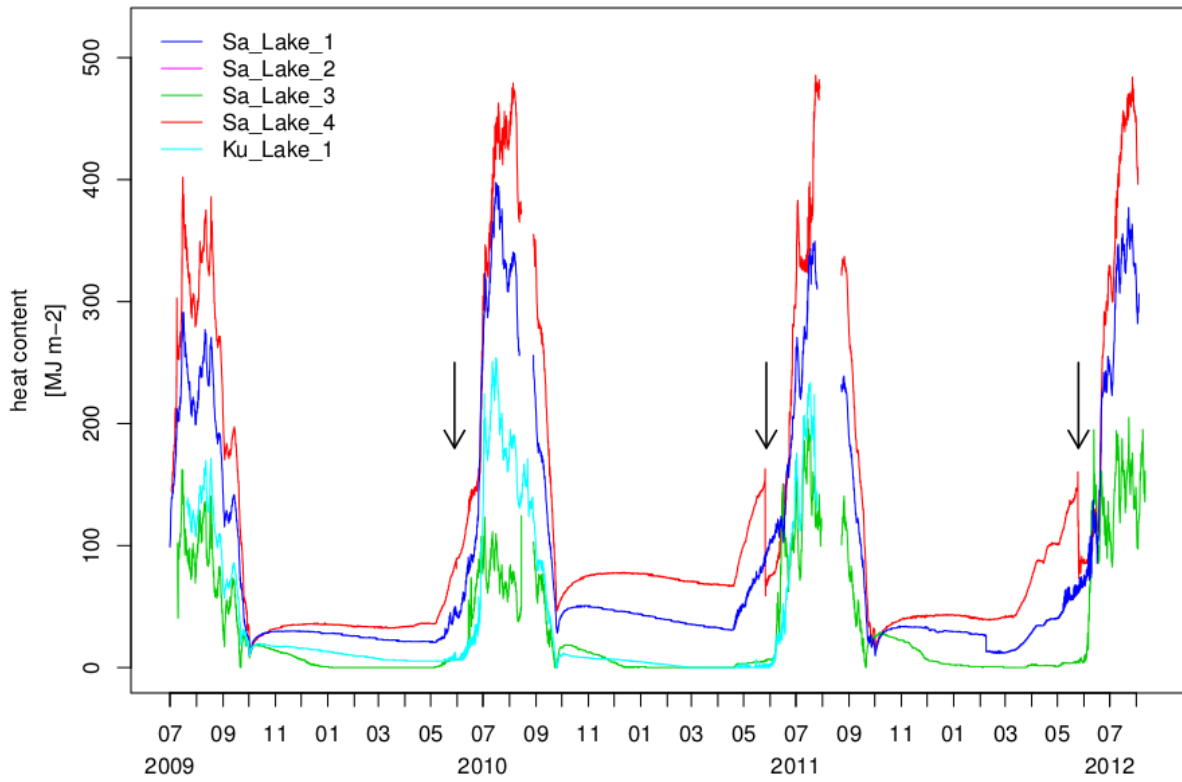
1

2 Figure 5. a) Hourly temperatures for the Lena River from July 2009 to July 2010, and for  
 3 Sa\_Lake\_4 (July 2009-August 2012): b) depth of bottom sensor as indicator for water level  
 4 changes: sharp increase in depth during May 2011 and 2012 indicates flooding with Lena  
 5 River water; c) water temperatures and ice cover duration (estimated from lake water  
 6 temperatures); d) Wedderburn number (dimensionless) calculated for the ice-free period.

7 Arrows indicate the timing of the lake's seasonal flooding by Lena river water.

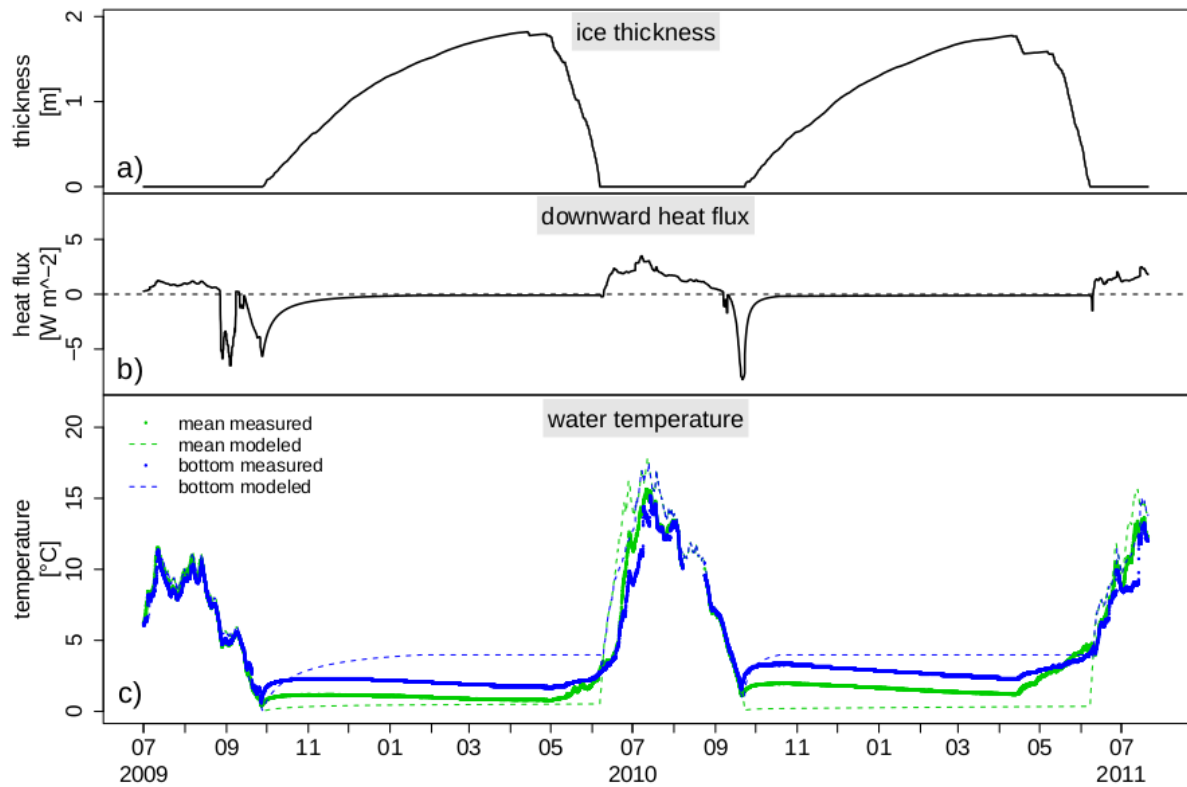


1  
 2 Figure 6. Relationship between mean monthly lake bottom temperatures for all five lakes  
 3 during the ice free period and the corresponding mean monthly air temperatures, from July  
 4 | 2009 to August 2012. [Data are also provided in the supplementary material of this paper.](#)



1  
2  
3  
4  
5

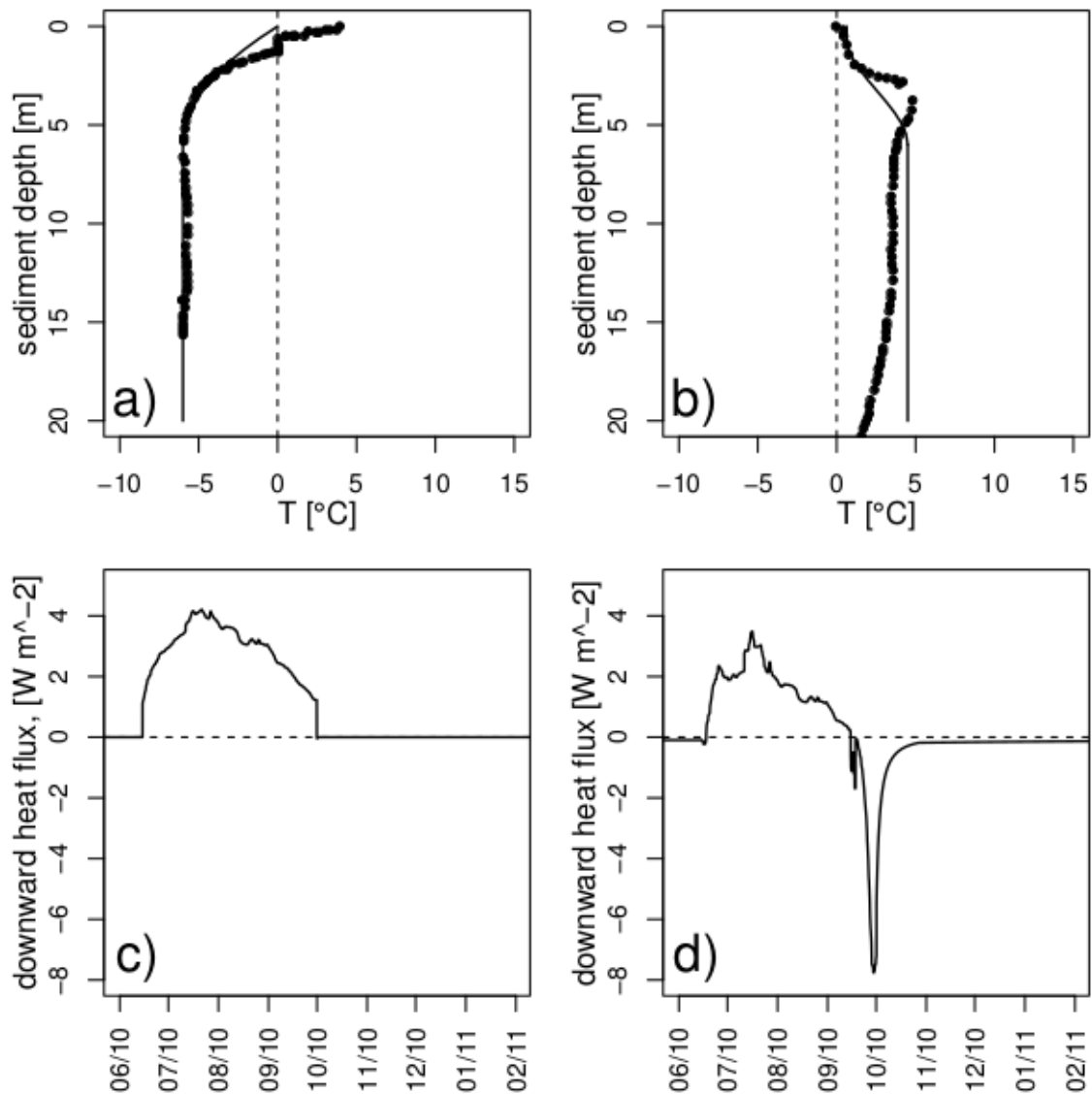
Figure 7. Sensible heat content (calculated using Equation 1) for the five lakes, from July 2009 to August 2012. Arrows indicate the timing of the lake's seasonal flooding by Lena river water.



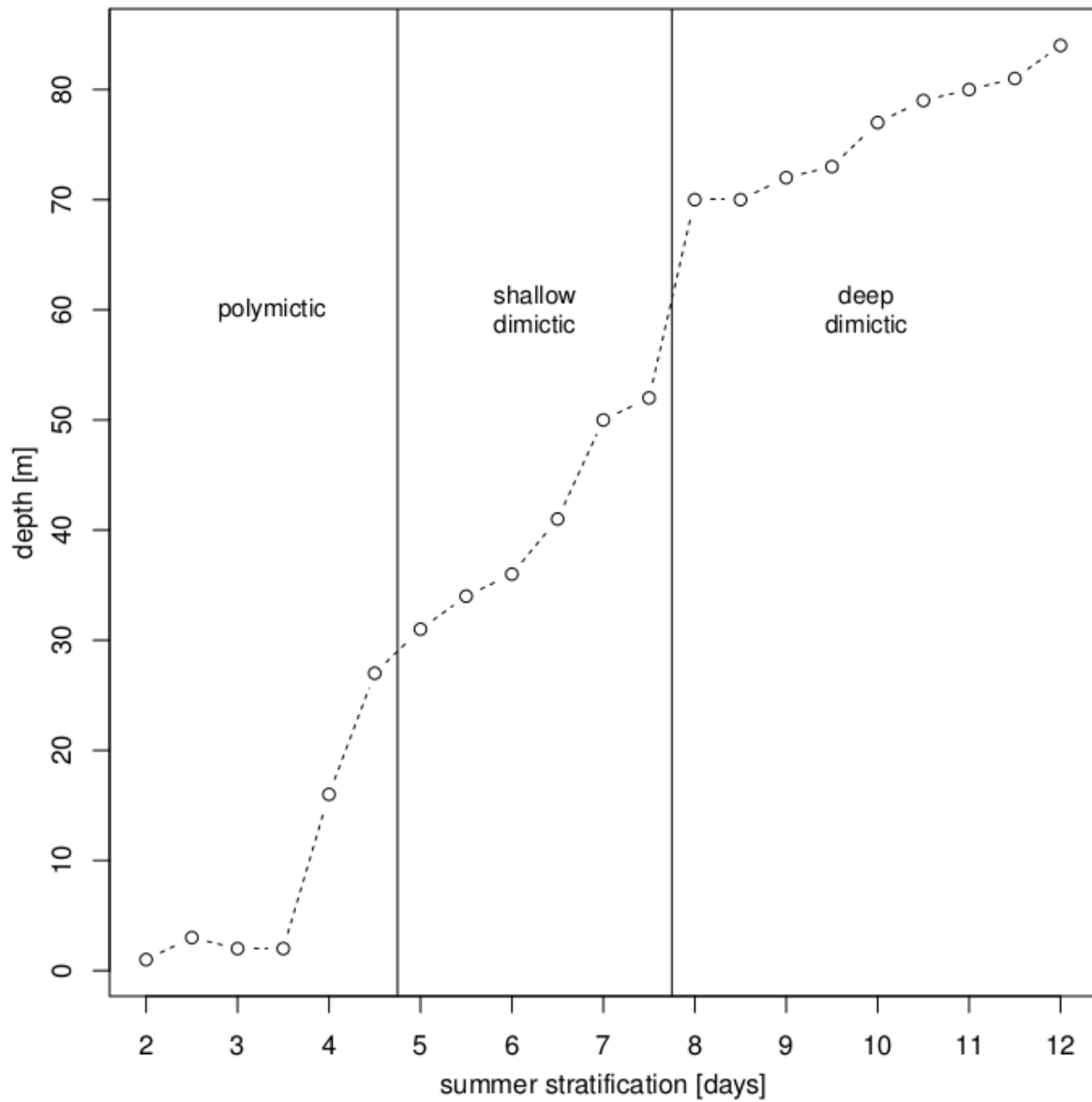
1

2 Figure 8. Modeled and measured hourly characteristics for Sa\_Lake\_1 from August 2009 to  
 3 August 2011. a) Modeled ice thickness; b) modeled vertical heat flux at the water-sediment  
 4 boundary: negative fluxes indicate fluxes from the sediment into the water column - a running  
 5 median filter was used to remove spikes; c) measured (continuous line) and modeled (dashed  
 6 lines) lake-bottom and mean water temperatures.



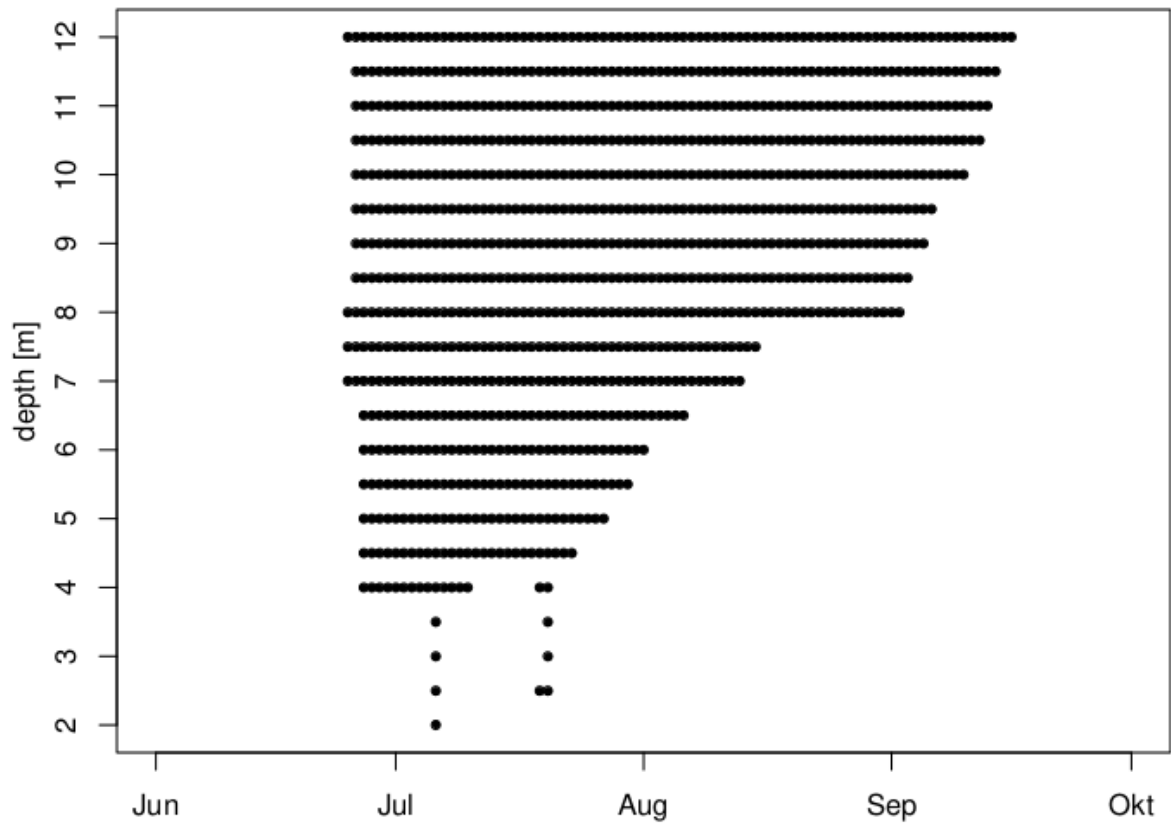


1  
 2 Figure 9. a & b) Measured temperature profiles (squares) beneath two lakes (with a) 1 m  
 3 water depth, and b) 5 m water depth) on the Bykovsky Peninsula, in the south-eastern part of  
 4 the Lena River Delta (Grigoriev, 1993). Temperatures were measured between 9 and 11 June  
 5 1984. Modeled sediment temperature profiles (continuous line) are for 10 June 2010 using  
 6 model parameters described in the Methods section. c & d) Modeled daily vertical heat flux at  
 7 the water-sediment boundary for c) the shallow lake, and d) the deep lake, 2010-2011.



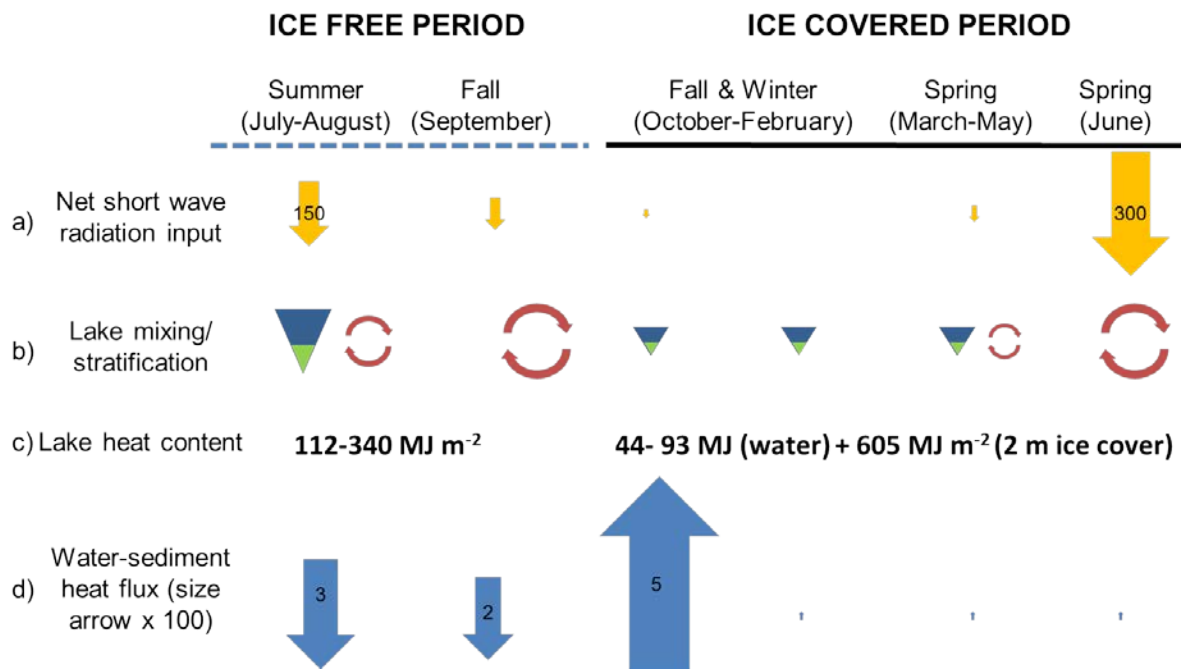
1

2 Figure 10. Total number of days with summer stratification in lakes of varying depths  
 3 modeled with FLake driven by the meteorological data from the Samoylov observatory  
 4 station for 2010. Existence of stratification was determined by the criterion  $(T_s - T_b) > 0.5^\circ\text{C}$ ,  
 5 where  $T_s$  and  $T_b$  are the modeled temperatures at lake surface and lake bottom, respectively.



1  
2  
3  
4  
5

Figure 11. Summer stratification duration in lakes of varying depth (see Fig. 10 for definitions).

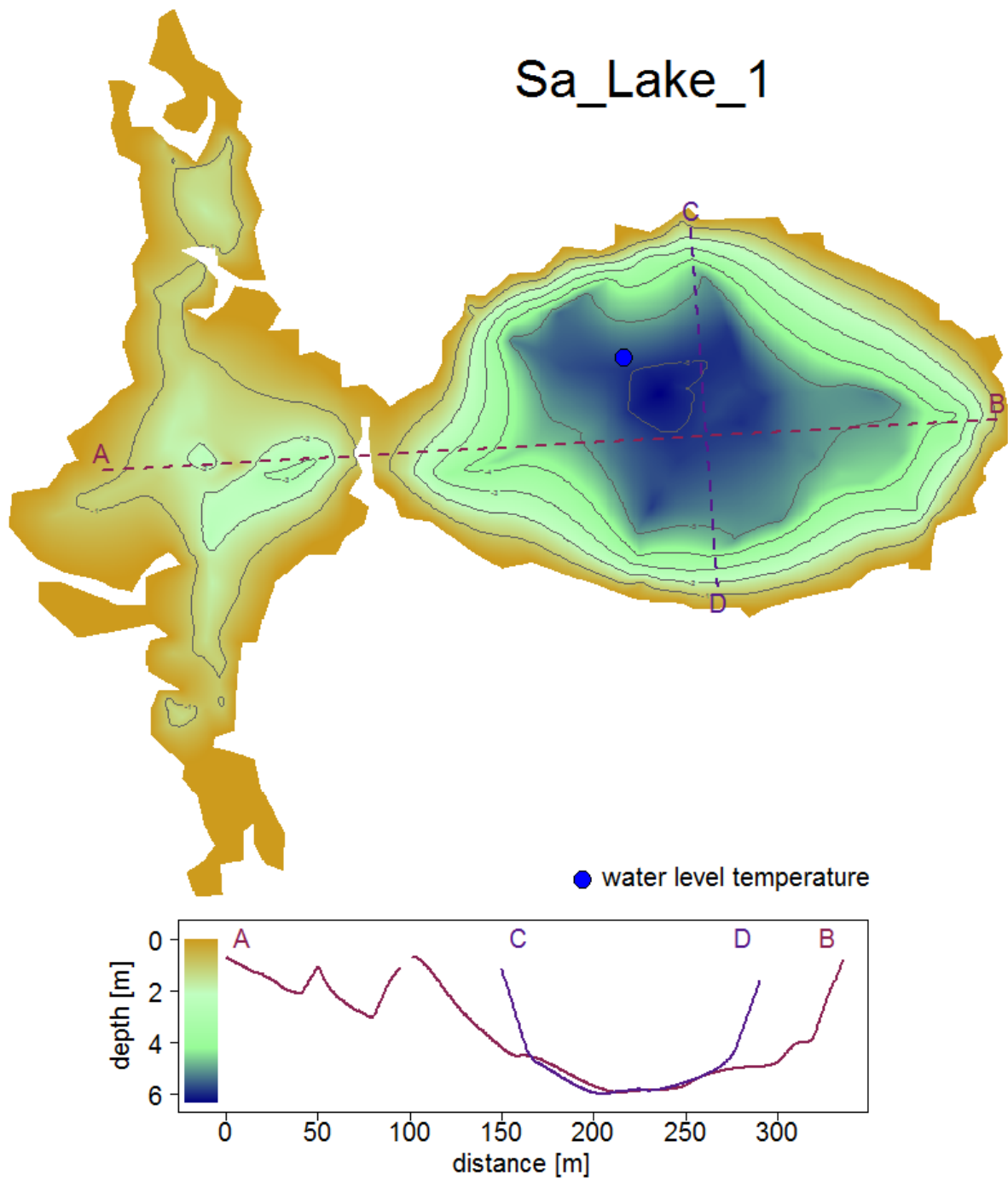


1  
2 | Figure 129. Summary of thermal processes in thermokarst lakes over a one year cycle. a) Net  
3 | short wave radiation input (measured at the climate station on Samoylov); b) dominant in-lake  
4 | processes (mixing and stratification) - size of symbol reflects intensity of process; c) lake heat  
5 | content (divided into summer and winter lake heat content according to Wetzel, 2001); d)  
6 | average heat fluxes across the lake's water-sediment boundary: downward arrows denote heat  
7 | flux into the sediment and upward arrows flux out of the sediment into the water column. The  
8 | size of the arrows and their numbers indicate the relative magnitudes of the fluxes [W m<sup>-2</sup>].  
9 | Note that the sizes of arrows representing bottom heat fluxes have been enlarged by a factor  
10 | of 100 due the small magnitude of the fluxes.

11  
12

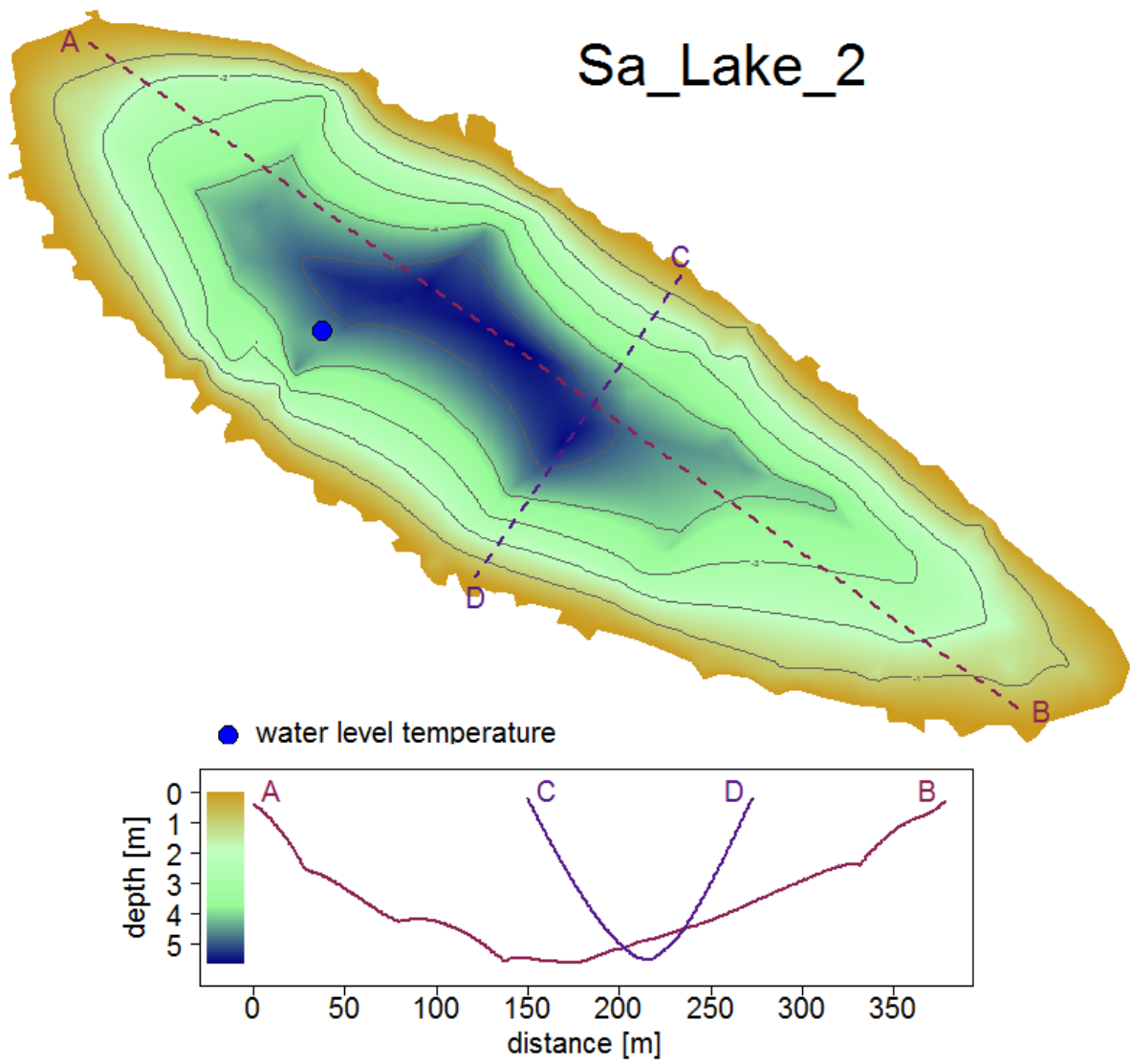
1 **Appendix A: Morphometry of lakes, hourly lake temperatures and lowest sensor depths**  
2 **data 2D Bathymetric contour plots and cross sections of the five lakes**

3 The topographic slope on the polygonal tundra (first terrace) is very low (< 5°). Aerial images  
4 of Sa Lake 2 and Sa Lake 3 show submerged polygons beneath the water surface,  
5 indicating that these lakes are likely to have been formed by the thawing of ground ice and ice  
6 wedges and the subsequent merging of polygonal ponds. The shorelines adjacent to shallow  
7 parts of these younger thermokarst lakes (with depths of 0-3 m) are very irregular and feature  
8 protrusions of different shapes and sizes (Figures A1-A4). Where deeper sections (> 3 m)  
9 occur close to the shore, the shorelines are smooth and the lakes tend to have an oval shape.  
10 The profiles of thermokarst lakes tend to be V-shaped rather than flat-bottomed and the  
11 thermokarst lakes investigated were up to 6.4 m deep. The deepest lake on this island, with up  
12 to 11.6 m water depth, is Sa Lake 4. It has an elongated shape and is one of three  
13 interconnected lakes that occur in an abandoned channel of the Lena River ("oxbow" or  
14 "perched" lakes; Figure A4). The largest monitored lake in this series of lakes was  
15 Ku Lake 1, located on sediments of the Pleistocene Ice Complex, which have high ice  
16 content. This lake is the largest of three residual lakes located within an alas that is more than  
17 20 m deep. This thermokarst basin evolved in two phases (Morgenstern et al., 2013). In the  
18 first phase the original large lake covered the entire basin. It drained abruptly through a  
19 thermos-erosional valley at about 5.7 ka BP, leaving the > 20 m deep alas with residual lakes.  
20 This was then followed by thermokarst processes of varying intensity during the second phase  
21 (5.7 ka BP to the present). This lake is an order of magnitude larger in surface area than the  
22 other four thermokarst lakes investigated and, in contrast to those lakes on Samoylov Island,  
23 has a regular oval shape, occurs within a basin with steep sides and has a smooth, flat  
24 shoreline. The maximum water depth is about 3.6 m and the profile is flat-bottomed (Figure  
25 A5).



1

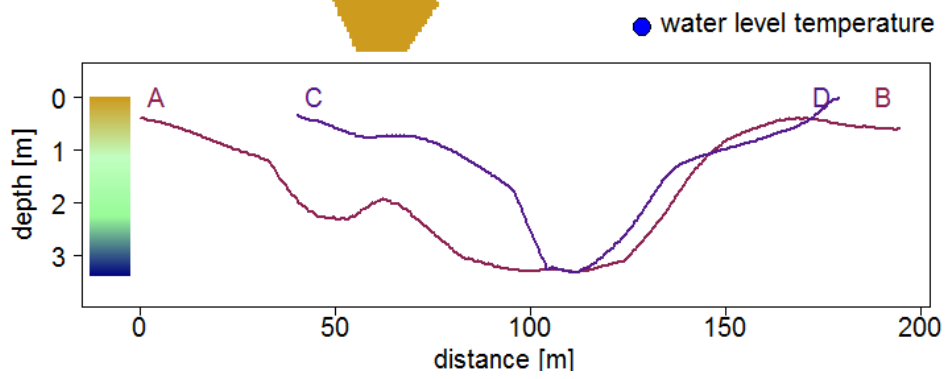
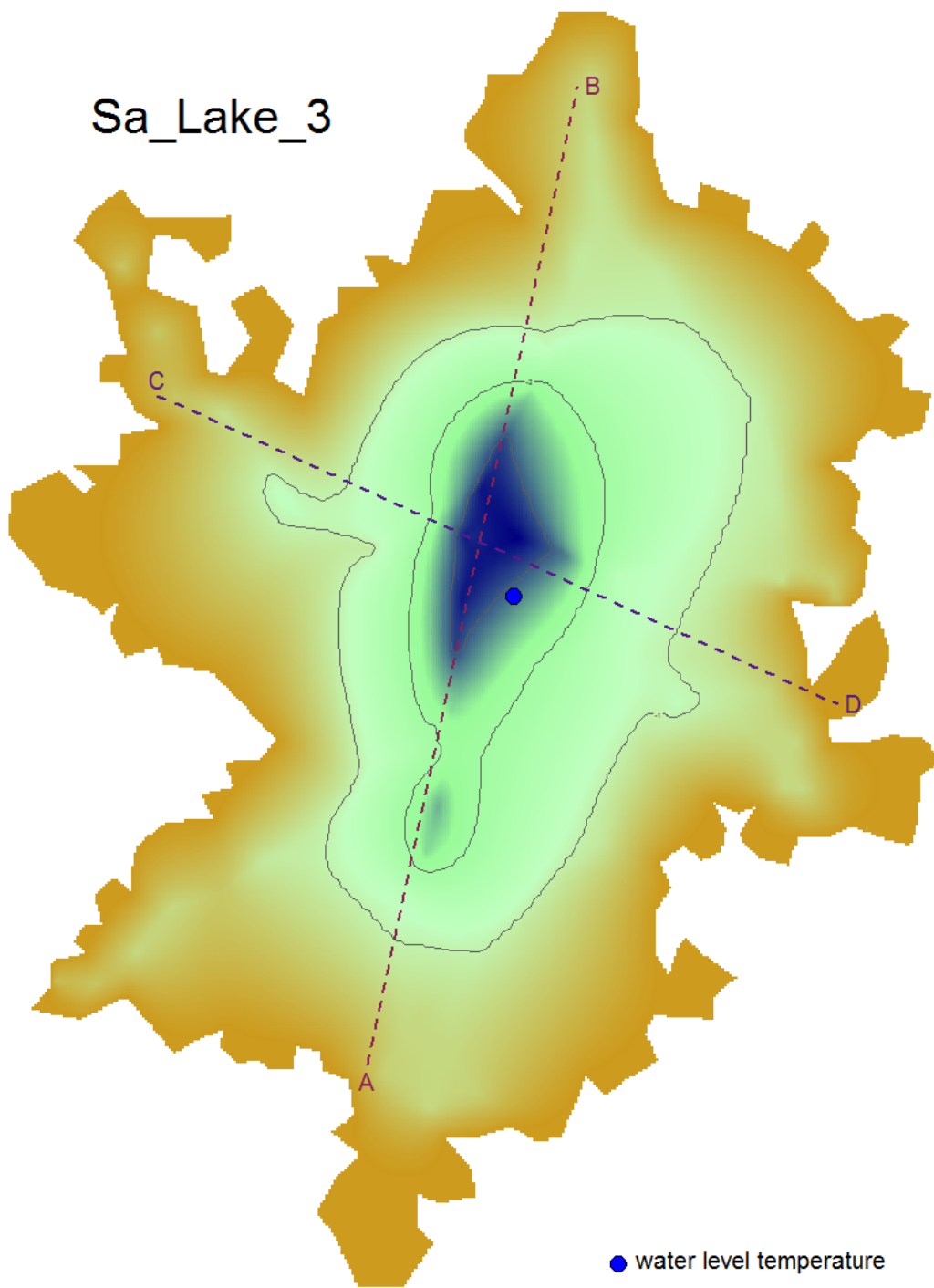
2 | Figure A1. Bathymetry and cross sections of Sa\_Lake\_1 with location of sensors.



1

2 | Figure A2. Bathymetry and cross sections of Sa\_Lake\_2 with location of sensors.

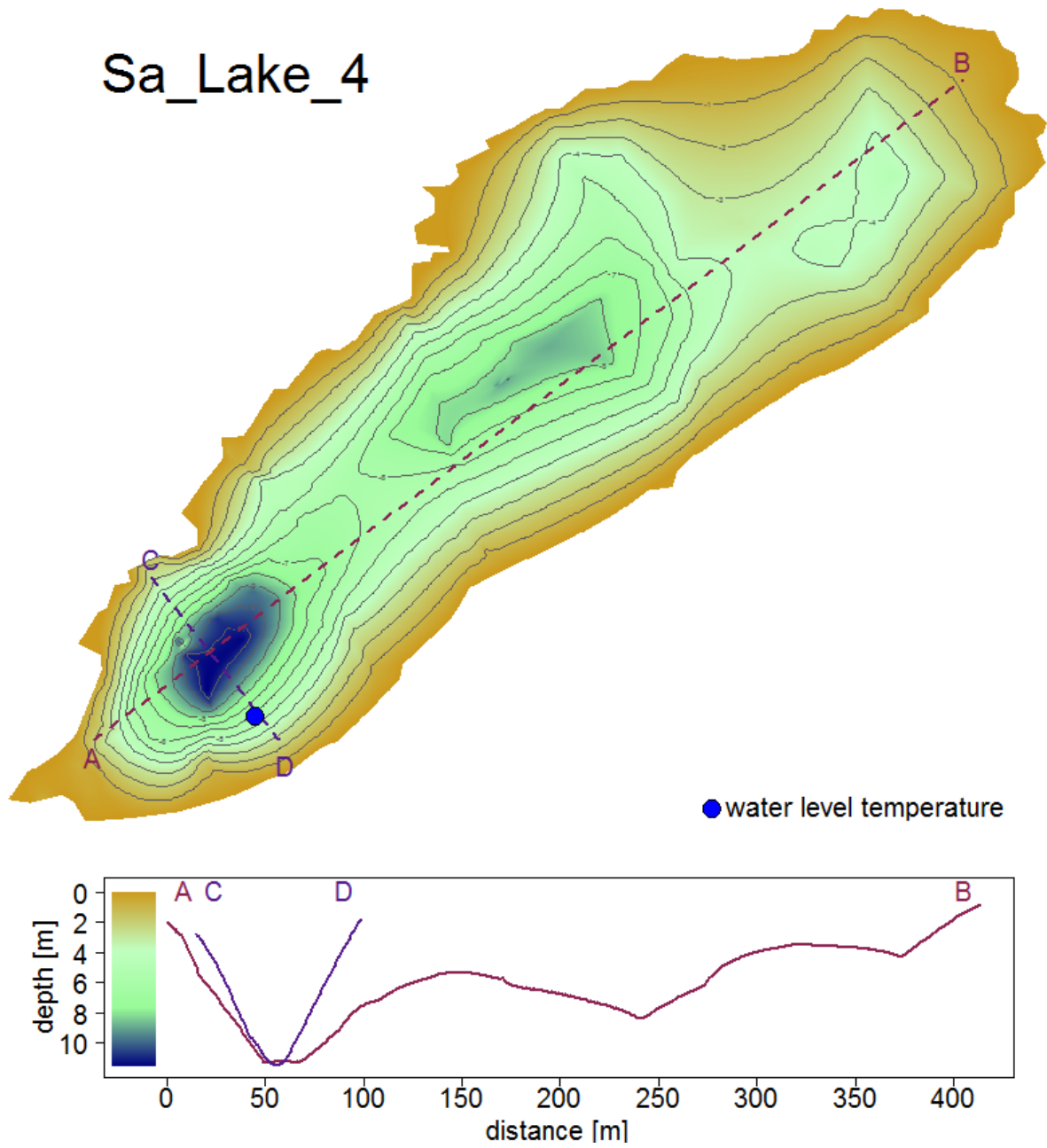
# Sa\_Lake\_3



1

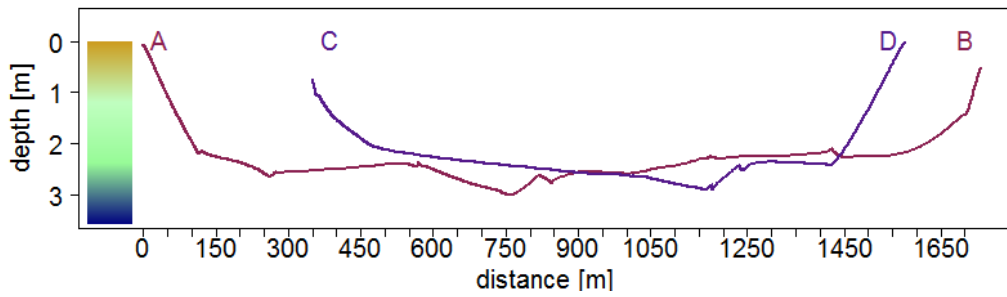
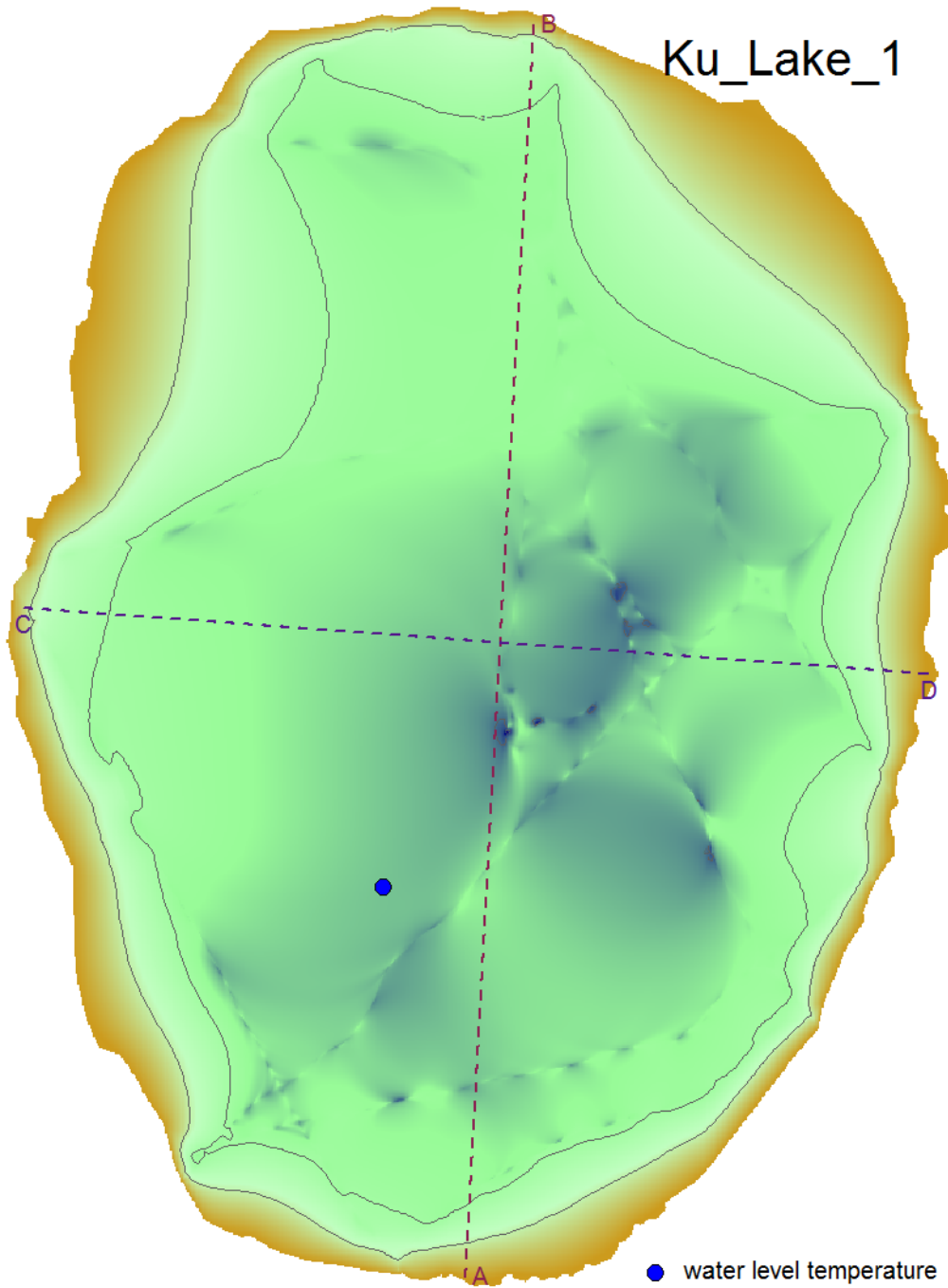


1 | Figure A3. Bathymetry and cross sections of Sa\_Lake\_3 with location of sensors.



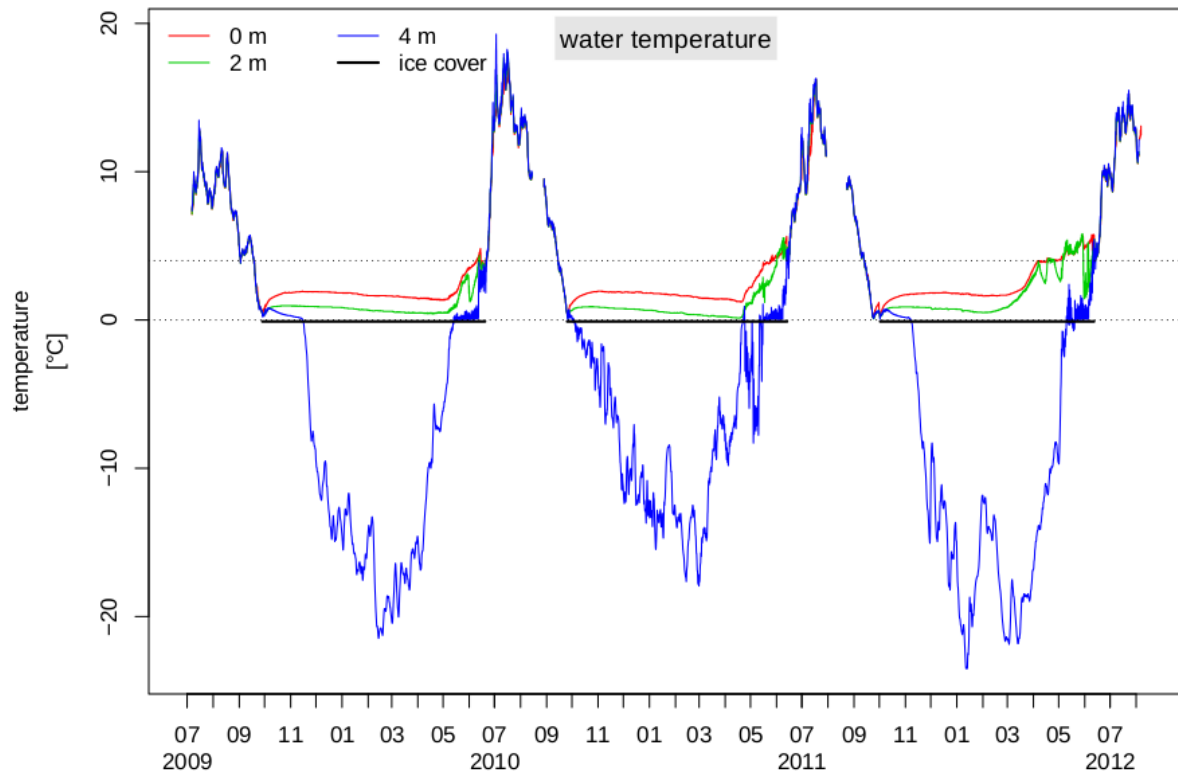
2

3 | Figure A4. Bathymetry and cross sections of Sa\_Lake\_4 with location of sensors.



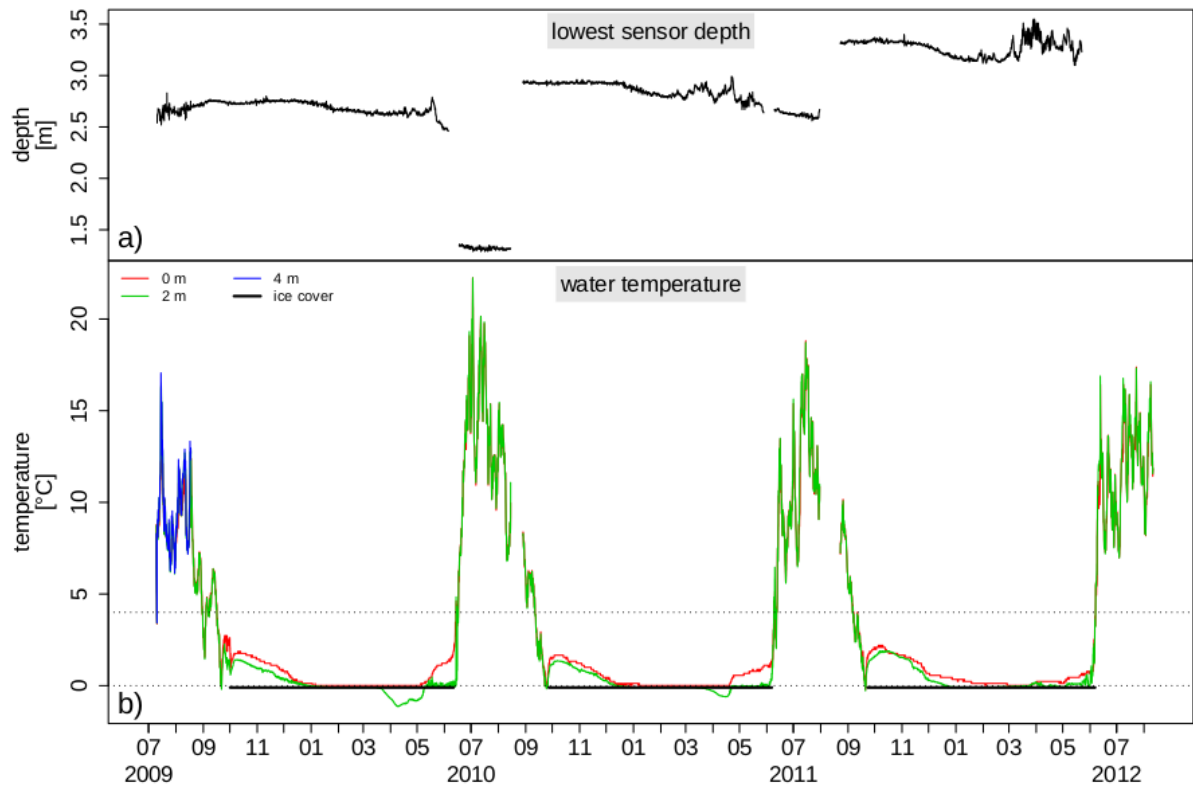
1

1 Figure A5. Bathymetry and cross sections of Ku\_Lake\_1. (Data from Morgenstern et al.,  
2 2011 [and http://doi.pangaea.de/10.1594/PANGAEA.848485](http://doi.pangaea.de/10.1594/PANGAEA.848485)).



3  
4 Figure A6. Hourly lake temperatures and lowest sensor depth (indicating water level changes)  
5 for Sa\_Lake\_2, from July 2009 to August 2012. Thick black lines indicate ice covered  
6 periods.

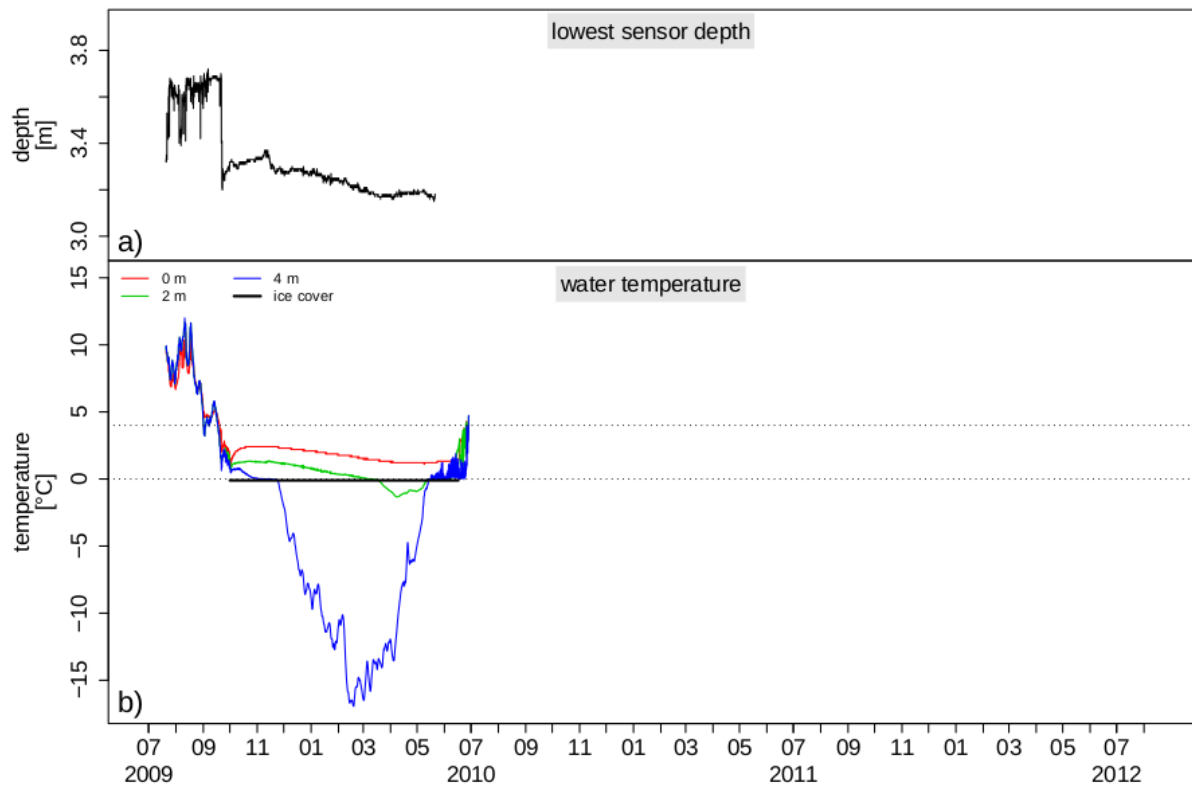
7



1

2 Figure A7. Hourly lake temperatures and lowest sensor depth (indicating water level changes)  
 3 for Sa\_Lake\_3, from July 2009 to August 2012. Thick black lines indicate ice covered  
 4 periods.

5



1

2 Figure A8. Hourly lake temperatures and lowest sensor depth (indicating water level changes)  
 3 for Ku\_Lake\_1, from July 2009 to August 2010. Thick black lines indicate ice covered  
 4 periods.

5

1

## 2 **Supplementary material: data and animations**

- 3 • Model data input (Samoylov); air temperature, air humidity, wind speed; radiation  
4 components

5 Samoylov\_2009\_2012.dat

6

- 7 • Model validation data: hourly lake temperatures and sensor depth (lake water level)  
8 data, where measured

9

10 Sa\_Lake\_1\_2009\_2012.dat

11 Sa\_Lake\_2\_2009\_2012.dat

12 Sa\_Lake\_3\_2009\_2012.dat

13 Sa\_Lake\_4\_2009\_2012.dat

14 Ku\_Lake\_1\_2009\_2010.dat

15 LenaRiver\_2009\_2010.dat

16

- 17 • Animation (movie) of temperatures in Sa\_Lake\_1 using daily average temperatures at  
18 depth and interpolated between depths using cubic interpolation. Daily temperature  
19 plots were added to produce the animation of temperatures

20 Sa\_Lake\_1\_2010-daily-color-.2s.gif

21

- 22 • [Summary table of mean monthly air and bottom lake temperatures:](#)  
23 [meanlake air temp.txt](#)

24

25

1 **Thermal processes of thermokarst lakes in the continuous**  
2 **permafrost zone of northern Siberia - observations and**  
3 **modeling (Lena River Delta, Siberia)**

4

5 **J. Boike<sup>1</sup>, C. Georgi<sup>1</sup>, G. Kirilin<sup>2</sup>, S. Muster<sup>1</sup>, K. Abramova<sup>3</sup>, I. Fedorova<sup>4,5,6</sup>, A.**  
6 **Chetverova<sup>4,5</sup>, M. Grigoriev,<sup>7</sup> N. Bornemann<sup>1</sup> and M. Langer<sup>1,8</sup>**

7 [1] Alfred Wegener Institute Helmholtz Center for Polar and Marine Research,  
8 Telegrafenberg A43, 14473 Potsdam, Germany

9 [2] Leibniz-Institute of Freshwater Ecology and Inland Fisheries (IGB), Mueggelseedamm  
10 310, 12587 Berlin, Germany

11 [3] Lena Delta Nature Reserve, Ak. Fedorova 28, 678400 Tiksi, Sakha Republic, Russia

12 [4] Institute of Earth Science, Saint-Petersburg State University, 10th line of Vasiljevsky  
13 Island, 33-35. 199178 Saint-Petersburg, Russia

14 [5] Arctic and Antarctic Research Institute, 38, Beringa str., St. Petersburg, 199397, Russia

15 [6] Kazan Federal University, 18, Kremlyovskaya str., Kazan, Russia

16 [7] Melnikov Permafrost Institute, Siberian Branch, Russian Academy of Sciences, Yakutsk,  
17 Russia

18 [8] Laboratoire de Glaciologie et Géophysique de l'Environnement (LGGE), 38402 St Martin  
19 d'Hères Cedex, France

20

21 Correspondence to: J. Boike (Julia.Boike@awi.de)

## 1 **Abstract**

2 Thermokarst lakes are typical features of the northern permafrost ecosystems, and play an  
3 important role in the thermal exchange between atmosphere and subsurface. The objective of  
4 this study is to describe the main thermal processes of the lakes and to quantify the heat  
5 exchange with the underlying sediments. The thermal regimes of five lakes located within the  
6 continuous permafrost zone of northern Siberia (Lena River Delta) were investigated using  
7 hourly water temperature and water level records covering a three year period (2009-2012),  
8 together with bathymetric survey data. The lakes included thermokarst lakes located on  
9 Holocene river terraces that may be connected to Lena River water during spring flooding,  
10 and a thermokarst lake located on deposits of the Pleistocene Ice Complex. Lakes were  
11 covered by ice up to 2 m thick that persisted for more than 7 months of the year, from October  
12 until about mid-June. Lake-bottom temperatures increased at the start of the ice-covered  
13 period due to upward-directed heat flux from the underlying thawed sediment. Prior to ice  
14 break-up, solar radiation effectively warmed the water beneath the ice cover and induced  
15 convective mixing. Ice break-up started at the beginning of June and lasted until the middle or  
16 end of June. Mixing occurred within the entire water column from the start of ice break-up  
17 and continued during the ice-free periods, as confirmed by the Wedderburn numbers, a  
18 quantitative measure of the balance between wind mixing and stratification that is important  
19 for describing the biogeochemical cycles of lakes. The lake thermal regime was modelled  
20 numerically using the FLake model. The model demonstrated good agreement with  
21 observations with regard to the mean lake temperature, with a good reproduction of the  
22 summer stratification during the ice free period, but poor agreement during the ice covered  
23 period. Model sensitivity to lake depth demonstrated that lakes in this climatic zone with  
24 mean depths  $>5$  m develop continuous stratification in summer for at least one month. The  
25 modeled vertical heat flux across the bottom sediment tends towards an annual mean of zero,  
26 with maximum downward fluxes of about  $5 \text{ W m}^{-2}$  in summer and with heat released back  
27 into the water column at a rate of less than  $1 \text{ W m}^{-2}$  during the ice-covered period.

28 The lakes are shown to be efficient heat absorbers and effectively distribute the heat through  
29 mixing. Monthly bottom water temperatures during the ice-free period range up to  $15^{\circ}\text{C}$  and  
30 are therefore higher than the associated monthly air or ground temperatures in the surrounding



1 frozen permafrost landscape. The investigated lakes remain unfrozen at depth, with mean  
2 annual lake –bottom temperatures of between 2.7 and 4°C.  
3 The data are available in the supplementary material for this paper and through the  
4 PANGAEA website (<http://doi.pangaea.de/10.1594/PANGAEA.846525>).

# 1   **1   Introduction**

2   Lakes can be interpreted as sensitive climatic indicators that respond to a range of different  
3   influences affecting the world’s climate. They can also exert an important influence on the  
4   local, regional, and global climate and hydrology by regulating heat and water fluxes, but  
5   their thermal dynamic represented in RCMs and GCMs is rather simple, and does not include  
6   all physical processes that are necessary for reproducing atmosphere-lake interaction (Walsh  
7   et al., 1998; Martynov et al., 2012). Lakes are often typical features of northern hemisphere  
8   ecosystems (Figure 1). In permafrost areas, which occupy about 25% of the world's landmass,  
9   lakes influence not only the thermal regime of the surrounding and underlying permafrost, but  
10   also the atmospheric heat and water fluxes, due to their large thermal heat reservoirs and heat  
11   capacities. The winter heat flux into the atmosphere through the ice cover from deep lakes  
12   that remain unfrozen at depth is several times greater than that from the surrounding tundra  
13   (Jeffries et al., 1999). Even smaller polygonal water bodies (thermokarst ponds), which freeze  
14   to the bottom every winter, have heat fluxes that are an order of magnitude greater than those  
15   from the surrounding permafrost (Langer et al., 2011b). The large thermal heat reservoir in  
16   lakes prevents the sediment beneath those lakes with a water depth greater than about 2 or 3  
17   meters from freezing, thus allowing a talik to develop (Lachenbruch, 1962). However, little  
18   data exists on the thermal conditions of lakes in north and central Yakutia, or the taliks  
19   beneath them (Grigoriev, 1960, 1966; Are, 1974; Pavlov et al., 1981). These unfrozen layers  
20   of lake sediment can enhance mobilization of the carbon reservoir by enabling year-round  
21   microbial decomposition in otherwise frozen surroundings, and water bodies can thus be  
22   hotspots for CO<sub>2</sub> and CH<sub>4</sub> emissions (Langer et al., 2015; Schneider von Deimling et al.,  
23   2014; Walter et al., 2006; Abnizova et al., 2012; Laurion et al., 2010). Water bodies are also  
24   important because they provide habitats for zooplankton, fish, and migratory birds (Vincent  
25   and Hobbie, 2000; Alerstam et al., 2001), and are a source of drinking water for northern  
26   communities, of water for irrigation, and of water for industry, exploration, and ice-road  
27   construction in winter (Vincent et al., 2013).

28   Measuring the water temperatures in lakes over both short and long terms is therefore  
29   important, not only for modeling the development of the subsurface thermal regime, but also  
30   for understanding and modeling ecological and physical dynamics. Few investigations have,  
31   however, been carried out into the physical and thermal characteristics of Arctic water bodies,

1 especially over the long term, and there is a particular shortage of data from northern Siberia.  
2 A notable exception is the long term biological, physical and chemical lake study initiated in  
3 1975 at the Toolik Lake Long Term Ecological Research (LTER) site in Alaska. The lakes  
4 studied are located on the North Slope of Alaska, in the foothills of the Brooks Range, and are  
5 classified as low Arctic lakes (Hobbie and Kling, 2014). Toolik Lake and most of the other  
6 lakes in this area are “kettle lakes” that formed as a result of glaciation; their lake  
7 morphometries (surface areas, depths) are a result of the glaciation history and the age of the  
8 landscape. Water depths can range up to 25 m, as is the case in Toolik Lake (Hobbie and  
9 Kling, 2014). The thermal stratification varies considerably between lakes (depending on the  
10 lake’s morphometry), as well as between years (Luecke et al., 2014). Also in northern Alaska,  
11 Arp et al. (2010) made use of an original method that combined short term (for example, over  
12 one year) measured lake surface temperatures (from depths of 0.5 m and 1.0 m) with  
13 meteorological and remote sensing data on lake surface temperatures and ice thicknesses. The  
14 latter variables were compared with measured temperatures and ice thicknesses, and with  
15 modeled results (Arp et al., 2010). The advantage of this approach is that, following  
16 successful calibration, a monitoring network can be established that is based purely on remote  
17 sensing data. Monitoring in some of these lakes on the Alaskan Coastal Plain has continued  
18 since 2010 as part of the new Circum-Arctic Lakes Observation Network (CALON) initiative  
19 (<http://www.arcticlakes.org/calon-lakes.html>; Hinkel et al., 2012). An initial series of data for  
20 vertical temperature profiles from the summer of 2010 has been provided for a number of  
21 lakes, together with time series of hourly temperature data, in order to demonstrate the  
22 seasonal and temporal variability (Hinkel et al., 2012).

23 Sporadic measurements of lake temperatures have been obtained in conjunction with  
24 limnological studies (for example, by Keatley et al., 2007, or Pienitz et al., 1997),  
25 paleolimnological investigations (such as in the 172 m deep El’gygytgyn Lake of north-  
26 eastern Siberia, a meteoritic impact crater; Nolan and Brigham-Grette, 2006), and physical  
27 experiments (such as dye tracing under the ice cover in a small Arctic lake; Welch and  
28 Bergmann, 1985). Vincent et al. (2008) measured temperatures and salinity in a high Arctic,  
29 125 m deep, perennially ice-covered lake on Ellesmere Island in Nunavut, Canada. The  
30 authors then successfully modeled the lake’s temperature regime using a one-dimensional  
31 heat diffusion equation and including heat transfer by radiation through ice and water. For

1 lakes within the Mackenzie Delta (Northwest Territories of Canada), Burn (2002, 2005)  
2 demonstrated that the temperatures in the deep central pool of a thermokarst lake on Richards  
3 Island remained positive throughout the winter, with a mean annual temperature of 3.5°C,  
4 whereas freezing occurred in the shallow littoral terrace of the lake (mean annual temperature  
5 -3.7°C).

6 This paper aims to quantify the seasonal thermal dynamics of lakes in the Eurasian north,  
7 where monitoring observatories have recently been established in the central part of the Lena  
8 River Delta. Our objectives are (i) to describe the thermal patterns and processes in both  
9 thermokarst lakes and “perched” lakes (which can have seasonal connections to river water),  
10 and (ii) to make use of measured data to validate the freshwater model FLake, as well as  
11 estimate water sediment heat exchange. FLake offers a good compromise between  
12 computational efficiency and physical reality, and has been coupled to several regional and  
13 global climate models (Thiery et al., 2014; Martynov et al., 2010). FLake has been used in  
14 various 1 dimensional modeling studies, for a wide range of lakes, including tropical lakes,  
15 and in lake model intercomparison projects (LakeMIP; Thiery et al., 2014; Stepanenko et al.,  
16 2010). However, it has not been used for Arctic lakes and this study tests the ability of FLake  
17 to reproduce the temperature regimes of thermokarst lakes in northern Siberia.

18

19

## 20 **2 Site description**

21 The Lena River Delta in northern Yakutia is one of the largest deltas in the Arctic and has one  
22 of the largest catchment areas (2,430,000 km<sup>2</sup>) in the whole of Eurasia (Costard and Gautier,  
23 2007). The Lena River discharges about 525 km<sup>3</sup> of water through the delta into the Arctic  
24 Ocean every year, with an average annual discharge rate of 16,800 m<sup>3</sup> s<sup>-1</sup> (Gordeev and  
25 Sidorov, 1993). This discharge rate has been reported to be increasing (Fedorova et al., 2015;  
26 Rawlins et al., 2009). As it passes through its estuarine area, the main flow of the Lena River  
27 splits into numerous arms and transverse branches to form the most extensive delta in the  
28 Russian Arctic, covering 25,000 km<sup>2</sup> and including about 1,500 islands and 60,000 lakes.

29 Continuous cold permafrost (with a mean annual temperature of -10°C at 10 m depth)  
30 underlies the study area to between about 400 and 600 m below the surface. Since

1 observations started in 2006, the permafrost at 10.7 m depth has warmed by  $> 1.5^{\circ}\text{C}$  (Boike et  
2 al., 2013; <http://gtnpdatabase.org/boreholes/view/53/>).

3 The main features of the annual energy balance for these sites with continuous permafrost in  
4 the subsurface typically include low net radiation, higher atmospheric latent heat flux than  
5 sensible heat flux, and a large proportion of soil heat flux (Boike et al., 2008; Langer et al.,  
6 2011a, 2011b). Previous publications have reported that shallow ( $< 1$  m deep) ponds freeze  
7 completely in winter, but that the timing of freeze-back can vary by up to 2 months between  
8 years, depending on the surface energy balance (Langer et al., 2011b; Langer et al., 2015).

9 The study areas are located on the islands of Samoylov and Kurungnakh, within the central  
10 part of the Lena River Delta (Figure 1). Samoylov Island ( $72^{\circ}22'\text{N}$ ,  $126^{\circ}28'\text{E}$ ) lies within one  
11 of the main river channels in the southern part of the delta and is relatively young, with an age  
12 of between 4 and 2 ka BP (Schwamborn et al., 2002), which is also the estimated maximum  
13 age of the investigated lakes on the island. In contrast, Kurungnakh Island forms part of the  
14 third terrace of the Lena Delta and is an erosional remnant of a late-Pleistocene accumulation  
15 plain. It consists of fluvial sands overlain by Yedoma-type ice complex deposits, which  
16 accumulated between 100 and 50 ka BP and since 50 ka BP, respectively, and a Holocene  
17 cover (8 to 3 ka BP) (Schwamborn et al., 2002; Wetterich et al., 2008). Large thermokarst  
18 lakes and basins are major components of the ice-rich permafrost landscape of Kurungnakh  
19 Island; they have formed since 13 to 12 ka BP (Morgenstern et al., 2011, 2013).

20 The lakes presented in this paper are of thermokarst origin which is common for the lowland  
21 tundra permafrost areas of North East Siberia. These areas were not ice-covered during the  
22 latest glacial period (70,000-10,000 years ago) and are characterized by high to moderate  
23 ground ice content and thick sediment cover. Arctic lowlands with similar landscape  
24 characteristics and lake distributions can be found in Central and East Siberia, Interior and  
25 Northern Alaska as well as Northwest Canada (Grosse et al., 2013).

26 The landscape on both of these islands, and in the delta as a whole, has generally been shaped  
27 by water through erosion and sedimentation (Fedorova et al., 2015), and by thermokarst  
28 processes (Morgenstern et al., 2013). The proportion of the total land surface of the delta  
29 covered by surface water can amount to more than 25% (Muster et al., 2012). Up to 50% of  
30 the total surface water area in permafrost landscapes is attributed to small lakes and ponds  
31 with surface areas of less than  $10^5$  m<sup>2</sup>, which have the potential to grow into large thermokarst

1 lakes (Muster et al., 2012). Water budget modeling for the tundra landscape has shown a  
2 small positive balance since 1953, which has been confirmed by satellite observations (since  
3 1964) of the surface areas of water bodies (Boike et al., 2013). The chemical and isotopic  
4 signals from the water in lakes on Samoylov Island generally indicate low levels of  
5 mineralization (Table 1). The stable isotopic ratios indicate that the thermokarst lake water is  
6 sourced mainly from thawed ground ice mixed with precipitation and the water in shallow  
7 ponds is sourced mainly from summer precipitation (Abnizova et al., 2012).

8 Small ponds and lakes emit more CO<sub>2</sub> and CH<sub>4</sub> per square meter than the surrounding tundra,  
9 and greenhouse gas production continues during winter in those lakes that do not freeze to the  
10 bottom (Langer et al., 2015). Modeling studies have demonstrated that an unfrozen layer of  
11 lake sediment is maintained throughout the year beneath thermokarst lakes (Yi et al., 2014).  
12 During high spring floods some of the lakes on the first terrace are flooded with Lena River  
13 water. Observations in 2014 on Samoylov Island, for example, confirmed the flooding of a  
14 large part of the first terrace on the island, including most of the lakes.

15 Additional detailed information concerning the climate, permafrost, land cover, vegetation,  
16 and soil characteristics of these islands in the Lena River Delta can be found in Boike et al.  
17 (2013) and Morgenstern et al. (2013).

18

### 19 **3 Methods**

#### 20 **3.1 Field instrumentation and ground surveys**

21 In July 2009, water level and temperature sensors (HOBO Temp Pro v2, HOBO U20, Onset,  
22  $\pm 0.2^{\circ}\text{C}$  across a temperature range from  $0^{\circ}\text{C}$  to  $70^{\circ}\text{C}$ , and  $\pm 0.4^{\circ}\text{C}$  across a temperature range  
23 from  $-40^{\circ}\text{C}$  to  $0^{\circ}\text{C}$ ) were installed within the water columns of the investigated lakes on  
24 Samoylov and Kurungnakh Island. Figure 1 shows the locations of the lakes (labelled  
25 Sa\_Lake\_1-4 for Samoylov and Ku\_Lake\_1 for Kurungnakh) and the location of the long  
26 term weather station. Gaps in the climate data record (air temperature, radiation, humidity,  
27 wind speed and direction, and snow depth) were filled whenever possible with data from  
28 temporary climate and eddy covariance stations located in close proximity to the weather  
29 station (Boike et al., 2013). Temperature and water depth sensors were placed directly above

1 the sediment-water interface and then temperature sensors at 2 m intervals up to 2 m below  
2 the water surface (Figure 2). The sensors were suspended in the water column from a buoy  
3 and anchored in the sediment below. The sensor at the bottom of the lake (just above the  
4 sediment) was labelled as “0 m”, the sensor 2 m above the sediment as “2 m”, and so on. The  
5 uppermost sensors were usually about 2 m below the water surface since we were concerned  
6 about the formation of ice and the potential drift of sensors with the shifting of ice cover. End-  
7 of-winter ice thickness (obtained by drilling) was measured in 2014; it ranged between 1.9  
8 and 2 m in lakes Sa\_Lake\_1-4 on Samoylov Island. During some winters the uppermost  
9 sensors became enclosed within the ice cover (for example, Sa\_Lake\_1 in 2012), but they  
10 were not moved out of position. One sensor was installed in the Lena River during August  
11 2009 (Figure 1) and recorded data from July 2009 to August 2010 but was lost during the  
12 following year.

13 Sensors were usually retrieved once a year (in August) and then re-launched in approximately  
14 the same position. The temperature record was therefore briefly interrupted during the period  
15 when the sensors were retrieved and read. The water depth (“sensor depth”) recorded by the  
16 bottom sensor sometimes changed following retrieval due to a change in the sensor position,  
17 although the actual water level of the lake remained the same. For example, for Sa\_Lake\_4 (a  
18 perched lake), sensors that were deployed at a water depth of about 8.5 m in 2009 were  
19 reinstalled at a depth of about 9.5 m in August 2010. Water level variations due to water  
20 balance changes (when the sensor position had not changed), for example during the summer  
21 period, were usually less than 0.5 m.

22 Data is only available over a one-year period for the lake on Kurungnakh Island (2009-2010)  
23 as the loggers were subsequently displaced, presumably during ice break-up. For the lakes on  
24 Samoylov Island, however we obtained continuous temperature and water level data over a  
25 period of 3 years from 2009 to 2012. All data and metadata are provided in the supplementary  
26 material for this publication and through the PANGAEA website  
27 (<http://doi.pangaea.de/10.1594/PANGAEA.846525>).

28 Bathymetric surveys were carried out in 2009 and 2010 on all of the investigated thermokarst  
29 lakes, using a GPSMAP 178 C echo sounder, a GPSMAP 421S plotter and a GPS 60  
30 navigator, all from Garmin. The shorelines were mapped either by GPS field survey or by  
31 manually digitizing the shoreline from high resolution aerial images. The accuracy of the echo

1 sonder equipment was about 0.1 m and was regularly checked using manual profiling. Depth  
2 measurements were taken along the longest lake axis as well as along a zigzag track in order  
3 to cover most of the lake surface and to locate any local “holes” that might exist as a result of  
4 thermokarst processes. Surface areas, mean and maximum depths, volumes, and hypsographic  
5 (depth/area) curves were calculated for the five lakes investigated using linear distance  
6 nearest neighbor interpolation in ArcGIS software (v.10.1) (Table 1). A description of the  
7 morphometry, including two-dimensional contour plots and cross sectional profiles of the  
8 lakes can be found in the appendix of this paper (Figures A1 to A5). Bathymetric records  
9 were also obtained for eight additional lakes (Chetverova et al., 2013) but are not included  
10 herein since temperature sensors were not installed. Bathymetric data, metadata and  
11 morphometric descriptions can be found in the appendix material for this publication, as well  
12 as through the PANGAEA website (<http://doi.pangaea.de/10.1594/PANGAEA.846525>).

13

### 14 **3.2 Heat content**

15 The ability of lakes to store and redistribute additional heat at seasonal time scales may affect  
16 the heat budget of adjacent permafrost areas at the landscape spatial scale. For this reason, we  
17 observe the thermal regime of tundra lakes to make inferences about their effect on heat  
18 exchange processes. The heat content of each lake ( $H_l$ ) was calculated at hourly time steps  
19 from the thermal energy stored in a water column from the lake's surface to its maximum  
20 depth ( $z_{\max}$ ):

$$21 \quad H_l = c_w \rho_w \int_0^{z_{\max}} T(z, t) dz \quad (1)$$

22 where  $c_w$  is the specific heat capacity of water,  $\rho_w$  is the freshwater density, and  $T$  is the  
23 temperature. The calculated heat budgets were divided into different time periods, as  
24 proposed by Wetzel (2001). The summer heat income is defined as the amount of heat  
25 required to raise the temperature of the lake from isothermal conditions at 4°C to the  
26 maximum observed depth-averaged summer temperature (summer heat content). The winter  
27 heat income is the amount of heat required to raise the temperature from the minimum  
28 temperatures to 4°C. The annual heat budget is the total amount of heat necessary to raise the  
29 water from the minimum temperature to maximum summer temperature. The winter heat



1 income and the annual heat budget must include the latent heat of fusion for the ice cover,  
2 especially for high latitude lakes (Wetzel, 2001). The ice cover thickness was measured  
3 during May 2014 and varied slightly from 2 m (Sa\_Lake\_1, Sa\_Lake\_2) to 1.9 m  
4 (Sa\_Lake\_4). The ice cover in these lakes melts completely every summer so that freezing  
5 and melting energies usually balance out over a year. The timing of spring ice break-up  
6 extends from the first ice melt, through moat formation and drifting of the ice cover, to the  
7 complete disappearance of ice. It is defined herein as the time at which the temperatures from  
8 all sensors indicate isothermal conditions, with temperature differences from the bottom to the  
9 top of the water column of  $< 0.1^{\circ}\text{C}$  following the period of stratification that occurs during ice  
10 cover, i.e. the time at which the lake water becomes completely mixed. The ice formation in  
11 fall is defined by the start of stratification in lake temperatures, i.e. when temperature  
12 differences from bottom to top exceed  $0.1^{\circ}\text{C}$ . The uncertainties in these determined times are  
13 estimated to be  $\pm 5$  days and are based on comparison with (infrequently available) satellite  
14 data (Table 1).

15

### 16 **3.3 Modeling of lake thermodynamics**

17 FLake is a freshwater lake model (Mironov, 2005) aimed at predicting the vertical thermal  
18 structure and mixing conditions in lakes over periods ranging from a few hours to a few years.  
19 The model is based on a two-layer parametric representation of the evolving temperature  
20 profile in the water column and on the integrated heat and kinetic energy budgets. The upper  
21 mixed layer is treated as thermally homogeneous, while the structure of the stratified layer  
22 between the upper mixed layer and the bottom of the basin (the lake thermocline) is described  
23 using the concept of self-similarity (or assumed shape) of the temperature-depth curve. The  
24 same self-similarity concept is used to describe the temperature structure of the thermally  
25 active upper layer of bottom sediments (Golosov and Kirillin, 2010) and of the ice (Mironov  
26 et al., 2012). It should be noted that no change in water depth as a result of winter ice  
27 formation is included in the computation, and the water depth is therefore assumed to be  
28 constant. Precipitation is also not included as an input into the model and snow accumulation  
29 is therefore not computed. Visual observations confirm that the lakes are usually snow free

1 due to the generally low snowfall (although a few areas with snow and hardened wind crusts  
2 occur locally), combined with high wind speeds blowing the snow away.

3 The following input data and settings were used for the lakes investigated in this study and  
4 tested with data for Sa\_Lake\_1, i.e. a lake depth of 4 m (93% of this lake has a water depth of  
5 not more than 4 m), a water optical light extinction coefficient of  $0.5 \text{ m}^{-1}$ , a 6 m thickness for  
6 the thermally active sediment layer beneath the lake, and a temperature at the bottom of the  
7 thermally active sediment layer of  $4.5^\circ\text{C}$ . Due to their very low contents of organic material  
8 and low levels of biological productivity the lakes are usually very clear: in shallow lakes (for  
9 example, Sa\_Lake\_3) the lake bottom is visible even at 2 m water depths. The thermal  
10 characteristics of the sediment are based on sediment temperatures measured beneath two  
11 lakes in the Lena River Delta (on the Bykovsky Peninsula; Grigoriev, 1993) and are discussed  
12 in the Sects. 4 and 5. Two temperature profiles were obtained in June 1984 for one shallow (1  
13 m) and one deep (5 m) lake, down to a sediment depth of 16 and 21 m below the lake bed,  
14 respectively. These temperature profiles are used as input for the model experiments since the  
15 assumption of thermal equilibrium does not necessarily exist for the lakes in the permafrost  
16 landscape.

17 Two meteorological datasets were used to drive the model: (1) hourly data from the on-site  
18 weather station (air temperature at 2 m height, wind speed, humidity, and radiation  
19 components), and (2) 6-hourly NCEP/NCAR reanalysis data provided by the  
20 NOAA/OAR/ESRL PSD, Boulder, Colorado, USA (<http://www.esrl.noaa.gov/psd/>; Kalnay  
21 et al., 1996). The two driving datasets were compared and were found to be in good  
22 agreement with each other, having some discrepancies in the short wave radiation  
23 components (Figure 3). The modeled lake temperatures were nearly identical in both  
24 datasets (not shown), indicating that reanalysis data sets perform well for lake modeling in  
25 these remote areas, where on-site meteorological information is often limited. For further  
26 analysis we used the measured on-site meteorological dataset, which can be found in the  
27 supplementary material for this publication. The FLake model output parameters (water  
28 temperatures, ice cover thickness, bottom sediment heat flux) for one of the lakes  
29 (Sa\_Lake\_1) are compared for the time period 9 July 2009 to 29 July 2011 with the measured  
30 parameters in Sect. 4. The model was used to:

- 1 - validate the 1-dimensional modeling approach and qualify the main mechanisms governing
- 2 features of the lake thermal regime, such as summer stratification, water-sediment heat
- 3 exchange, and ice melt
- 4 - characterize the water-sediment heat exchange at annual time scales
- 5 - establish a relationship between the morphometry and summer stratification duration.

6 The “Lake Analyzer” numerical tool (<http://lakeanalyzer.gleon.org/>; Read et al., 2011) was  
7 used to determine the dimensionless Wedderburn number (Wd), a quantitative measure of the  
8 balance between wind mixing and stratification that is important for describing the  
9 biogeochemical cycles of lakes (Spigel and Imberger 1980). A Wd number of 1 indicates a  
10 threshold value at which the wind shear brings the thermocline to the lake's surface along the  
11 upwind shoreline. For large Wedderburn numbers ( $\gg 1$ ) the buoyancy force is much greater  
12 than the wind stress suggesting strong vertical stratification. For small Wedderburn numbers  
13 ( $\ll 1$ ) the wind stress is much greater than the buoyancy force suggesting destruction of the  
14 vertical thermal stratification in the lake. On-site weather data from hourly time series of  
15 water temperature, wind speed, and bathymetric data were used as model inputs for the  
16 calculation of Wd.

17

18

## 19 **4 Results**

### 20 **4.1 Lake thermal dynamics based on observations**

21 The following analyses were based on temperature and sensor depth (water depth) data  
22 collected over the course of three years (2009-2012) from the investigated lakes, covering a  
23 range of morphometric characteristics and located on two geomorphologically different  
24 terraces (consisting of sediments of the Pleistocene Ice Complex on Kurungnakh and a  
25 Holocene flood plain on Samoylov). The seasonal thermal dynamics are only discussed in  
26 detail for two of these lakes: Sa\_Lake\_1 which is a thermokarst lake, and Sa\_Lake\_4 which is  
27 a perched/oxbow lake (Figures 4 and 5; an animation of the daily temperatures of Sa\_Lake\_1  
28 is also provided in the supplement). These lakes were selected as they have the best data  
29 records, taking into account the temporal coverage and the total number of sensors in each

1 lake profile. The seasonal temperature dynamics of the other lakes (Sa\_Lake\_2, Sa\_Lake\_3,  
2 and Ku\_Lake\_1) are illustrated in the Appendix of this paper (Figures A6-A8).

### 3 **4.2 Fall & winter**

4 During fall, cooling and complete mixing occurs at about the end of September resulting in  
5 isothermal conditions at 0°C immediately prior to ice cover formation (Figures 4 & 5). The  
6 ice cover growth can be briefly interrupted due to short-lived warming events during the fall  
7 (as was observed, for example, in late September and early October of 2008) but the ice cover  
8 then persists from October through to June (Figures 4b & 5c; Table 1). The water column  
9 becomes stratified following the formation of the ice cover and the initial isothermal  
10 conditions change so that lake-bottom temperatures are consistently warmer than those higher  
11 up in the water column (towards the water/ice interface). This bottom temperature  
12 development under ice, which involves rapid warming immediately after ice-cover formation  
13 followed by subsequent gradual cooling, takes place in all lakes but the rates of warming and  
14 cooling vary (Figures 4b, 5c, A6-8). In Sa\_Lake\_1 the maximum vertical temperature  
15 gradient was less than 1°C m<sup>-1</sup> (with a maximum of 1°C m<sup>-1</sup>) in the winter of 2010/2011 and  
16 decreased over the course of the winter (Figure 4b). In Sa\_Lake\_4, the maximum temperature  
17 gradient was less than 0.2°C m<sup>-1</sup> and, in contrast, increased over the course of the winter  
18 (Figure 5c). The waters in both lakes remained stratified during the winter, with gradual  
19 overall cooling of the stratified profile continuing until the end of winter.

### 20 **4.3 Spring**

21 The snow cover on the tundra landscape was usually very thin during the winter (< 0.5 m) and  
22 had usually thawed by the end of May or early June. Field observations during a number of  
23 spring field campaigns showed that the frozen surfaces of the lakes were normally kept snow-  
24 free by wind action. It is interesting to note that the under-ice warming of the water column  
25 (Figures 4b, 5c) started as early as the beginning of March (e.g., in 2012), when air  
26 temperatures were still well below 0°C, as a result of strong solar radiation input through the  
27 ice. A temperature increase of about 4°C over the 6 week period prior to ice break-up is equal  
28 to an energy input of about 30 W m<sup>-2</sup>. With solar radiation returning after the polar night, the  
29 shortwave net radiation on the ice surface is about 50 W m<sup>-2</sup> in March and increases to about

1 300 W m<sup>-2</sup> by the end of May or the beginning of June (Figure 3b). The net shortwave  
2 radiation penetrating to the water column is thus reduced by about 15-20% as a result of  
3 transmission through the ice cover. Radiation can penetrate to great water depths depending  
4 on the optical properties of the lake water. Assuming light extinction in the water column to  
5 be 0.5 m<sup>-1</sup>, about 13% of the radiation penetrating the ice cover (or ~ 4 W m<sup>-2</sup>) will reach the  
6 lake floor beneath 4 m of water. The solar radiative heating of the water (still below its  
7 maximum density at 4°C) and subsequent convective mixing effectively reduced the  
8 temperature gradient beneath the ice cover to less than 0.5°C m<sup>-1</sup> for Sa\_Lake\_1 and less than  
9 0.1°C m<sup>-1</sup> for Sa\_Lake\_4 (Figures 4b & 5c), this being a well-known mechanism in ice-  
10 covered fresh water lakes during spring (Mironov et al., 2002; Kirillin et al., 2012). Continued  
11 solar radiation and air temperature warming induce lake ice melt, which can also be  
12 accelerated by high wind speeds. For example, in 2009 the ice cover on Sa\_Lake\_1 was  
13 observed to drift, break-up, shrink, and then disappear, over the course of just a few days due  
14 to strong, warm winds. Satellite radar observations from 2011 show that the ice cover break-  
15 up occurred over a period of about 10 days from the beginning of June, starting with the  
16 formation of a moat. On 10<sup>th</sup> June all lakes had an ice cover with a moat (i.e. an unfrozen ring  
17 close to the shoreline); on 21<sup>st</sup> June, Sa\_Lakes 1, 2, and 3 were ice free but the largest and  
18 deepest lakes (Ku\_Lake\_1 and Sa\_Lake\_4) still had 40-50% ice cover (Table 1). Complete  
19 mixing of the water, as indicated by the first isothermal conditions after the winter  
20 stratification (Table 1), had already occurred during the early part of ice break-up (Table 1;  
21 Figures 4b, 5c). The lakes were usually ice free by the middle or end of June (Table 1).

22 Seasonal flooding by the Lena River was an additional process that had an important effect on  
23 the water temperatures in Sa\_Lake\_4 (which was formed in a former river channel) and  
24 Sa\_Lake\_1. River ice break-up and flooding took place at the end of May in all three years,  
25 when the lakes were still ice covered (Table 1). Lena River temperatures recorded over a  
26 complete year (2009-2010) showed that the river temperatures remained around 0°C during  
27 the winter, warmed up briefly for about 2 days to a peak temperature of 1.1°C (31 May 2010)  
28 and then cooled again to 0°C before steadily increasing thereafter to reach a maximum of  
29 19.4°C on 20 July 2010 (Figure 5a). Radiative under-ice warming and convection in  
30 Sa\_Lake\_4 continued until lake ice break-up in 2010, but this spring under-ice warming was  
31 interrupted in both 2011 and 2012 by intense flooding with cold Lena River water, as

1 indicated by both the temperature profiles and the water depth data (Figure 5b). The water  
2 level in this lake rose by about 1 m over the course of a few hours (28-29 May 2011 & 27-28  
3 May 2012), returning to the original level within 4-5 days. Concomitant with water level rise  
4 in Sa\_Lake\_4, the water temperatures fell to 0°C in the upper sensors (immediately beneath  
5 the ice). Lake\_Sa\_1 was also connected to the river during the flood events, as can be  
6 recognized by the slight increase in water depth at the end of May in 2010 and 2011 (no water  
7 depth data are available for 2012), but the increase was less than in Sa\_Lake\_4 (< 10 cm  
8 variation; Figure 4a).

#### 9 **4.4 Summer**

10 During the summer months positive air temperatures and continuous heat input from solar  
11 radiation steadily raised the water temperatures of the lakes at all depths, until September.  
12 Heat input from net shortwave radiation supplied about 150 W m<sup>-2</sup> in mid-July (Figure 3).  
13 Maximum air temperatures occurred over very short (daytime) periods, reaching up to more  
14 than 25°C. The highest air temperatures were recorded in July 2010, reaching a maximum of  
15 31.9°C on 5<sup>th</sup> July.

16 All of the lakes experienced short periods of thermal stratification during the summer, which  
17 varied both between the lakes and between the summers; the highest temperature gradient  
18 reached was about 5°C m<sup>-1</sup> in the deepest lake, Sa\_Lake\_4 (Figure 5). Maximum water  
19 temperatures of around 20°C were usually reached in mid-July, with up to 22°C recorded for  
20 the shallow lake (Sa\_Lake\_3). Mean monthly bottom temperatures during periods with no ice  
21 cover ranged between 4°C and 15°C (Figure 6), and can therefore be considerably higher  
22 during the summer than their annual means (Table 1).

23 The monthly bottom temperatures for some lakes were also warmer than the corresponding  
24 monthly air temperatures (Figure 6), confirming that radiation input is an important additional  
25 energy source, as well as effective mixing of the lake waters. Starting with colder mean  
26 bottom temperature in July, gradual warming creates warmest mean bottom temperatures in  
27 the deepest lake (Sa\_Lake\_4) in August and in the shallowest lake (Sa\_Lake\_3) in July. For  
28 all other lakes, maximum bottom temperatures occur either in July or August, depending on  
29 the timing of ice break up and the lake's seasonal energy balance.

1 The Wedderburn numbers are in agreement with the observed short periods of weak  
2 stratification during the ice-free period (Figures 4c, 5d). Remarkably,  $W_d$  remain rather low  
3 throughout the whole summer (between 1 and 8 for Sa\_Lake\_1 and Sa\_Lake\_4) and there are  
4 even short periods with  $W_d < 1$ . These  $W_d$  values indicate that buoyancy and wind stress  
5 were almost in equilibrium, suggesting favorable conditions for occasional upwelling of the  
6 thermocline along the upwind shorelines of the lakes, which would make an additional  
7 contribution to the mixing of water in the lakes and to the heat/mass exchange between the  
8 lakes and the atmosphere. During short periods with  $W_d < 1$  the wind stress is much greater  
9 than the buoyancy, effectively destroying the thermal stratification.

#### 10 **4.5 Lake heat content**

11 The heat content in the investigated lakes at times varied by up to  $\pm 50 \text{ MJ m}^{-2}$  over just a  
12 few days (Figure 7), with the maximum heat content being reached at the end of July or in  
13 early August. The summer heat income of the lakes was of the order of 100 to 400  $\text{MJ m}^{-2}$  and  
14 had a linear relationship with their depths (see Equation 1). The winter heat income of the  
15 lake water beneath the ice cover varied between 50 and 150  $\text{MJ m}^{-2}$ , not including the heat  
16 transfer associated with the formation of the ice cover. However, if a 2 m thick ice cover is  
17 taken into account (which is especially important for Arctic lakes; Wetzel, 2001), the annual  
18 heat budget can reach up to about 1  $\text{GJ m}^{-2}$  (Table 1).

19 Sa\_Lake\_4, which can be subjected to substantial seasonal flooding during spring, showed a  
20 reduction in heat content of about 100  $\text{MJ m}^{-2}$  (in 2010 and 2011) within a few hours, thus  
21 suppressing the ongoing radiative warming of the lake water. Although the Lena River carries  
22 a substantial amount of heat into its delta every year ( $\sim 0.49 * 10^{12} \text{ J s}^{-1}$ ; Alekseevsky, 2007)  
23 due to very warm summer temperatures, the flooding of the lakes occurs when its  
24 temperatures are at their coldest.

#### 25 **4.6 Modeled seasonal lake thermal dynamics**

26 A comparative analysis of the modeling results and observational data has revealed the  
27 capabilities of, and flaws in, the use of one-dimensional modeling to reproduce the thermal  
28 dynamics of lakes formed on permafrost, as well as providing additional quantitative insights  
29 into the major mechanisms governing the seasonal thermal dynamics of Siberian lakes. The

1 FLake model results for the Sa\_Lake\_1 over a period of 2 years (2009-2011) have been in  
2 overall good agreement with on-site observations with regard to seasonal variations in lake  
3 temperatures, the mean and maximum temperatures in winter and summer, and the durations  
4 of the open water and ice cover seasons (Figure 8a-c).

5 To quantify the model performance for thermokarst lakes we applied standard measures (e.g.  
6 Thiery et al., 2014) of the model's ability to reproduce the observed mean temperature ( $T_m$ ),  
7 the standard deviation ratio ( $SD_{\text{model}}/SD_{\text{obs}}$ ), the centered root mean squared error (RMSEc),  
8 and the Pearson correlation coefficient ( $r$ ). In contrast to other lake model evaluations using  
9 surface temperature  $T_s$  (for example, from African and West European lakes), we used  $T_m$   
10 since no temperature probes were installed at the surface due to the seasonal ice cover. FLake  
11 demonstrated good performance with regard to the mean lake temperature. The statistics—  
12 Pearson correlation coefficient  $r = 0.97$ ,  $SD_{\text{model}}/SD_{\text{obs}} 1.28$ , RMSE 1.49 °C are slightly worse  
13 than those reported previously for temperate lakes ( $r = 0.988$ ; Stepanenko et al., 2010) and  
14 better than FLake performance on deep tropical lakes ( $r = 0.78$ ,  $SD_{\text{model}}/SD_{\text{obs}} 1.25$ , RMSE  
15 0.75 °C; Thiery et al., 2014). The model reproduced summer stratification during the ice free  
16 period ( $r = 0.93$ ,  $SD_{\text{model}}/SD_{\text{obs}} 1.25$ , RMSE 1.82 °C). Solar heating of the water below the ice  
17 is not included in the model and thus the agreement between model and observations is lower  
18 during the ice-covered period ( $r = -0.42$ ,  $SD_{\text{model}}/SD_{\text{obs}} 0.37$ , RMSE 0.66 °C). The resulting  
19 uncertainties in the ice break up prediction affect also the model performance with regard to  
20 the lake heat content at the beginning of the open water period in early summer (Figure 8). As  
21 thermal dynamics under the ice cover are crudely reproduced by the majority of 1-  
22 dimensional lake models used in coupled climate modeling systems (Stepanenko et al., 2010),  
23 estimation of the role played by thermokarst lakes in regional climate requires integration of a  
24 cost-effective and physically sound sub-model of winter lake thermodynamics into lake  
25 parameterization schemes for climate models (e.g. Oveisy and Boegman 2014).

26

#### 27 **4.6.1 Open water period and summer stratification**

28 The duration of the warming and cooling periods, as well as the mean water temperatures  
29 during the autumn cooling, are well simulated by the model suggesting that the model  
30 adequately captures the net heat storage of the lakes. The model was also able to reproduce



1 the development of weak thermal stratification in summer (i.e. the short periods during which  
2 the bottom temperatures differed from the mean temperatures of the lakes in June and July,  
3 2010 and 2011: Figure 8c). The largest discrepancies in the water temperatures produced by  
4 the model occurred during the period of spring warming, with maximum deviations of about  
5 6°C from the measured mean temperatures (Figure 8). These deviations can be explained by  
6 the ice break-up being modeled too early, with subsequent early warming of the lake. Lake  
7 temperatures were consequently consistently overestimated during the warming period in  
8 2010.

#### 9 **4.6.2 Ice duration and thickness, and water temperatures beneath the ice** 10 **cover**

11 The mean rate of ice growth modeled with FLake was about 0.92 cm day<sup>-1</sup> for 2010  
12 (minimum 0.021 cm day<sup>-1</sup>, maximum 8 cm day<sup>-1</sup>) and 0.89 cm day<sup>-1</sup> for 2011 (minimum  
13 0.026 cm day<sup>-1</sup>, maximum 4.6 cm day<sup>-1</sup>), with the maximum thickness of ice cover remaining  
14 below 2 m. The modeled ice thickness of no more than 2 m agrees well with the temperature  
15 data from the sensor located 4 m above the sediment (approximately 2 m from the lake  
16 surface) in Sa\_Lake\_1 (Figure 4b). This sensor did not record any freezing in 2010 or 2011,  
17 but in 2012 the sensor froze into the lake ice (Figure 4b), recording sub-zero temperatures and  
18 thus indicating thicker ice (> 2 m) in 2012.

19 The modeled melting of the ice cover in spring and subsequent warming of lake temperatures  
20 is, in general, well reproduced by the model. The measured development of under-ice bottom  
21 temperatures (with warming following the onset of ice cover formation, followed by a later  
22 winter cooling) is only partly reproduced in the modeled results due to rather simplified  
23 parameterization of the under-ice thermodynamics in the FLake model, with a linear vertical  
24 temperature profile in the ice-covered water column and no solar radiation penetrating the ice  
25 cover.

#### 26 **4.6.3 Thermal properties of the lake sediments and water-sediment heat flux**

27 Heat conduction from a lake's water column to the underlying sediment is a key  
28 thermodynamic process for understanding the role of lakes in the permafrost landscape. The  
29 Flake model incorporates simulation of seasonal temperature variations within the thermally  
30 active sediment layer, based on an assumption of thermal equilibrium in the sediment over

1 longer-than-seasonal time scales (i.e. a constant temperature beneath the seasonally thermally  
2 active sediment layer, ensuring zero mean annual flux across the water-sediment boundary;  
3 Golosov and Kirillin, 2010). Since this thermal equilibrium does not necessarily exist in lakes  
4 on permafrost, we performed two separate model experiments with different thermal  
5 conditions beneath the lakes, based on temperature profiles measured in lake sediments at  
6 comparable sites in the Lena River Delta (Grigoriev 1993; Figure 9). While the sediment  
7 temperature beneath the shallow lake fell to below 0°C at about 2 m depth and reached -6°C  
8 at 15 m depth, the temperatures beneath the deeper lake indicated an unfrozen layer to about  
9 25 m depth, with a maximum temperature of about 4.5°C at a depth of about 3 m beneath the  
10 lake floor (Figure 9 a, b). The reported temperatures at depth, where seasonal variations were  
11 minimal, ranged from -6°C beneath the 1 m deep lake to 4°C beneath the 5 m deep lake.  
12 Using the measured temperature profile below the 5 m deep lake, the thickness of the  
13 sediment layer with appreciable seasonal variations in temperature was estimated to be ~6 m  
14 (Figure 9 b). The FLake modeled heat flux at the lake-sediment boundary for different ground  
15 temperatures revealed two characteristic seasonal patterns of lake-permafrost heat exchange:  
16 the flux across the frozen sediment beneath the shallow lake was directed downwards during  
17 the summer, with a magnitude of up to 4 W m<sup>-2</sup>, the fast release of heat from the sediment  
18 during autumn cooling, and the water-sediment heat flux of ~0 W m<sup>-2</sup> during the entire ice-  
19 covered period (Figure 9 c). This seasonal pattern suggests an annually positive heat budget  
20 of the under-lake ground and thawing of the permafrost, which is continuously heated by the  
21 lake above. For a lake with deep temperatures approaching 4°C, the annual mean flux across  
22 the sediment tended towards zero, with maximum downward fluxes in summer of 3 W m<sup>-2</sup>, a  
23 maximum of 7 W m<sup>-2</sup> heat released back into the water column during early freeze back, and  
24 a continuous low rate of < 1 W m<sup>-2</sup> during the ice-covered winter (Figure 9 d). In the absence  
25 of any additional information available on the ground temperatures under Sa\_Lake\_1, the  
26 latter case was adopted for the longer model run (Figures 8b, c), with an “equilibrium state”  
27 suggesting little or no permafrost thawing beneath the lake. The maximum modeled heat flux  
28 at the sediment-water interface was about 4 W m<sup>-2</sup> into the sediment (in summer) and about 7  
29 W m<sup>-2</sup> (to almost zero) from the sediment into the water column during the ice-covered  
30 period. The rapidly changing (negative) hourly heat fluxes during the fall cooling period were  
31 due to rapid cooling of the water column, which could not be reproduced by the model.

1 Overall, the calculated energy density for the lake with mean annual water temperature of 3°C  
2 is about 65 MJ m<sup>-3</sup>, thus more than six times the amount for the permafrost soil of about 10  
3 MJ m<sup>-3</sup>. Lakes are therefore effective for energy storage compared to the frozen landscape,  
4 and the fraction of landscape covered by thermokarst lakes has the potential to significantly  
5 affect the land-atmosphere energy exchange.

6

7

## 8 **5 Discussion**

9 Lakes can be considered to represent “hot spots” in the permafrost landscape. This study has  
10 demonstrated that the investigated lakes remain unfrozen throughout the winter and have  
11 mean bottom water temperatures (between 2.7 to 4.0°C) that are significantly warmer than the  
12 mean annual air temperature (~ -13°C) or the permafrost temperature (-9.2°C at 10.7 m  
13 depth). This is in agreement with observations made by Jorgenson et al. (2010) who reported  
14 thermokarst lake-bottom temperatures in Alaska that were up to 10°C warmer than the mean  
15 annual air temperatures. Harris (2002) attributed the anomalously high mean annual  
16 temperature in a shallow lake in western Canada to convective heat exchange and the  
17 absorption of radiation through the water column. Mean annual lake-bottom temperatures in  
18 northern Alaska also showed a similar range of values (Arp et al. 2012; CALON), and this  
19 range has therefore been used in previous modeling studies to estimate the development of  
20 talik (Burn, 2002; Ling and Zhang, 2003). Differences in heat content are related to  
21 morphometric parameters, particularly to water depth. Burn (2002) found mean annual lake-  
22 bottom temperatures of between 1.5°C and 4.8°C for the deeper pools in tundra lakes on  
23 Richards Island (north-western Canada). Ensom et al. (2012) reported mean annual bottom  
24 temperatures of between 3.4°C and 5.5°C from a number of lakes and channels in the  
25 Mackenzie Delta (Canada) and computed that 60% of the lakes maintained taliks.

26 Mean bottom lake temperatures, which ranged between 2.7 and 4 °C in this study, depend on  
27 lake depth and are important for constraining future numerical modeling experiments on talik  
28 development. Our study also confirms previous findings that there is a “critical lake depth”  
29 (lake depth > winter ice cover thickness) for water to remain unfrozen beneath the ice cover

1 (Arp et al., 2012; Burn, 2002). All lakes in this study had a depth > 3 m, which exceeds the  
2 maximum ice thickness of about 2 m.

3 The bottom temperatures in the lakes varied significantly between summer and winter but  
4 their annual mean temperatures and temperature dynamics were similar despite the range of  
5 morphometric and geomorphological characteristics. The Wd numbers indicated that the lakes  
6 were all well-mixed during the summer periods, and it can therefore be assumed that both  
7 heat and dissolved gases, in particular, oxygen, are effectively transported through the water  
8 column. This assumption is supported by the measured oxygen concentrations in these lakes,  
9 which ranged between 8 and 10 mg l<sup>-1</sup>, and the lack of any detected vertical stratification (R.  
10 Osudar, personal communication, 2015).

11 We observed and simulated short stratification periods in summer in the studied lakes  
12 (Figures 4 & 5). These stratification events are probably the major physical factor affecting  
13 biogeochemical processes in lakes. In particular, the duration of the thermal stratification in  
14 summer affects the concentration and vertical distribution of dissolved oxygen. Longer  
15 summer stratification provokes deep anoxia and favors methanogenesis in the deep water  
16 column and upper sediment (Golosov et al., 2012). Under equal climatic forcing, lake depth is  
17 the primary factor determining the duration of summer stratification (the second one being the  
18 water transparency, Kirillin, 2010). Sensitivity model runs with the lake depth varying in the  
19 range 2-12 m using the same meteorological input data from Samoylov demonstrated that  
20 lakes in this climatic zone with mean depths >5 m should have dimictic stratification regimes,  
21 i.e. develop continuous stratification in summer with a duration of 1 month or longer (Figure  
22 10). This also supports the observation of summer stratification in deeper (> 6 m) Alaskan  
23 thermokarst lakes (Sepulveda-Jáuregui et al., 2015). In lakes of about 8 m depth or more, the  
24 summer stratification duration significantly increases since high thermal inertia prevents  
25 vertical mixing during the autumn cooling in August-September (Figure 11).

26 The summer heat budgets of Arctic lakes are much smaller than those of low-latitude lakes.  
27 The only previously reported summer heat budget for an Arctic lake (Chandler Lake, Alaska)  
28 was 240 MJ m<sup>-2</sup>, which lies in the same range as the heat budgets in this study (Wetzel, 2001).  
29 In contrast, the summer heat budget for a large lake such as Lake Superior on the Canada-  
30 USA border is much larger at about 1.3 GJ m<sup>-2</sup>. In comparison, the annual heat budget of  
31 Lake Baikal in Siberia is estimated to be about 2.7 GJ m<sup>-2</sup> (Wetzel, 2001). The total annual

1 heat budget for all of the investigated lakes (including the latent heat of the ice cover)  
2 amounts up to about  $1 \text{ GJ m}^{-2}$  (Table 1). In view of the large proportion of land covered by  
3 water bodies in this landscape (25%) and the volumes of water that they contain, their energy  
4 storage and turnover within the permafrost landscape are of considerable significance.  
5 Furthermore, changes in the heat content of lakes occur much more rapidly than changes in  
6 the heat content of the surrounding permafrost soils as a result of efficient energy absorption  
7 and effective mixing. In contrast, progressive deepening of the seasonally thawing upper layer  
8 of permafrost (the active layer) of the polygonal tundra landscape at this site takes several  
9 months and only reaches a maximum thaw depth of about 0.6 m (Boike et al., 2013). Lakes  
10 also have an important effect on the subsurface thermal conditions beneath the lake and  
11 potentially also in the surrounding permafrost. Our results show that, during the summer, heat  
12 is continuously transferred from lake water into the bottom sediment. The importance of  
13 summer heat gain and its dissipation into the water body and the underlying sediment was  
14 first discussed by Vtyurina (1960), using data from a 12 m deep lake in Siberia. Her findings  
15 showed heat fluxes directed into the sediments during winter (Figure 5 in Vtyurina, 1960; also  
16 reported in Grosse et al., 2013) which, according to our findings, is an indicator of permafrost  
17 thaw. Our modeling results, however, suggest that the temperature increase associated with  
18 permafrost thaw eventually results in a net annual heat equilibrium between deeper lakes and  
19 the underlying sediments, characterized by a continuous negative heat flux (i.e. heat loss from  
20 the sediment into the water column) during the long ice-covered winter and heat gain by the  
21 sediment during the open water summer period. The warming of lake-bottom temperatures  
22 with the onset of ice cover was initially attributed by Brewer (1958) to heating by shortwave  
23 solar radiation and by Mortimer and Mackereth (1958) to the heat release from the lake  
24 sediment. Our observed near-bottom temperatures increased beneath the ice cover and the  
25 modeling experiments suggested this warming was solely due to heat flow from the sediment,  
26 with typical rates of  $< 10 \text{ W m}^{-2}$ . However, the heat flux from the sediment in tundra lakes  
27 appears to decay within less than one month, which is much faster than in ice-covered lakes  
28 of the temperate and boreal climates (cf. Rizk et al. 2014), and is followed by a gradual  
29 decrease of the deep water temperatures. The latter is not reproduced by the parameterized  
30 sediment module of FLake.

31

1 Our numerical modeling of the thermal dynamics of lakes has shown that the basic processes  
2 can be accurately reproduced for the summer. However, the model parameters that yielded the  
3 best fit for the seasonal heat budget and ice cover duration resulted in less accurate predictions  
4 of the bottom temperature under ice. Lake temperatures increase, starting in spring 1-2  
5 months before ice-off, apparently by radiative solar heating. This temperature increase  
6 suggests that radiation can make a significant direct contribution to sediment heating in  
7 shallow and clear-water thermokarst lakes – a contribution that is usually neglected in lake  
8 models. The concept of self-similarity cannot account for the permafrost-talik specific lake  
9 processes, such as (i) warming of bottom waters immediately following onset of ice formation  
10 and (ii) phase change in the lake’s frozen sediment, i.e. annual freeze thaw processes and  
11 thawing at the talik-permafrost boundary. While the short period of warming of bottom water  
12 is due to heat flux from the sediment into the water body, the cooling in winter from mid-  
13 winter onwards suggests a loss of heat. This heat loss may occur through transmission into  
14 both the sediment and the atmosphere, the latter being of minor importance due to isolation of  
15 the water column by the ice cover. Further investigations into these processes of warming and  
16 subsequent gradual cooling under the ice cover would require a more advanced lake model  
17 that is able to take into account deep, continuously frozen sediments and characteristic  
18 processes such as thawing.

19

## 20 **6 Summary and conclusions**

21 We have measured and modeled the thermal dynamics of lakes in the Lena River Delta of  
22 northern Siberia over a three year period (2009-2012), with the objective of understanding  
23 and quantifying the important thermal processes that operate in this permafrost environment.  
24 The investigated lakes were situated in two different geomorphologic settings (sediments of  
25 the Pleistocene Ice Complex and on a younger river terrace) with a range of morphometric  
26 characteristics. Some of the lakes were seasonally connected to the Lena River through high  
27 floods that occurred during spring. Such annual flooding of these lakes by cold river water  
28 results in a significant reduction in the ongoing warming (and thus sensible heat storage),  
29 depending on the magnitude of the flooding. A schematic summary of our results is provided  
30 in Figure 12.

1 The lakes were shown to receive substantial energy for warming from net shortwave radiation  
2 during the summer. Warming also occurs during the ice cover period in spring, resulting in  
3 convective mixing beneath the ice cover. Mixing also occurs following ice break-up, during  
4 the summer, and during the fall cooling, resulting in efficient heat transfer to bottom waters  
5 and across the sediment-water interface. Numerical modeling suggests that the annual mean  
6 net heat flux across the bottom sediment boundary is approximately zero, with positive  
7 summer downward fluxes during the ice-free period (4 months) and heat-release back into the  
8 water column at much lower rates during the ice-covered period (8 months). Overall, the ice  
9 formation and thaw together account for most of the annual variations in a lake's heat content.  
10 Furthermore, their timing and durations determine the magnitude and direction of bottom  
11 sediment heat fluxes and the timing of water column mixing. Future warming may result in  
12 changes to the ice cover but may also produce more pronounced summer stratification, thus  
13 potentially reducing the heat input into the sediment layers.

14 In view of the large area covered by water bodies in permafrost landscapes (25% of the land  
15 surface) and their efficiency at energy absorption and mixing, these water bodies are clearly  
16 of considerable importance with respect to energy storage and turnover, atmospheric fluxes,  
17 and sediment heat fluxes in permafrost landscapes.

18 The investigated thermokarst lakes are representative of Arctic tundra lowlands characterized  
19 by thermokarst processes that are common for large regions in Central and East Siberia,  
20 Interior and Northern Alaska as well as Northwest Canada. Despite their importance,  
21 however, lakes are not yet included in earth system models. Future work should therefore  
22 include lakes in these models and test their sensitivity to possible future changes in climate.

23

24 Author contributions: J. Boike designed the research and led the discussions, supported by G.  
25 Kirilin and M.Langer. The FLake modeling was carried out by G. Kirilin and C. Georgi. The  
26 paper was written by J.Boike, with comments from all authors.

27

28 Acknowledgements: The logistical support provided by the Russian Research station on  
29 Samoylov Island is gratefully acknowledged. Field support, including data collection, was  
30 provided by Grigoriy Soloviev, Waldemar Schneider, Günther Stoof, and Karoline

1 Wischnewski. Elizabeth Miller, Max Heikenfeld, Wil Lieberman-Cribbin and Stephan Lange  
2 assisted with the data analysis and helpful discussions. The authors acknowledge the financial  
3 support provided through the European Union's FP7-ENV PAGE21 project under contract  
4 number GA282700, and through the Feodor Lynen grant from the Alexander-von-Humboldt  
5 Foundation awarded to Moritz Langer. The research was carried out under the Russian  
6 government's Program of Competitive Growth, Kazan Federal University.



## 1 **References**

- 2 Alekseevsky, N. I. (Ed.): Geocological state of Russian Arctic coast and their safety of  
3 nature management (in Russian), GEOS Publ., Moscow, Russia, 586 pp., 2007.
- 4 Abnizova, A., Siemens, J., Langer, M., and Boike, J.: Small ponds with major impact: The  
5 relevance of ponds and lakes in permafrost landscapes to carbon dioxide emissions, *Global*  
6 *Biogeochem. Cycles*, 26, GB2041, doi: 10.1029/2011gb004237, 2012.
- 7 Alerstam, T., Gudmundsson, G. A., Green, M., and Hedenström, A.: Migration along  
8 orthodromic sun compass routes by arctic birds, *Science*, 291, 300-303, 2001.
- 9 Are F. E.: Thermal regime of small thermokarst lakes in the Siberian Taiga zone (for example  
10 of Central Yakutia) (in Russian), Collection of papers "Lakes of Cryolithozone of Siberia",  
11 edited by: Are F.E., Nauka, Siberian brunch, 98-116, 1974.
- 12 Arp, C. D., Jones, B. M., Whitman, M., Larsen, A., and Urban, F. E.: Lake Temperature and  
13 Ice Cover Regimes in the Alaskan Subarctic and Arctic: Integrated Monitoring, Remote  
14 Sensing, and Modeling, *J. Am. Water Resour. Assoc.*, 46, 777-791, doi: 15, 10.1111/j.1752-  
15 1688.2010.00451.x, 2010.
- 16 Arp, C. D., Jones, B. M., Lu, Z., and Whitman, M. S.: Shifting balance of thermokarst lake  
17 ice regimes across the Arctic Coastal Plain of northern Alaska, *Geophys. Res. Lett.*, 39, doi:  
18 10.1029/2012gl052518, 2012.
- 19 Boike, J., Wille, C., and Abnizova, A.: Climatology and summer energy and water balance of  
20 polygonal tundra in the Lena River Delta, Siberia, *J. Geophys. Res.*, 113, G03025,  
21 doi:10.1029/2007JG000540, 2008.
- 22 Boike, J., Kattenstroth, B., Abramova, K., Bornemann, N., Chetverova, A., Fedorova, I.,  
23 Fröb, K., Grigoriev, M., Grüber, M., Kutzbach, L., Langer, M., Minke, M., Muster, S., Piel,  
24 K., Pfeiffer, E. M., Stoof, G., Westermann, S., Wischnewski, K., Wille, C., and Hubberten, H.  
25 W.: Baseline characteristics of climate, permafrost and land cover from a new permafrost  
26 observatory in the Lena River Delta, Siberia (1998-2011), *Biogeosciences*, 10, 2105-2128,  
27 doi: 10.5194/bg-10-2105-2013, 2013.
- 28 Burn, C. R.: Tundra Lakes and Permafrost, Richards Island, Western Arctic Coast, Canada,  
29 *Canadian Journal Earth Science*, 39, 1281-1298, doi:10.1139/E02-035, 2002.

- 1 Burn, C. R.: Lake-bottom Thermal Regimes, Western Arctic Coast, Canada, Permafr.  
2 Periglac. Proc., 16, 355–367, doi: 10.1002/PPP.542, 2005.
- 3 Brewer, M. C.: The thermal regime of an arctic lake, EOS Transactions ,American  
4 Geophysical Union, 39, 2, 278-284, doi: 10.1029/TR039i002p00278, 1958: Costard, F., and  
5 Gautier, E.: The Lena River: Hydromorphodynamic Features in a Deep Permafrost Zone, in:  
6 Large Rivers: Geomorphology and Management, edited by: Gupta, A., John Wiley & Sons,  
7 Ltd, West Sussex, England, 225-233, 2007.
- 8 Chetverova, A., Fedorova, I., Potapova, T., Boike, J.: Hydrological and geochemical features  
9 of lakes of Samoylov Island of the Lena River Delta./ Proceedings of AARI, № 1 (95), 97-  
10 110, 2013 (in Russian).
- 11 Ensom, T. P., Burn, C. R., and Kokelj, S. V.: Lake- and channel-bottom temperatures in the  
12 Mackenzie Delta, Northwest Territories, Can. J. Earth Sci., 49, 16, 963-978, doi:  
13 10.1139/e2012-001, 2012.
- 14 Fedorova, I., Chetverova, A., Bolshiyarov, D., Makarov, A., Boike, J., Heim, B.,  
15 Morgenstern, A., Overduin, P. P., Wegner, C., Kashina, V., Eulenburg, A., Dobrotina, E., and  
16 Sidorina, I.: Lena Delta hydrology and geochemistry: long-term hydrological data and recent  
17 field observations, Biogeosciences, 12, 345-363, doi: 10.5194/bg-12-345-2015, 2015.
- 18 Golosov, S., and Kirillin, G.: A parameterized model of heat storage by lake sediments,  
19 Environ. Model. Software, 25, 793-801, doi: 10.1016/j.envsoft.2010.01.002, 2010.
- 20 Golosov, S., Terzhevik, A., Zverev, I., Kirillin, G. and Engelhardt, C.: Climate change impact  
21 on thermal and oxygen regime of shallow lakes. Tellus A, 64, 17264, doi:  
22 10.3402/tellusa.v64i0.17264, 2012.
- 23 Gordeev, V. V., and Sidorov, I. S.: Concentrations of major elements and their outflow into  
24 the Laptev Sea by the Lena River, Marine Chemistry, 43, 33-45, 1993.
- 25 Grigoriev, M.: Cryomorphogenesis of the Lena River mouth area (in Russian), Siberian  
26 Branch, USSR Academy of Sciences, Yakutsk, 176 pp., 1993.
- 27 Grigoriev, N. F.: The temperature of permafrost in the Lena delta basin–deposit conditions  
28 and properties of the permafrost in Yakutia (in Russian), Yakutsk, 2, 97-101, 1960.

1 Grigoriev, N. F. Perennially frozen rocks of the maritime lowlands of Yakutia (in Russian),  
2 Moscow, Nauka, 80, pp, 1966.

3 Grosse, G., Jones, B., and Arp, C. D.: Thermokarst Lakes, Drainage, and Drained Basins, in:  
4 Treatise on Geomorphology, edited by Giardino, R. & Harbor, J., 8 Glacial and Periglacial  
5 Geomorphology, 29, 325-353, Academic Press, San Diego, CA, doi: 10.1016/B978-0-12-  
6 374739-6.00216-5, 2013.

7 Harris, S. A.: Causes and consequences of rapid thermokarst development in permafrost or  
8 glacial terrain, *Permafr. Periglac. Proc.*, 13, 237-242, doi: 10.1002/ppp.419, 2002.

9 Hinkel, K. M., Lenters, J. D., Sheng, Y., Lyons, E. A., Beck, R. A., Eisner, W. R., Maurer, E.  
10 F., Wang, J., and Potter, B. L.: Thermokarst Lakes on the Arctic Coastal Plain of Alaska:  
11 Spatial and Temporal Variability in Summer Water Temperature, *Permafr. Periglac. Proc.*, 23,  
12 207-217, doi: 10.1002/ppp.1743, 2012.

13 Hobbie, J. E., and Kling, G. W.: Alaska's changing Arctic: Ecological consequences for  
14 tundra, streams, and lakes, Oxford University Press, 352 pp., 2014.

15 Jeffries, M. O., Zhang, T., Frey, K., and Kozlenko, N.: Estimating Late-Winter Heat Flow to  
16 the Atmosphere from the Lake-Dominated Alaskan North Slope, *Journal Glaciology*, 45, 315-  
17 347, 1999.

18 Jorgenson, M. T., Romanovsky, V., Harden, J., Shur, Y., O'Donnell, J., Schuur, E. A. G.,  
19 Kanevskiy, M., and Marchenko, S.: Resilience and vulnerability of permafrost to climate  
20 change, *Canadian Journal of Forest Research*, 40, 1219-1236, doi: 10.1139/x10-060, 2010.

21 Kalnay, E., Kanamitsu, M., Kistler, R., Collins, W., Deaven, D., Gandin, L., Iredell, M., Saha,  
22 S., White, G., Woollen, J., Zhu, Y., Leetmaa, A., Reynolds, R., Chelliah, M., Ebisuzaki, W.,  
23 Higgins, W., Janowiak, J., Mo, K. C., Ropelewski, C., Wang, J., Jenne, R., and Joseph, D.:  
24 The NCEP/NCAR 40-Year Reanalysis Project, *Bull. Am. Meteorol. Soc.*, 77, 437-471, 1996.

25 Keatley, B. E., Douglas, M. S. V., and Smol, J. P.: Physical and chemical limnological  
26 characteristics of lakes and ponds across environmental gradients on Melville Island,  
27 Nunavut/N.W.T., High Arctic Canada, *Fundamental and Applied Limnology - Archiv für*  
28 *Hydrobiologie*, 168, 355–376, doi: 10.1127/1863-9135/2007/0168-0355, 2007.

- 1 Kirillin, G.: Modeling the impact of global warming on water temperature and seasonal  
2 mixing regimes in small temperate lakes. *Boreal Environ. Res*, 15, 279-293, 2010.
- 3
- 4 Kirillin, G., Leppäranta, M., Terzhevik, A., Granin, N., Bernhardt, J., Engelhardt, C.,  
5 Efremova, T., Golosov, S., Palshin, N., and Sherstyankin, P.: Physics of seasonally ice-  
6 covered lakes: a review, *Aquat. Sci.*, 74, 659-682, 2012.
- 7 Lachenbruch, A. H.: Mechanics of thermal contraction cracks and ice-wedge polygons in  
8 permafrost, *Special papers*, 70, Geological Society of America, New York, 69 pp., 1962.
- 9 Langer, M., Westermann, S., Muster, S., Piel, K., and Boike, J.: The surface energy balance  
10 of a polygonal tundra site in northern Siberia Part 1: Spring to fall, *The Cryosphere*, 5, 151-  
11 171, doi: 10.5194/tc-5-151-2011, 2011a.
- 12 Langer, M., Westermann, S., Muster, S., Piel, K., and Boike, J.: The surface energy balance  
13 of a polygonal tundra site in northern Siberia - Part 2: Winter, *The Cryosphere*, 5, 509-524,  
14 doi: 10.5194/tc-5-509-2011, 2011b.
- 15 Langer, M., Westermann, S., Heikenfeld, M., Dorn, W., and Boike, J.: Satellite-based  
16 modeling of permafrost temperatures in a tundra lowland landscape, *Remote Sensing of*  
17 *Environment*, 135, 12-24, doi: 10.1016/j.rse.2013.03.011, 2013.
- 18 Langer, M., Westermann, S., Walter Anthony, K., Wischnewski, K., and Boike, J.: Frozen  
19 ponds: production and storage of methane during the Arctic winter in a lowland tundra  
20 landscape in northern Siberia, Lena River delta, *Biogeosciences*, 12, 977-990, doi:  
21 10.5194/bg-12-977-2015, 2015.
- 22 Laurion, I., Vincent, W.F., Retamal, L., Dupont, C., Francus, P., MacIntyre, S. & Pienitz, R.:  
23 Variability in greenhouse gas emissions from permafrost thaw ponds. *Limnology and*  
24 *Oceanography* 55, 115-133, 2010.
- 25 Lehner, B., and Döll, P.: Development and validation of a global database of lakes, reservoirs  
26 and wetlands, *Journal of Hydrology*, 296, 1-22, 2004.
- 27 Ling, F., and Zhang, T.: Numerical simulation of permafrost thermal regime and talik  
28 development under shallow thaw lakes on the Alaskan Arctic Coastal Plain, *J. Geophys. Res.*,  
29 108, 4511, doi: 10.1029/2002JD003014, 2003.

1 Luecke, C., Giblin, A. E., Bettez, N. D., Burkart, G. A., Crump, B. C., Evans, M. A., Gettel,  
2 G., McIntyre, S., O'Brien, W. J., Rublee, P. A., and King, G. W.: The response of lakes near  
3 the Arctic LTER to environmental change, in: *Alaska's changing Arctic: ecological  
4 consequences for tundra, streams, and lakes*, edited by: Hobbie, J., and Kling, G. W., Oxford  
5 University Press, New York, 238-286, 2014.

6 Martynov, A., Sushama, L. and Laprise, R.: Simulation of temperate freezing lakes by one-  
7 dimensional lake models: performance assessment for interactive coupling with regional  
8 climate models. *Boreal Environ. Res.*, 15(2), 143-164, 2010.

9 Martynov, A., Sushama, L., Laprise, R., Winger, K., and Dugas, B.: Interactive lakes in the  
10 Canadian Regional Climate Model, version 5: the role of lakes in the regional climate of  
11 North America, *Tellus A*, 64, 16226, doi: 10.3402/tellusa.v64i0.16226, 2012.

12 Mironov, D. V., Terzhevik, A., Kirillin, G., Jonas, T., Malm, J., and Farmer, D.: Radiatively  
13 driven convection in ice-covered lakes: Observations, scaling, and a mixed layer model,  
14 *Journal of Geophysical Research: Oceans*, 107, 7, 1-16, doi: 10.1029/2001JC000892, 2002.

15 Mironov, D. V.: Parameterization of lakes in numerical weather prediction. Description of a  
16 lake model, COSMO technical report, 2005.

17 Mironov, D., B. Ritter, J.-P. Schulz, M. Buchhold, M. Lange, and E. Machulskaya:  
18 Parameterization of sea and lake ice in numerical weather prediction models of the German  
19 Weather Service. *Tellus A*, 64, 17330. doi: 10.3402/tellusa.v64i0.17330, 2012 Morgenstern,  
20 A., Grosse, G., Günther, F., Fedorova, I., and Schirrmeister, L.: Spatial analyses of  
21 thermokarst lakes and basins in Yedoma landscapes of the Lena Delta, *The Cryosphere*, 5,  
22 849-867, 10.5194/tc-5-849-2011, 2011.

23 Morgenstern, A., Grosse, G., Günther, F., Fedorova, I., and Schirrmeister, L.: Spatial analyses  
24 of thermokarst lakes and basins in Yedoma landscapes of the Lena Delta, *The Cryosphere*, 5,  
25 849-867, doi:10.5194/tc-5-849-2011, 2011.

26 Morgenstern, A., Ulrich, M., Günther, F., Roessler, S., Fedorova, I. V., Rudaya, N. A.,  
27 Wetterich, S., Boike, J., and Schirrmeister, L.: Evolution of thermokarst in East Siberian ice-  
28 rich permafrost: A case study, *Geomorphology*, 201, 363-379, doi:  
29 10.1016/j.geomorph.2013.07.011, 2013.

- 1 Mortimer, C. and Mackereth F: Convection and its consequences in ice-covered lakes. Verh  
2 Int Ver Limnol, 13, 923–932, 1958.
- 3
- 4 Muster, S., Langer, M., Heim, B., Westermann, S., and Boike, J.: Subpixel heterogeneity of  
5 ice-wedge polygonal tundra: a multi-scale analysis of land cover and evapotranspiration in the  
6 Lena River Delta, Siberia, *Tellus B*, 64, 17301, doi: 10.3402/tellusb.v64i0.17301, 2012.
- 7 Nolan, M., and Brigham-Grette, J.: Basic hydrology, limnology, and meteorology of modern  
8 Lake El'gygytgyn, Siberia, *J. Paleolimnol.*, 37, 17-35, doi: 10.1007/s10933-006-9020-y,  
9 2006.
- 10 Oveisy, A. and Boegman, L.: One-dimensional simulation of lake and ice dynamics during  
11 winter. *J. Limnol.*, 73, doi: 10.4081/jlimnol.2014.903, 2014.
- 12 Pavlov A.V., Tishin M.I.: Heat balance of a large lake and surrounding area in central Yakutia  
13 (in Russian), Collection of papers "Structure and thermal regime of frozen rocks", edited by:  
14 Katasonova E.G., Pavlov A.V., Nauka, Siberian branch, 53-62 1981.
- 15 Pienitz, R., Smol, J. P., and Lean, D. R. S.: Physical and Chemical limnology of 59 lakes  
16 located between the southern Yukon and the Tuktoyaktuk Peninsula, Northwest Territories  
17 (Canada), *Can. J. Fish. Aquat. Sci.*, 54, 330-346, 1997.
- 18 Rawlins, M. A., Serreze, M. C., Schroeder, R., Zhang, X., and McDonald, K. C.: Diagnosis of  
19 the record discharge of Arctic-draining Eurasian rivers in 2007, *Environmental Research*  
20 *Letters*, 4, 1-8, 2009.
- 21 Read, J. S., Hamilton, D. P., Jones, I. D., Muraoka, K., Winslow, L. A., Kroiss, R., Wu, C. H.,  
22 and Gaiser, E.: Derivation of lake mixing and stratification indices from high-resolution lake  
23 buoy data, *Environ. Model. Software*, 26, 1325-1336, doi: 10.1016/j.envsoft.2011.05.006,  
24 2011.
- 25 Rizk, W., Kirillin, G. and Leppäranta, M.: Basin-scale circulation and heat fluxes in ice-  
26 covered lakes. *Limnol. Oceanogr.*, 59, 445-464, 2014.
- 27 Sepulveda-Jauregui, A., Walter Anthony, K. M., Martinez-Cruz, K., Greene, S., and  
28 Thalasso, F.: Methane and carbon dioxide emissions from 40 lakes along a north–south

- 1 latitudinal transect in Alaska, *Biogeosciences*, 12, 3197-3223, doi:10.5194/bg-12-3197-2015,  
2 2015.
- 3 Schertzer, W. M.: Freshwater Lakes, in: *Surface climates of Canada*, edited by: Bailey, W. G.,  
4 Oke, T. R., and Rouse, W. R., McGill-Queens University Press, Montreal, 124-148, 1997.
- 5 Schneider von Deimling, T., Grosse, G., Strauss, J., Schirrmeister, L., Morgenstern, A.,  
6 Schaphoff, S., Meinshausen, M., and Boike, J.: Observation-based modelling of permafrost  
7 carbon fluxes with accounting for deep carbon deposits and thermokarst activity, *Biogeosci.*  
8 *Disc.*, 11, 16599-16643, doi: 10.5194/bgd-11-16599-2014, 2014.
- 9 Schwamborn, G., Rachold, V., and Grigoriev, M. N.: Late Quaternary sedimentation history  
10 of the Lena Delta, *Quat. Int.*, 89, 119-134, doi: 10.1016/S1040-6182(01)00084-2, 2002.
- 11 Sobiech, J., Boike, J., and Dierking, W.: Observation of melt onset in an Arctic Tundra  
12 landscape using high resolution TerraSAR-X and RADARSAT-2 data, *IGARSS*, Munich,  
13 Germany, 3552–3555, 2012.
- 14 Spigel, R. H., and Imberger, J. The classification of mixed-layer dynamics of lakes of small  
15 to medium size. *Journal of physical oceanography*, 10(7), 1104-1121, 1980.
- 16 Stefan, J.: Über die Theorie der Eisbildung, insbesondere über die Eisbildung im Polarmeere,  
17 *Annalen der Physik*, 278, 269-286, 1891.
- 18 Stepanenko, V.M., Goyette, S., Martynov, A., Perroud, M., Fang, X. and Mironov, D.: First  
19 steps of a lake model intercomparison Project: LakeMIP. *Bor. Environ. Res.*, 15, 191-202,  
20 2010.
- 21 Thiery, W., Stepanenko, V. M., Fang, X., Jöhnk, K. D., Li, Z., Martynov, A., Perroud, M.,  
22 Subin, Z. M., Darchambeau, F., Mironov, D., and van Lipzig, N. P. M.: LakeMIP Kivu:  
23 evaluating the representation of a large, deep tropical lake by a set of one-dimensional lake  
24 models, 2014, doi: 10.3402/tellusa.v66.21390, 2014.
- 25 Vincent, A. C., Mueller, D. R., and Vincent, W. F.: Simulated heat storage in a perennially  
26 ice-covered high Arctic lake: Sensitivity to climate change, *J. Geophys. Res.*, 113, C04036,  
27 doi: 10.1029/2007JC004360, 2008.
- 28 Vincent, W.F., Pienitz, R., Laurion, I. and Walter Anthony, K.: Climate impacts on Arctic  
29 lakes. In: Goldman, C.R., Kumagai, M. and Robarts, R.D. (eds). *Climatic Change and Global*

- 1 Warming of Inland Waters: Impacts and Mitigation for Ecosystems and Societies, John Wiley  
2 & Sons, Ltd, Chichester, U.K., 27-42, 2013.
- 3 Vtyurina, E. A.: Temperature regime of the Lake Glubokoe Trudy institute merzlotovedeniya  
4 im. V.A. Obrucheva. AN SSSR, Moscow, 132-140, 1960 (in Russian).
- 5 Walsh, S. E., Vavrus, S. J., Foley, J. A., Fisher, V. A., Wynne, R. H., and Lenters, J. D.:  
6 Global Patterns of Lake Ice Phenology and Climate: Model Simulation and Observation, J.  
7 Geophys. Res., 103, 28, 825-828, 1998.
- 8 Walter, K. M., Zimov, S. A., Chanton, J. P., Verbyla, D., and Chapin III, F. S.: Methane  
9 bubbling from Siberian thaw lakes as a positive feedback to climate warming, Nature, 443,  
10 71-75, doi: 10.1038/nature05040, 2006.
- 11 Welch, H. E., and Bergmann, M. A.: Water circulation in small arctic lakes in winter, Can. J.  
12 Fish. Aquat. Sci., 42, 506-520, 1985.
- 13 Wetterich, S., Schirrmeister, L., Meyer, H., Andreas, F. A., and Mackensen, A.: Arctic  
14 freshwater ostracods from modern periglacial environments in the Lena River Delta (Siberian  
15 Arctic, Russia): geochemical applications for palaeoenvironmental reconstructions, J.  
16 Paleolimnol., 39, 427-449, doi: 10.1007/s10933-007-9122-1, 2008.
- 17 Wetzel, R. G.: Limnology: lake and river ecosystems, 3rd ed., Gulf Professional Publishing,  
18 Orlando, 1006 pp., 2001.
- 19 Yi, S., Wischniewski, K., Langer, M., Muster, S., and Boike, J.: Freeze/thaw processes in  
20 complex permafrost landscapes of northern Siberia simulated using the TEM ecosystem  
21 model: impact of thermokarst ponds and lakes, Geoscientific Model Development, 7, 1671-  
22 1689, doi: 10.5194/gmd-7-1671-2014, 2014.
- 23



1 Table 1. Physical and chemical characteristics of the studied lakes in the Lena River Delta,  
 2 Siberia

	Sa_Lake_1	Sa_Lake_2	Sa_Lake_3	Sa_Lake_4	Ku_Lake_1
Area [m <sup>2</sup> ]	39,541	39,991	23,066	47,620	1,730,000 <sup>a</sup>
Max. depth [m]	6.4	5.7	3.4	11.6	3.6 <sup>a</sup>
Mean depth [m]	3	3.1	1.2	4.5	2.4
Volume [m <sup>3</sup> ]	106,500	103,600	18,800	175,121	3,321,000
Volume/Area [m]	2.7	2.6	0.8	3.7	1.8
Perimeter [m]	1,931	1,471	1,760	1,474	5,170 <sup>a</sup>
Period of data collection	04 July 2009 - 07 Aug. 2012	10 July 2009 - 07 Aug. 2012	13 July 2009 - 14 Aug. 2012	06 July 2009 - 06 Aug. 2012	24 July 2009 - 29 July 2010
Location	126.486 E, 72.373 N	126.496 E, 72.378 N	126.511 E, 72.374 N	126.505 E, 72.369 N	126.177 E, 72.328 N
Start of ice cover formation (temp. diff. from bottom to top > 0.1°C)	05 Oct. 2009 01 Oct. 2010 02 Oct. 2011	1 Oct. 2009 28 Sep. 2010 05 Oct. 2011	04 Oct. 2009 30 Sep. 2010 26 Sep. 2011	04 Oct. 2009 28 Sep. 2010 4 Oct. 2011	04 Oct. 2009 02 Oct. 2010
Start of ice cover break-up (temp.	04 July 2009 14 June 2010	12 July 2009 23 June 2010	24 June 2009 14 June 2010	07 July 2009 20 June 2010	24 July 2009 20 June 2010

diff. from bottom to top > 0.1°C)	08 June 2011	16 June 2011	10 June 2011	20 June 2011	
	15 June 2012	15 June 2012	10 June 2012	21 June 2012	
% ice cover (satellite radar data <sup>b)</sup> 2011	5 June:100%	5 June: 100%	5 June: 100%	5 June: 95%	5 June: 95%
	10 June: 95%	10 June: 100%	10 June: 90%	10 June: 95%	10 June: 95%
	16 June: 85%	16 June: 90%	16 June: ice free	16 June: 85%	16 June: 90%
	21 June: ice free	21 June: ice free		21 June: 50%	21 June: 40%
					27 June: ice free
2012	27 June: ice free	27 June: ice free	27 June: ice free	27 June: ice free	05 June: 90%
					27 June: ice free
Mean annual bottom temperature [°C] (2010-2011)	3.7	3.6	2.7	2.9	4.0
Winter lake water heat budget [MJ m <sup>-2</sup> ]	93	66	44	145	61
Summer lake water heat budget [MJ m <sup>-2</sup> ]	140	206	161	340	112
Annual lake heat budget	[233]	[272]	[205]	[485]	[173]
	838	877	810	1090	778

[MJ m<sup>-2</sup>]

(2010-2011)

c, d

Residence time [years] <sup>e</sup>	14	14	4	24	9
Electrical conductivity [μS cm <sup>-1</sup> ]	140 <sup>f</sup>	127 <sup>f</sup>	64 <sup>i</sup>	185 <sup>f</sup> 59 <sup>g</sup> 80 <sup>h</sup>	30 <sup>i</sup>
pH-value <sup>f</sup>	6.99 <sup>f</sup>	6.82 <sup>f</sup>	7.3 <sup>i</sup>	6.95 <sup>f</sup> 7.36 <sup>g</sup> 7.28 <sup>h</sup>	7.64 <sup>i</sup>

---

1

2 <sup>a</sup> data provided in Morgenstern et al. (2011, 2013) and <http://doi.pangaea.de/10.1594/PANGAEA.848485>

3 <sup>b</sup> Sobiech et al. (2012) & TerraSar-X data (copyright: DLR, 2011) where available with sufficiently high  
4 resolution

5 <sup>c</sup> numbers in brackets represent the total annual lake water budget (sensible heat), without taking into account the  
6 latent heat of ice cover formation

7 <sup>d</sup> includes latent heat for the formation of a 2 m ice cover (605 MJ m<sup>-2</sup>)

8 <sup>e</sup> residence time  $F = V/E$ ; roughly approximated by the ratio of the lakes's volume ( $V$ ) divided by the sum of  
9 evapotranspiration ( $E$ ) and runoff  $R$  ( $F = V/(E-R)$ ; Schertzer 1997). Within the study area, the annual  
10 evapotranspiration is about ~190 mm and runoff is to be negligible within the overall water balance (Boike et al.,  
11 2013)

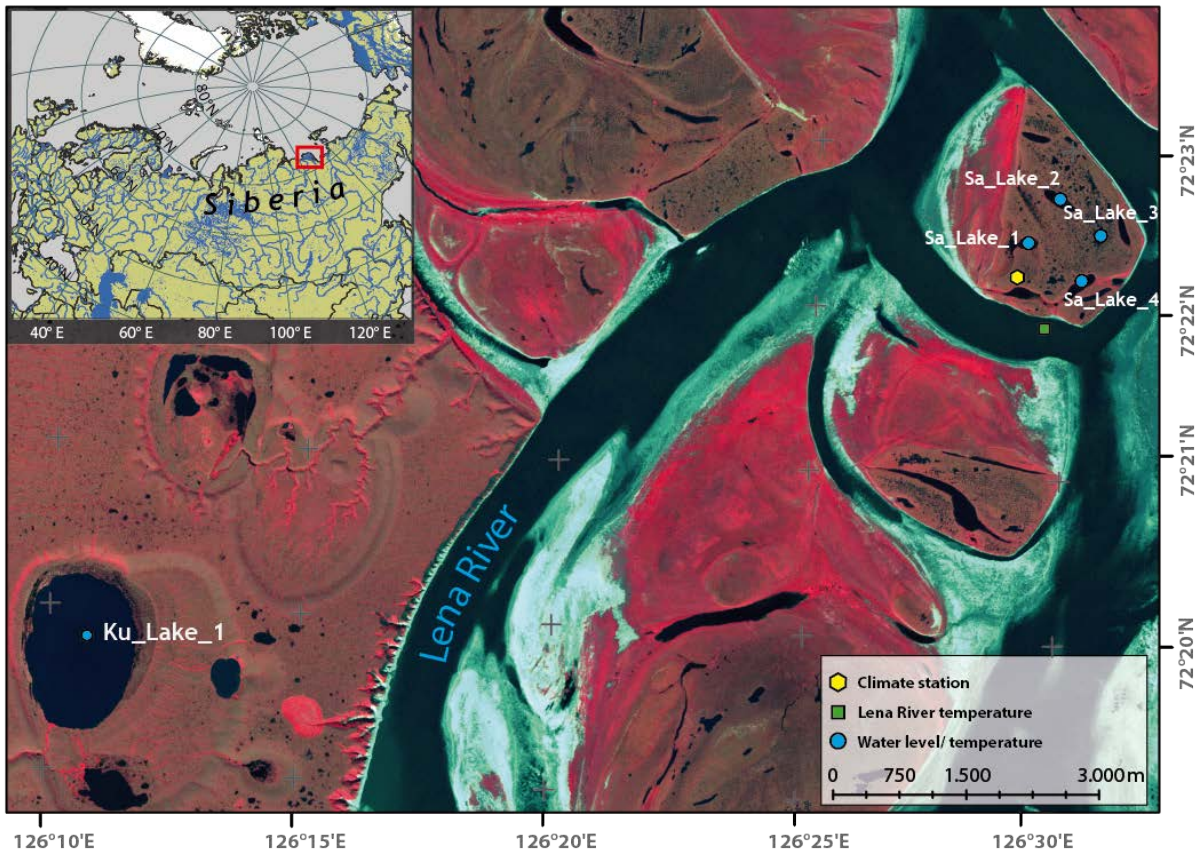
12 <sup>f</sup> mean value for ice-covered period (April – May 2014)

13 <sup>g</sup> mean value for the Lena River flood period (May – June 2014)

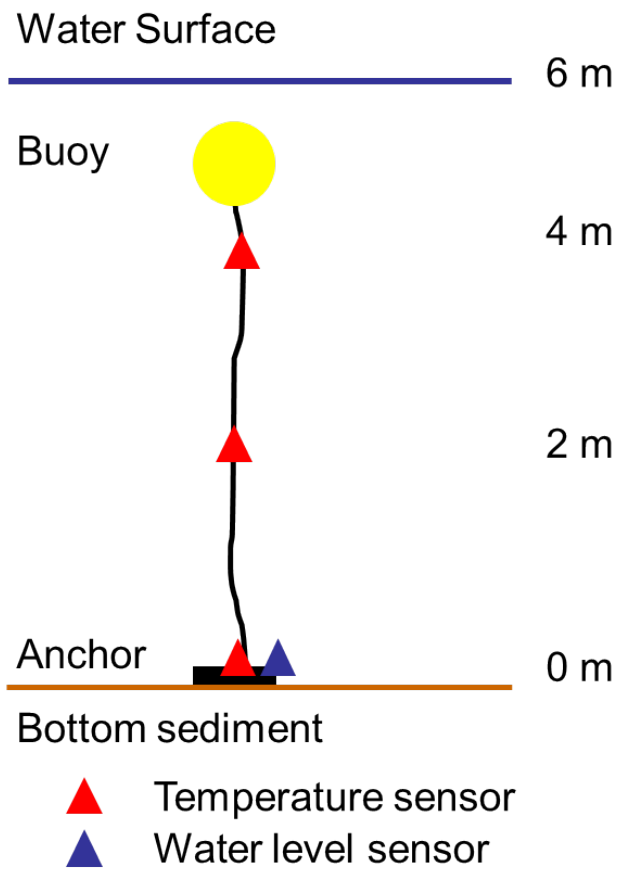
14 <sup>h</sup> mean value for summer period (July – August 2014)

15 <sup>i</sup> mean value for summer period (measured in July 2009)

16

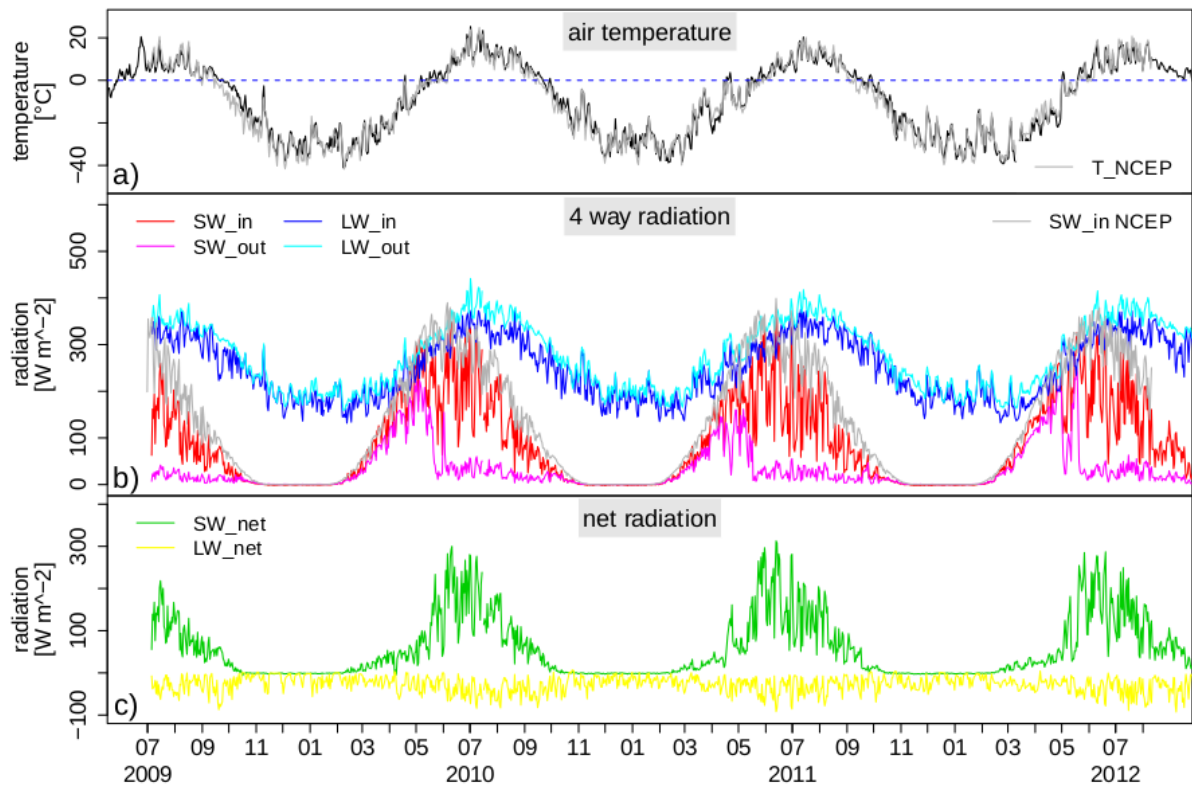


1 126°10'E 126°15'E 126°20'E 126°25'E 126°30'E  
 2 Figure 1. Location of the study sites in the Lena River Delta of eastern Siberia; sites are  
 3 within the zone of continuous permafrost on the islands of Kurungnakh (Ku\_Lake\_1), and  
 4 Samoylov (Sa\_Lakes\_1-4). The inset map shows the location of the Lena River Delta in  
 5 northern Eurasia and the distribution of lakes (Global lakes and wetland map; Lehner and  
 6 Döll, 2004).



1

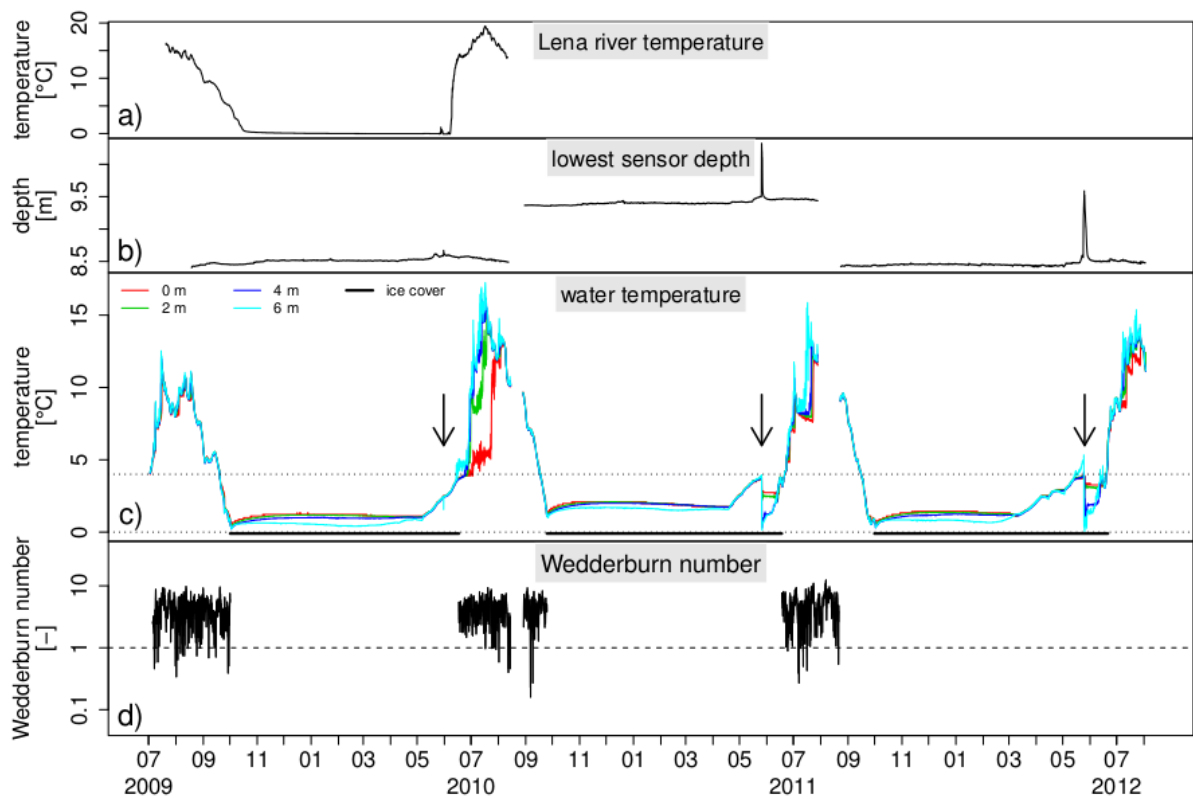
2 Figure 2. Schematic diagram showing the positions of sensors within the water column. To  
 3 prevent freezing of the buoy within the ice cover (maximum 2 m thick), sensors were  
 4 deployed 2 m below the water surface in most lakes. The water level sensor was located just  
 5 above the bottom sensor, referred to in Figures 4 & 5 as the “lowest sensor depth”.



1

2 Figure 3. a) Mean daily air temperature at 2 m above ground level from Samoylov and NCEP;  
 3 b) radiation balance (Samoylov) and shortwave incoming radiation (NCEP); c) net shortwave  
 4 and longwave radiation (Samoylov) and radiation balance measured at the Samoylov climate  
 5 station July 2009 - August 2012.

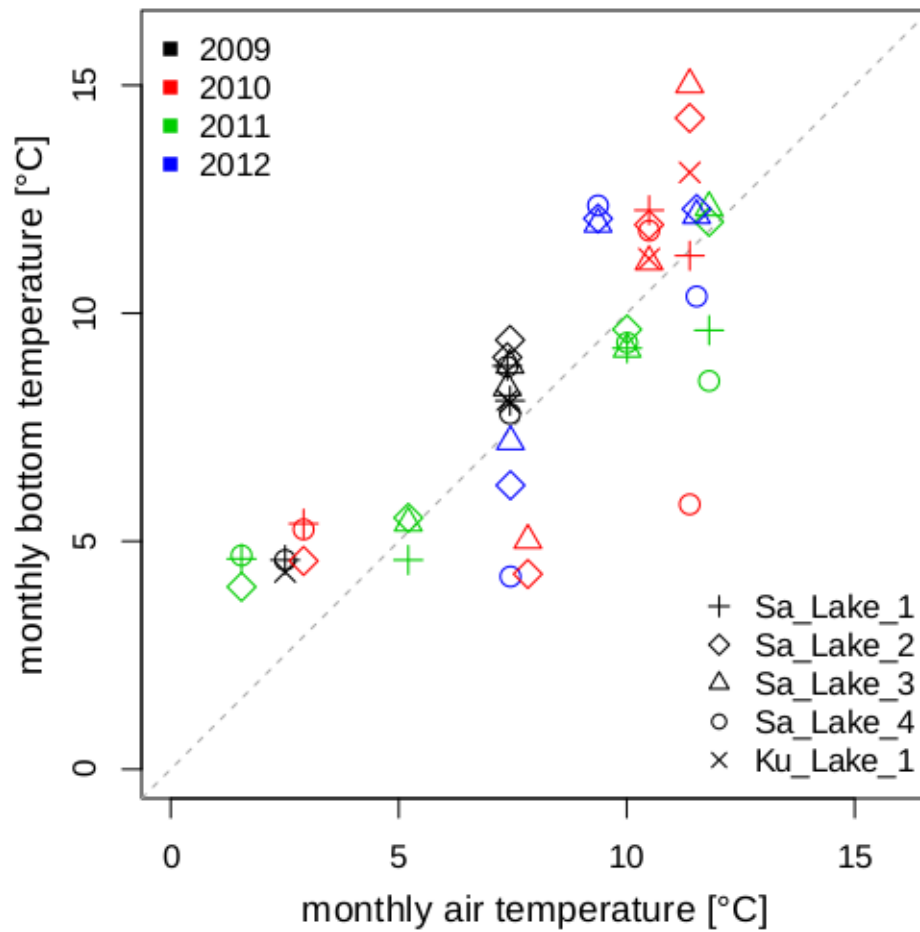




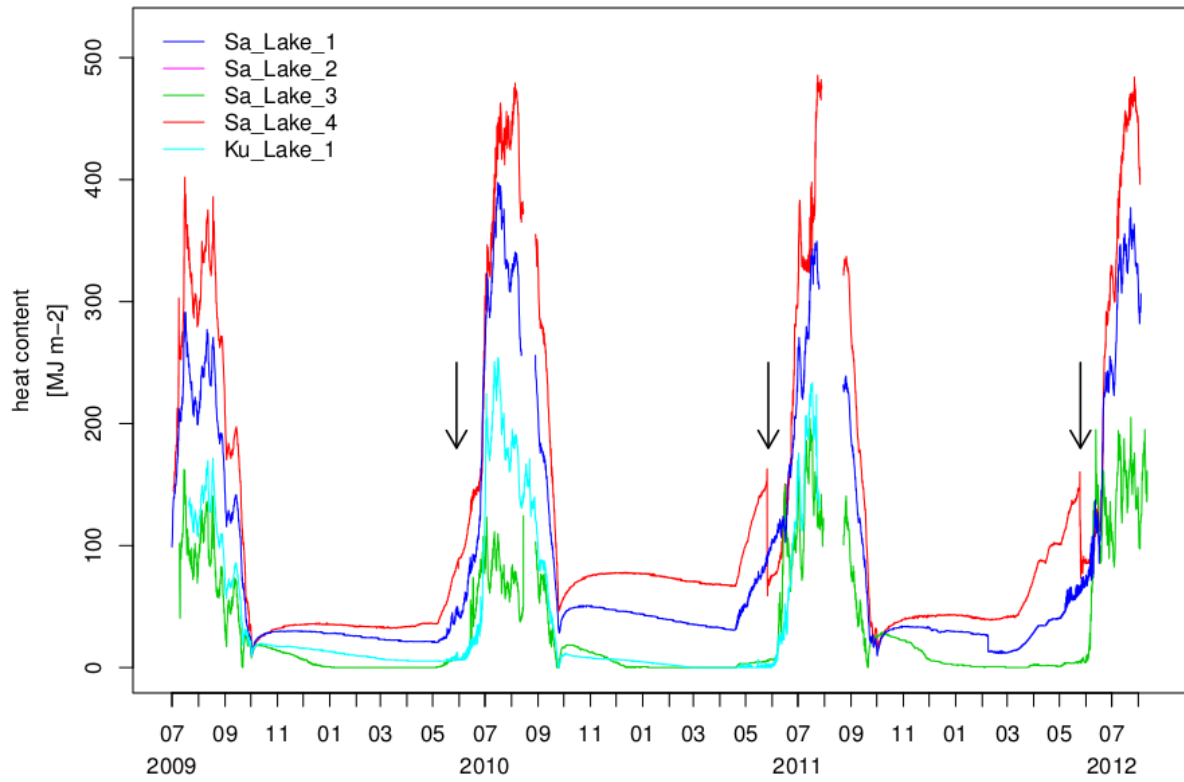
1

2 Figure 5. a) Hourly temperatures for the Lena River from July 2009 to July 2010, and for  
 3 Sa\_Lake\_4 (July 2009-August 2012): b) depth of bottom sensor as indicator for water level  
 4 changes: sharp increase in depth during May 2011 and 2012 indicates flooding with Lena  
 5 River water; c) water temperatures and ice cover duration (estimated from lake water  
 6 temperatures); d) Wedderburn number (dimensionless) calculated for the ice-free period.  
 7 Arrows indicate the timing of the lake's seasonal flooding by Lena river water.





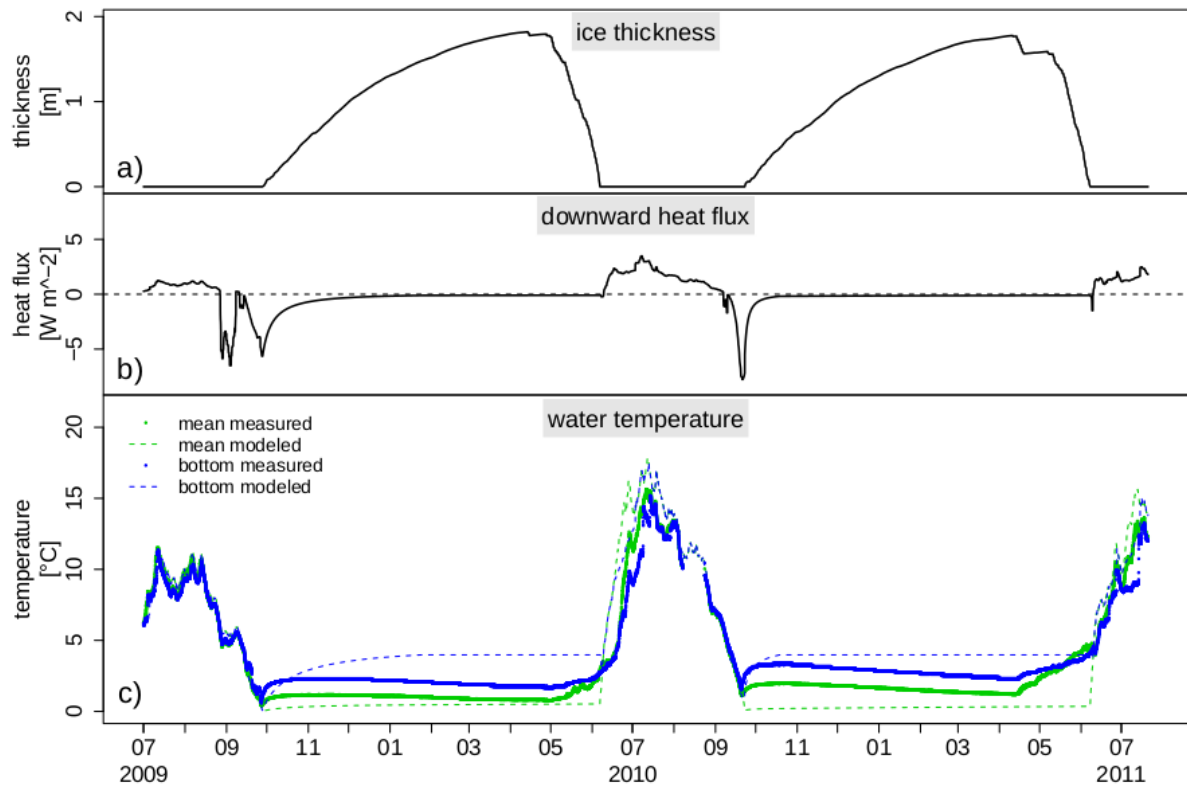
1  
 2 Figure 6. Relationship between mean monthly lake bottom temperatures for all five lakes  
 3 during the ice free period and the corresponding mean monthly air temperatures, from July  
 4 2009 to August 2012. Data are also provided in the supplementary material of this paper.



1

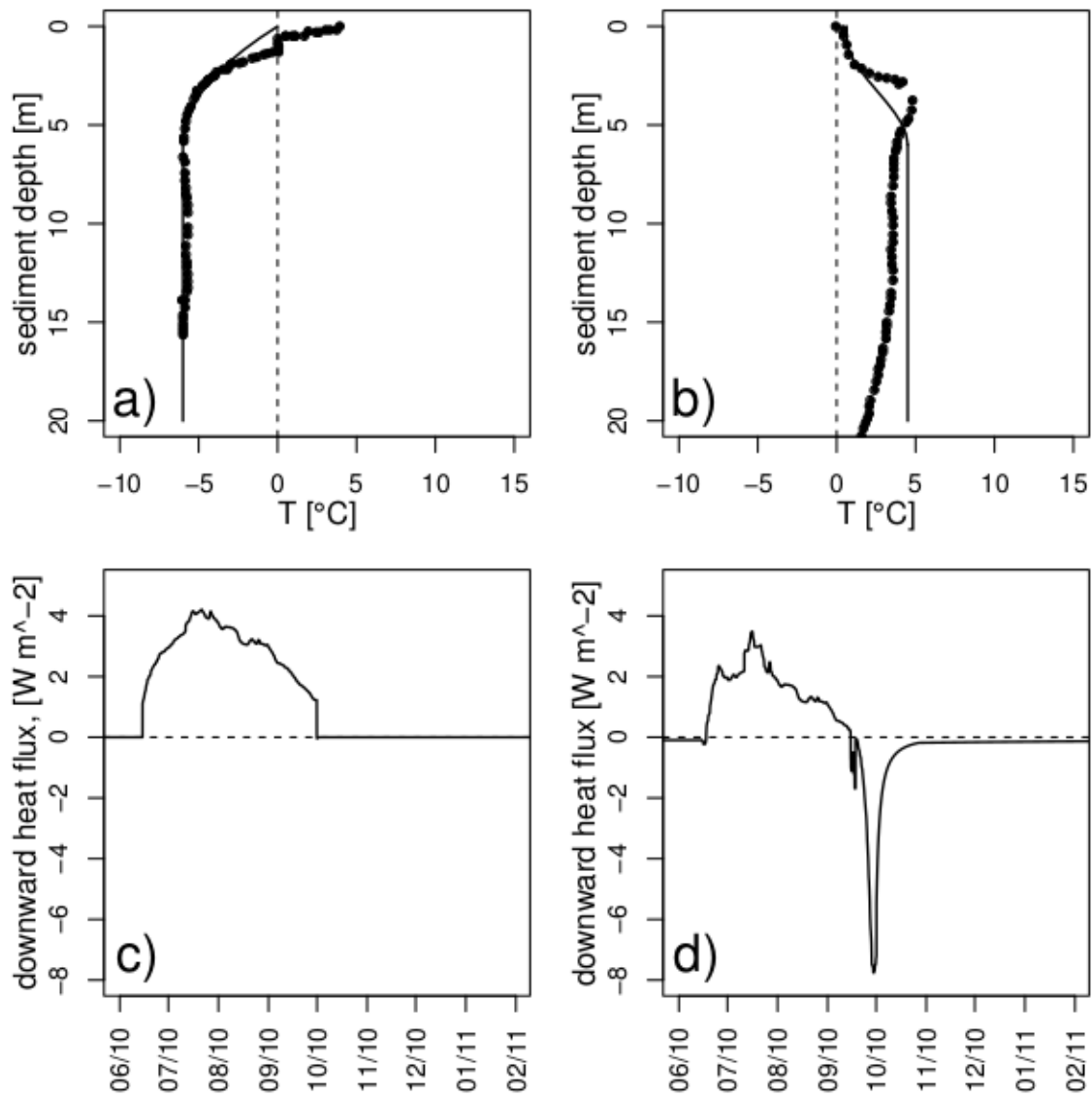
2 Figure 7. Sensible heat content (calculated using Equation 1) for the five lakes, from July  
 3 2009 to August 2012. Arrows indicate the timing of the lake's seasonal flooding by Lena river  
 4 water.

5

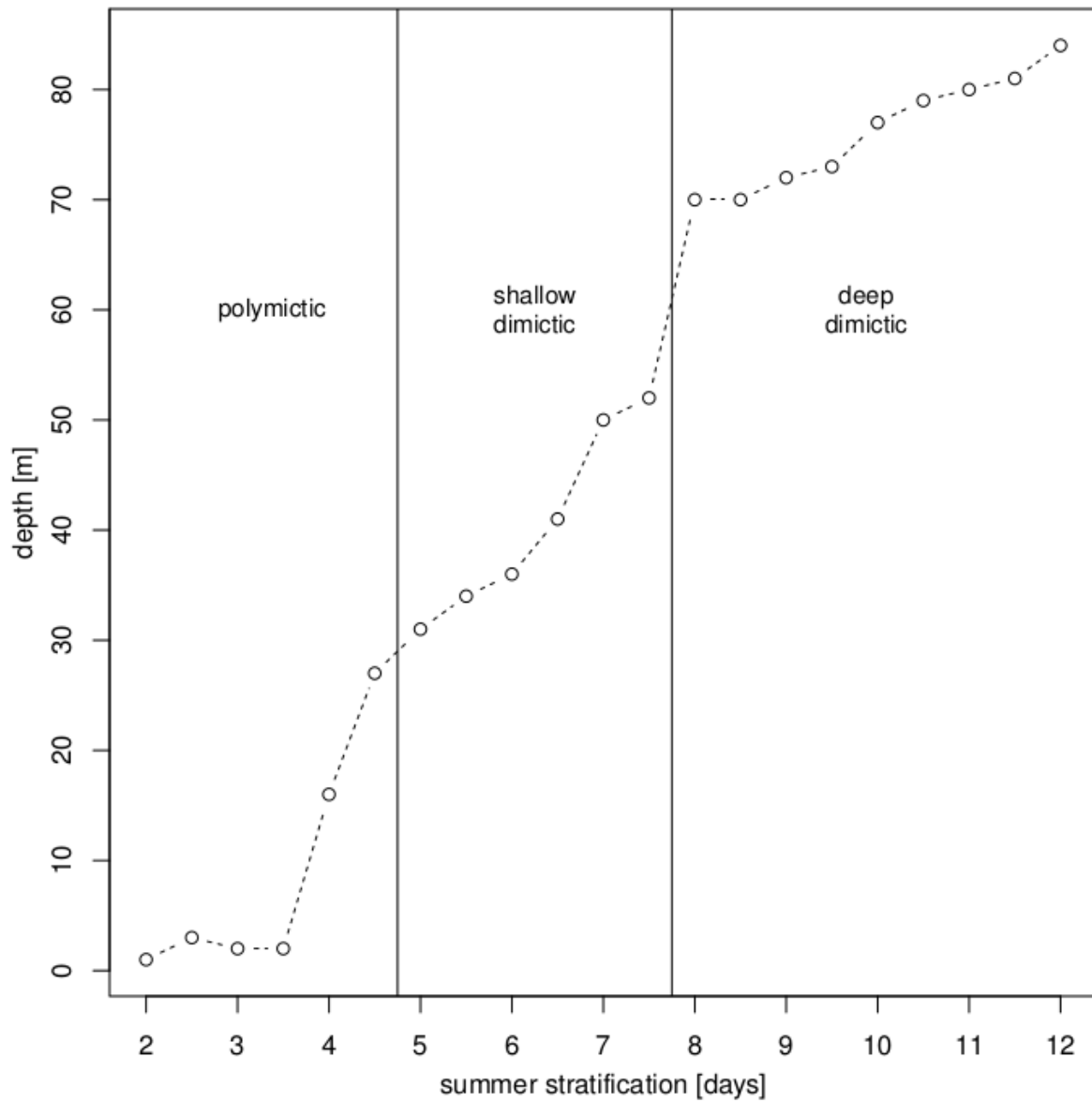


1

2 Figure 8. Modeled and measured hourly characteristics for Sa\_Lake\_1 from August 2009 to  
 3 August 2011. a) Modeled ice thickness; b) modeled vertical heat flux at the water-sediment  
 4 boundary: negative fluxes indicate fluxes from the sediment into the water column - a running  
 5 median filter was used to remove spikes; c) measured (continuous line) and modeled (dashed  
 6 lines) lake-bottom and mean water temperatures.

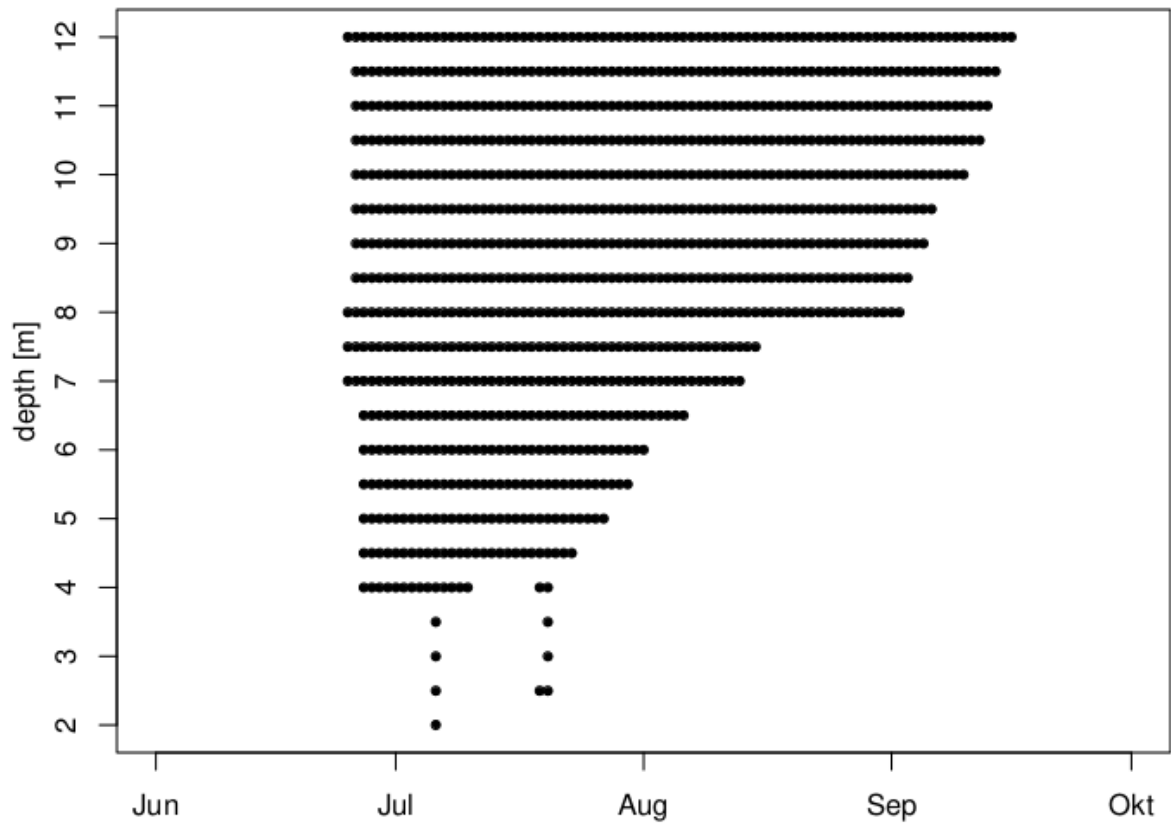


1  
 2 Figure 9. a & b) Measured temperature profiles (squares) beneath two lakes (with a) 1 m  
 3 water depth, and b) 5 m water depth) on the Bykovsky Peninsula, in the south-eastern part of  
 4 the Lena River Delta (Grigoriev, 1993). Temperatures were measured between 9 and 11 June  
 5 1984. Modeled sediment temperature profiles (continuous line) are for 10 June 2010 using  
 6 model parameters described in the Methods section. c & d) Modeled daily vertical heat flux at  
 7 the water-sediment boundary for c) the shallow lake, and d) the deep lake, 2010-2011.



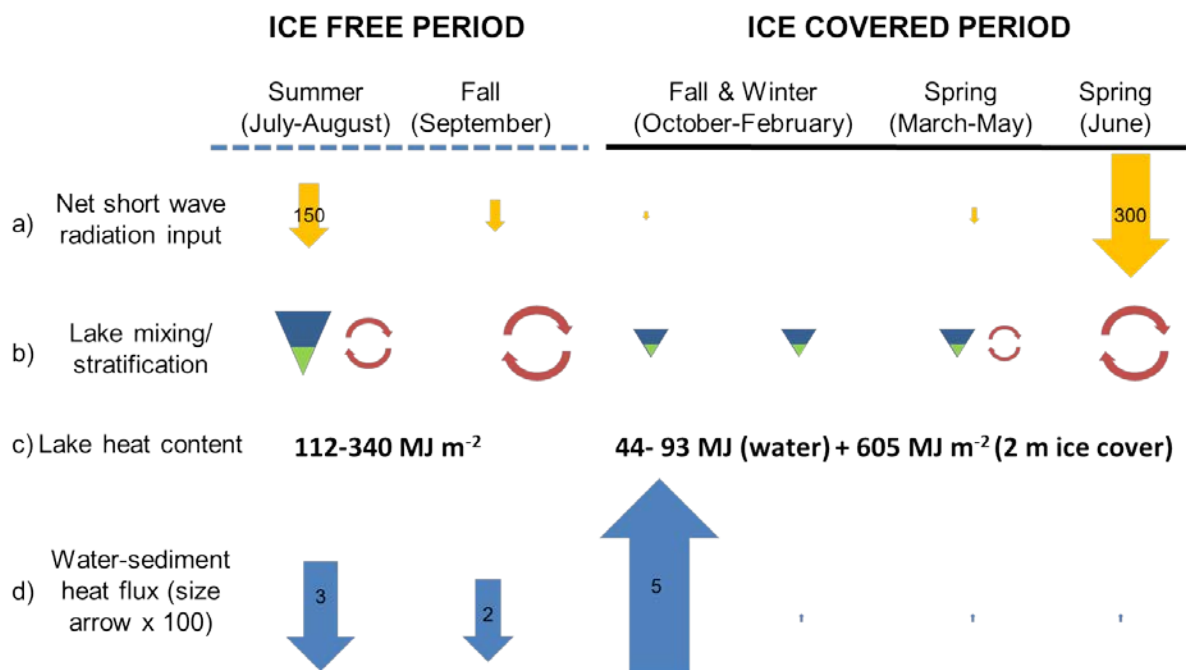
1

2 Figure 10. Total number of days with summer stratification in lakes of varying depths  
 3 modeled with FLake driven by the meteorological data from the Samoylov observatory  
 4 station for 2010. Existence of stratification was determined by the criterion  $(T_s - T_b) > 0.5^\circ\text{C}$ ,  
 5 where  $T_s$  and  $T_b$  are the modeled temperatures at lake surface and lake bottom, respectively.



1  
2  
3  
4  
5

Figure 11. Summer stratification duration in lakes of varying depth (see Fig. 10 for definitions).



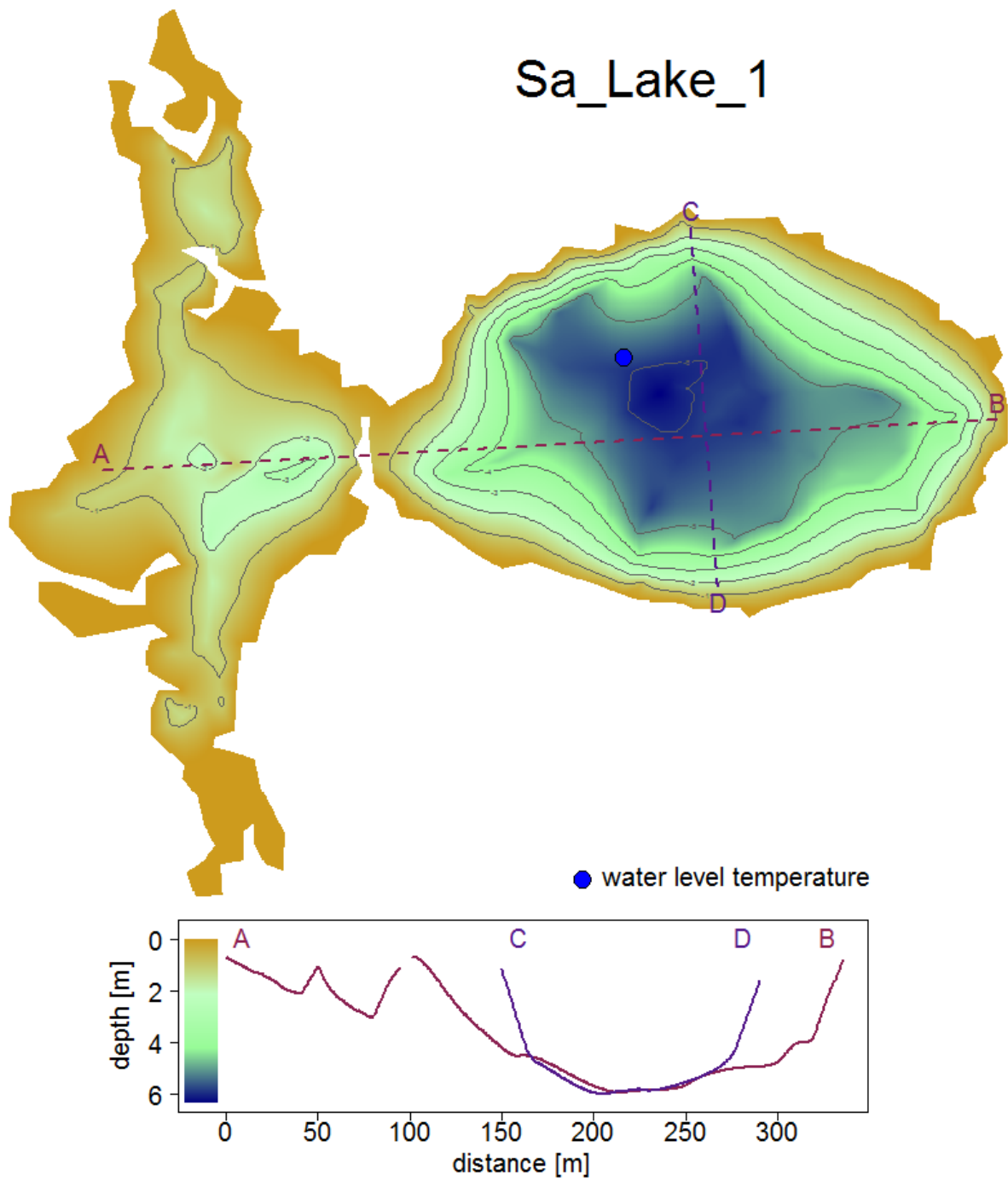
1  
2 Figure 12. Summary of thermal processes in thermokarst lakes over a one year cycle. a) Net  
3 short wave radiation input (measured at the climate station on Samoylov); b) dominant in-lake  
4 processes (mixing and stratification) - size of symbol reflects intensity of process; c) lake heat  
5 content (divided into summer and winter lake heat content according to Wetzel, 2001); d)  
6 average heat fluxes across the lake's water-sediment boundary: downward arrows denote heat  
7 flux into the sediment and upward arrows flux out of the sediment into the water column. The  
8 size of the arrows and their numbers indicate the relative magnitudes of the fluxes [W m<sup>-2</sup>].  
9 Note that the sizes of arrows representing bottom heat fluxes have been enlarged by a factor  
10 of 100 due the small magnitude of the fluxes.

11  
12

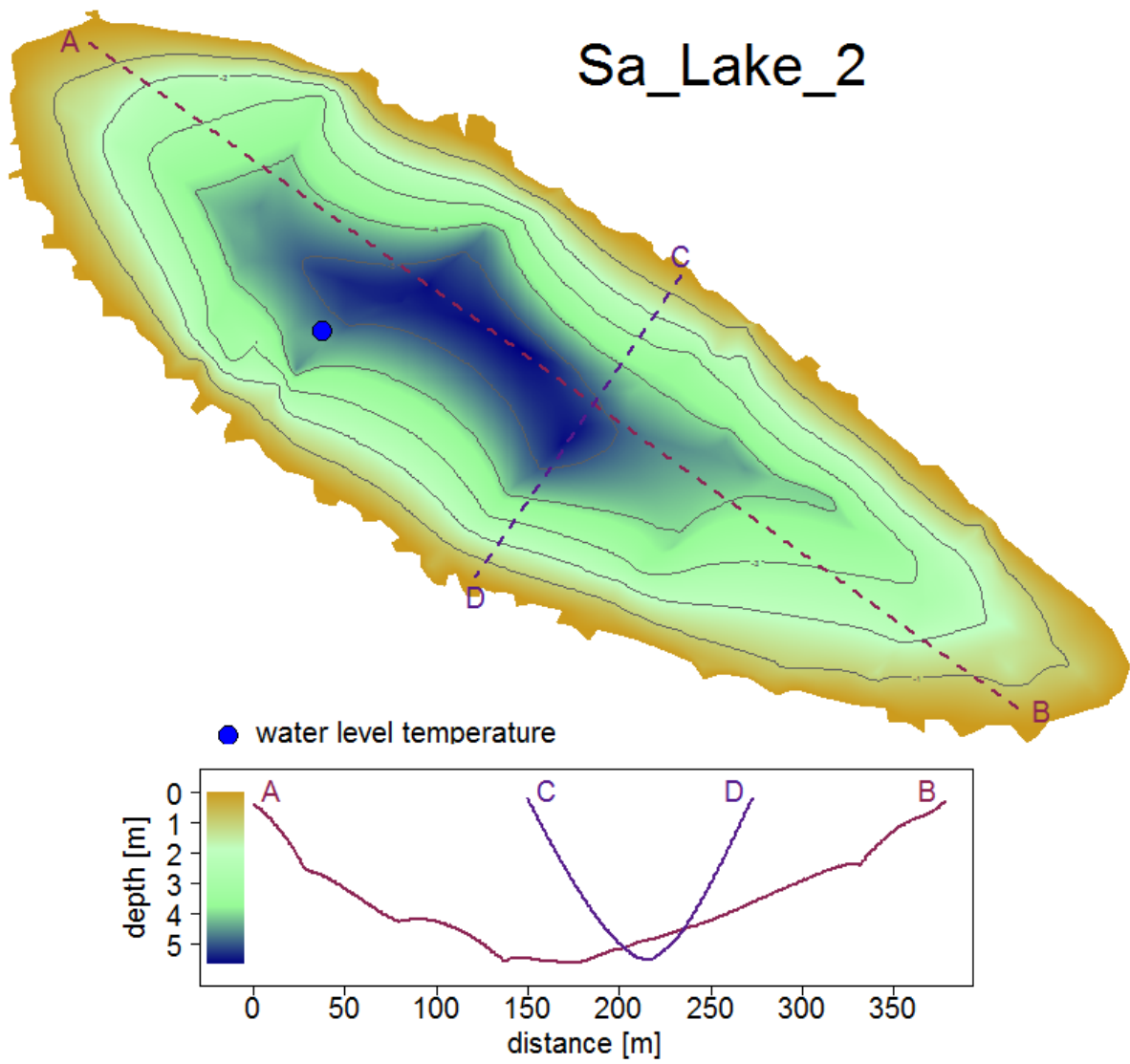
1 **Appendix A: Morphometry of lakes, hourly lake temperatures and lowest sensor depths**  
2 **data**

3 The topographic slope on the polygonal tundra (first terrace) is very low ( $< 5^\circ$ ). Aerial images  
4 of Sa\_Lake\_2 and Sa\_Lake\_3 show submerged polygons beneath the water surface,  
5 indicating that these lakes are likely to have been formed by the thawing of ground ice and ice  
6 wedges and the subsequent merging of polygonal ponds. The shorelines adjacent to shallow  
7 parts of these younger thermokarst lakes (with depths of 0-3 m) are very irregular and feature  
8 protrusions of different shapes and sizes (Figures A1-A4). Where deeper sections ( $> 3$  m)  
9 occur close to the shore, the shorelines are smooth and the lakes tend to have an oval shape.  
10 The profiles of thermokarst lakes tend to be V-shaped rather than flat-bottomed and the  
11 thermokarst lakes investigated were up to 6.4 m deep. The deepest lake on this island, with up  
12 to 11.6 m water depth, is Sa\_Lake\_4. It has an elongated shape and is one of three  
13 interconnected lakes that occur in an abandoned channel of the Lena River ("oxbow" or  
14 "perched" lakes; Figure A4). The largest monitored lake in this series of lakes was  
15 Ku\_Lake\_1, located on sediments of the Pleistocene Ice Complex, which have high ice  
16 content. This lake is the largest of three residual lakes located within an alas that is more than  
17 20 m deep. This thermokarst basin evolved in two phases (Morgenstern et al., 2013). In the  
18 first phase the original large lake covered the entire basin. It drained abruptly through a  
19 thermos-erosional valley at about 5.7 ka BP, leaving the  $> 20$  m deep alas with residual lakes.  
20 This was then followed by thermokarst processes of varying intensity during the second phase  
21 (5.7 ka BP to the present). This lake is an order of magnitude larger in surface area than the  
22 other four thermokarst lakes investigated and, in contrast to those lakes on Samoylov Island,  
23 has a regular oval shape, occurs within a basin with steep sides and has a smooth, flat  
24 shoreline. The maximum water depth is about 3.6 m and the profile is flat-bottomed (Figure  
25 A5).





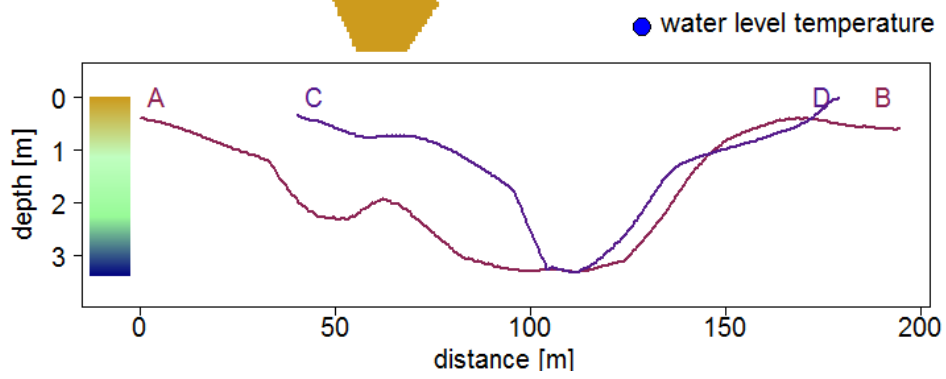
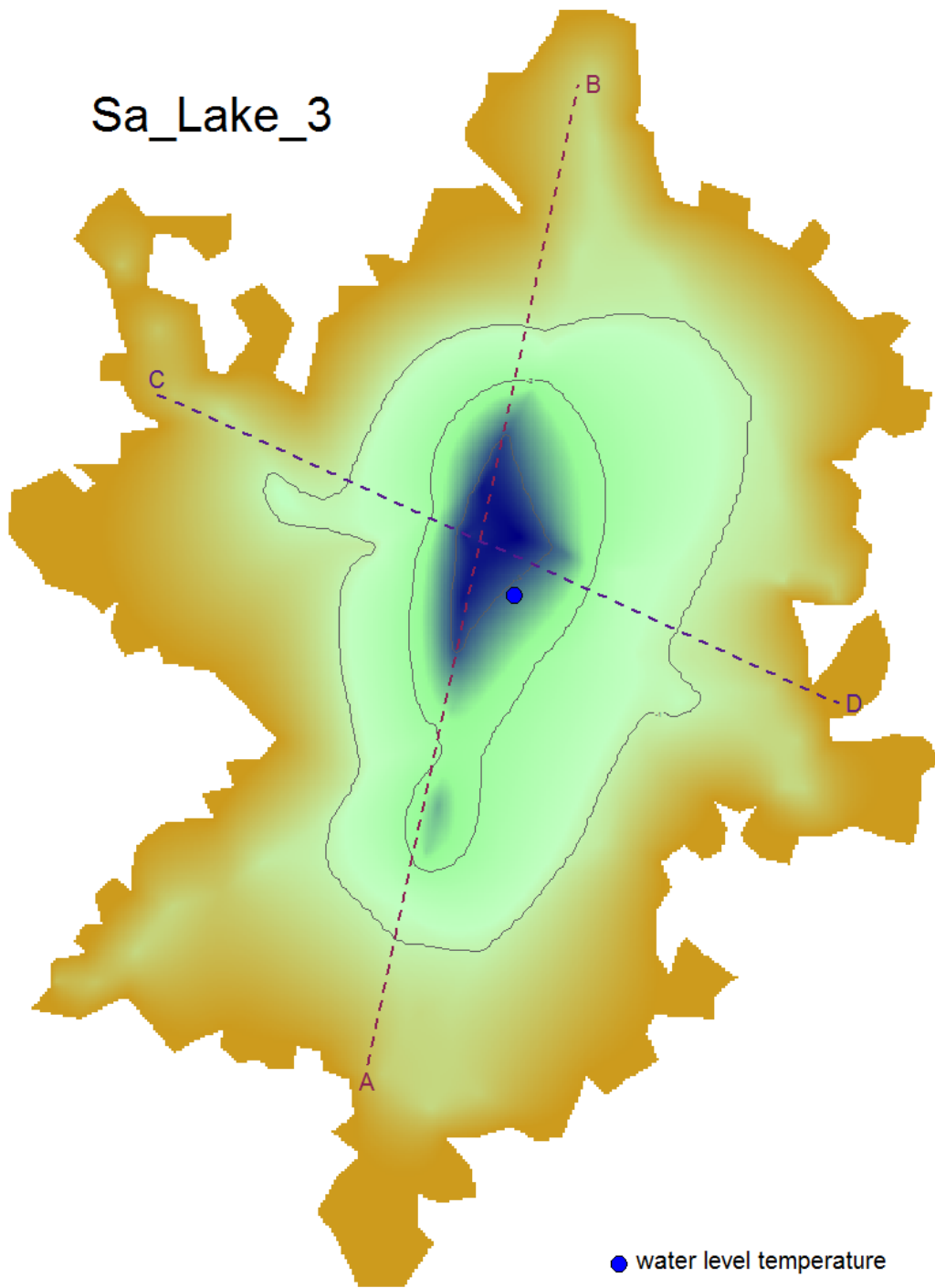
- 1
- 2 Figure A1. Bathymetry and cross sections of Sa\_Lake\_1 with location of sensors.



1

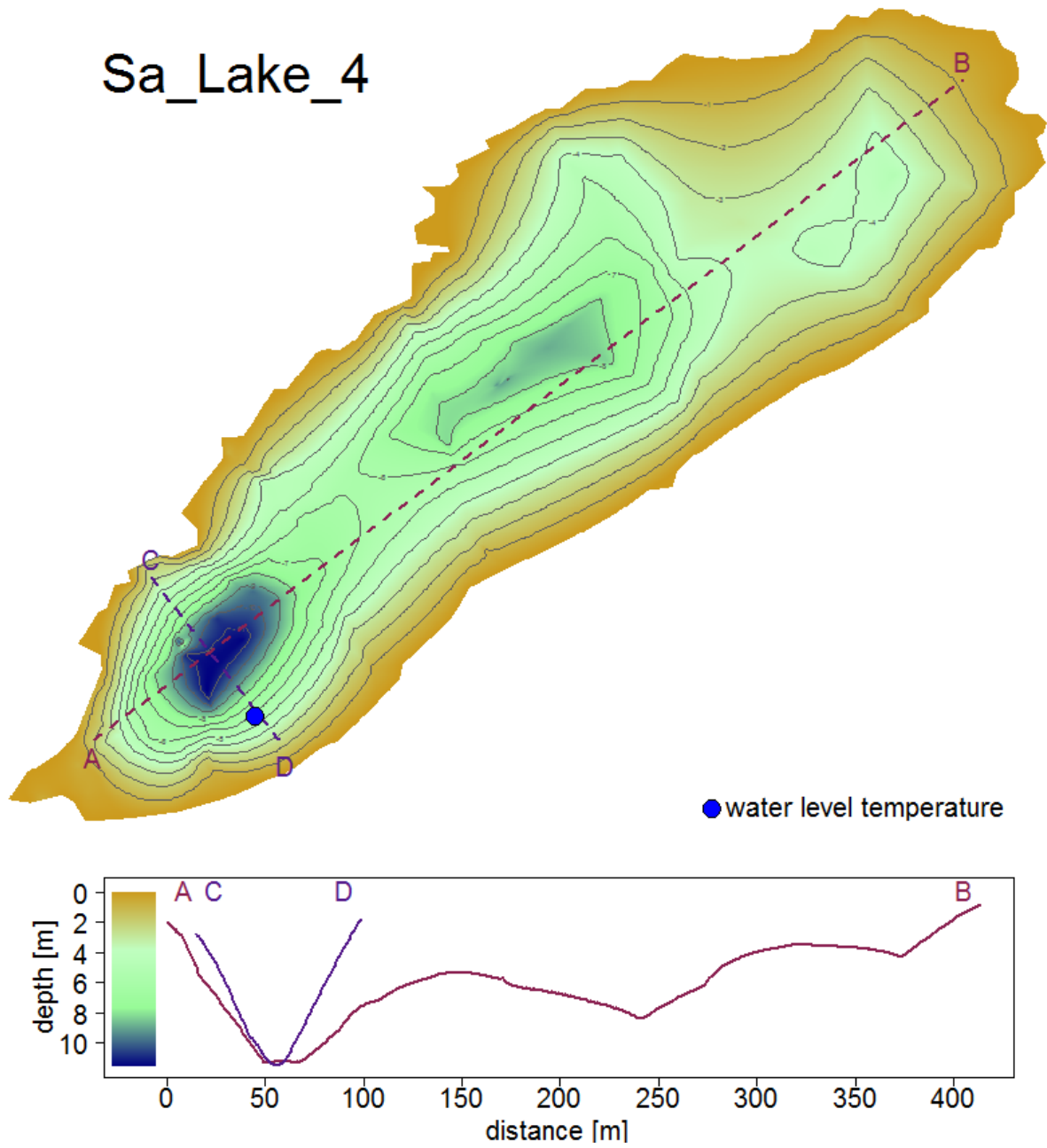
2 Figure A2. Bathymetry and cross sections of Sa\_Lake\_2 with location of sensors.

# Sa\_Lake\_3



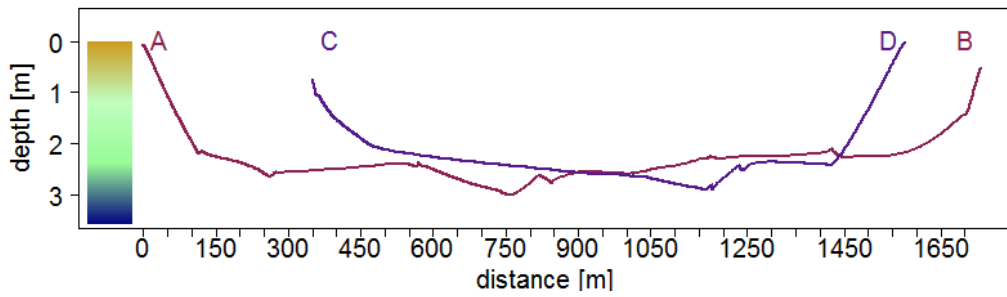
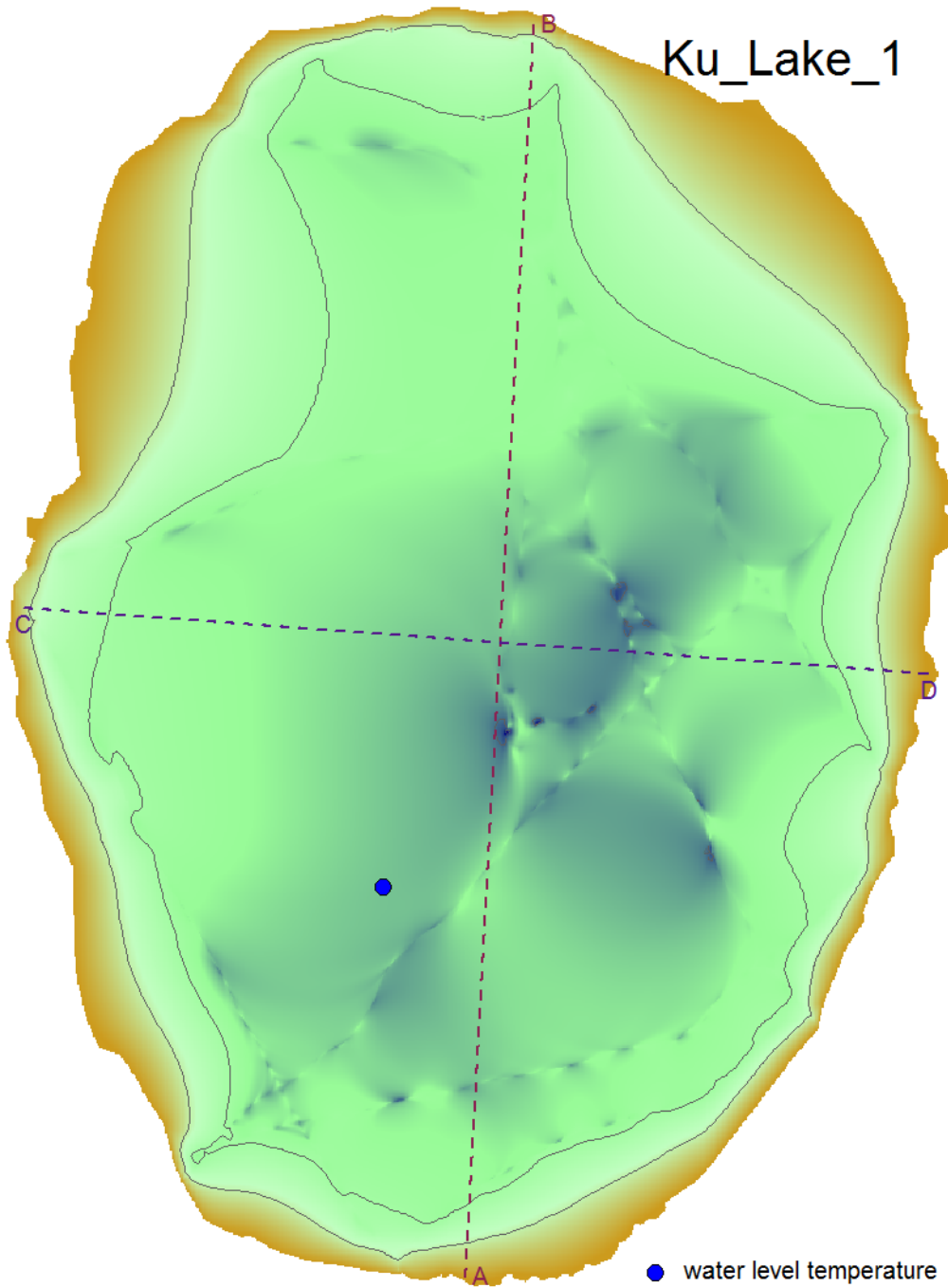
1

1 Figure A3. Bathymetry and cross sections of Sa\_Lake\_3 with location of sensors.



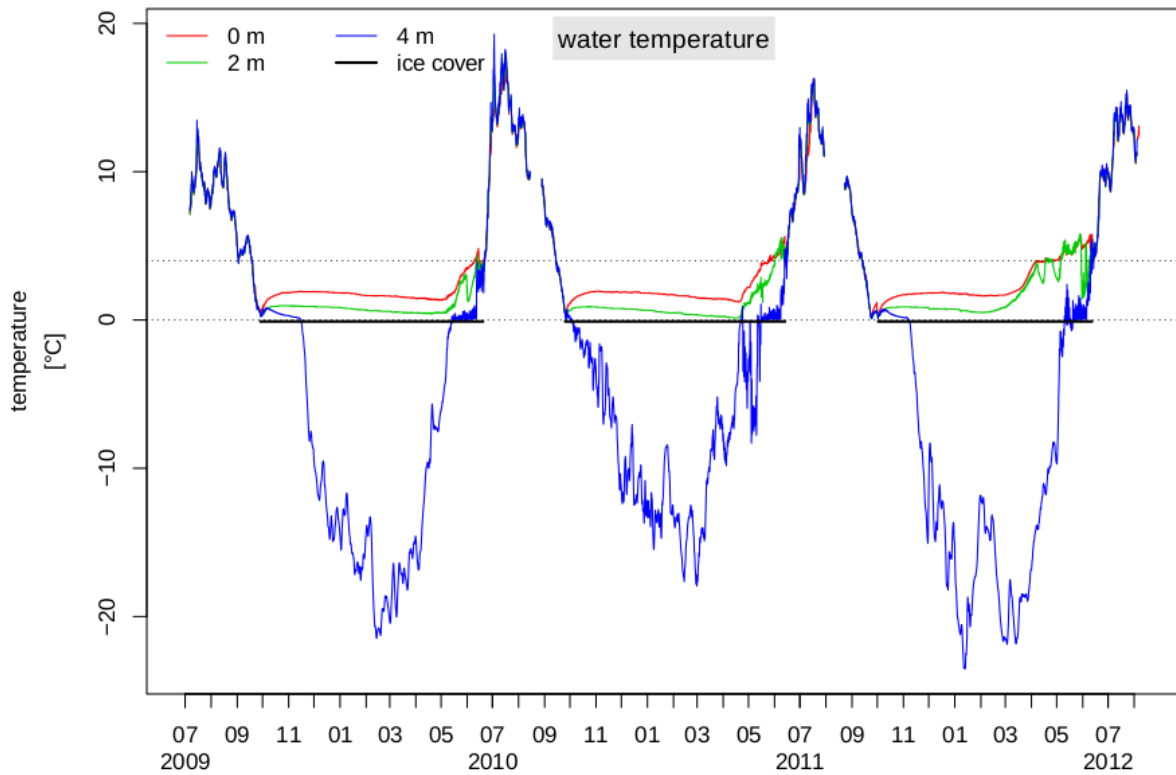
2

3 Figure A4. Bathymetry and cross sections of Sa\_Lake\_4 with location of sensors.



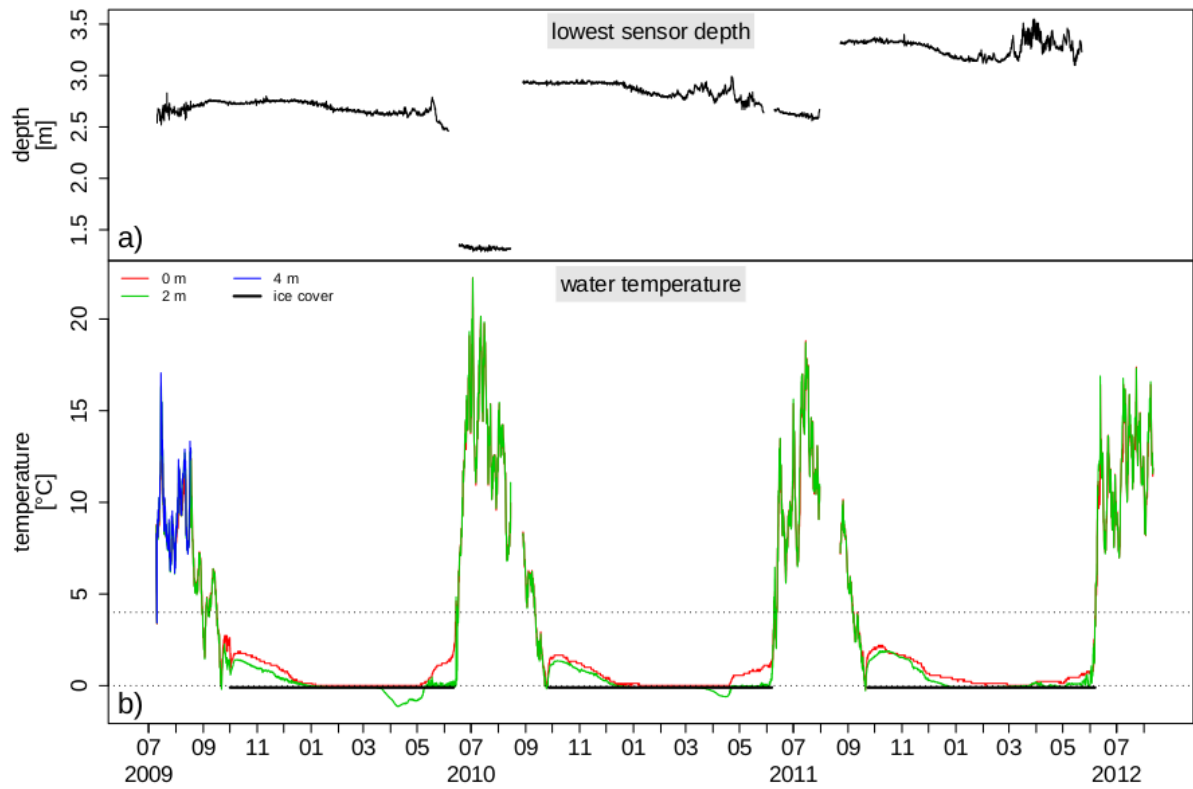
1

1 Figure A5. Bathymetry and cross sections of Ku\_Lake\_1. (Data from Morgenstern et al.,  
2 2011 and <http://doi.pangaea.de/10.1594/PANGAEA.848485>).



3  
4 Figure A6. Hourly lake temperatures and lowest sensor depth (indicating water level changes)  
5 for Sa\_Lake\_2, from July 2009 to August 2012. Thick black lines indicate ice covered  
6 periods.

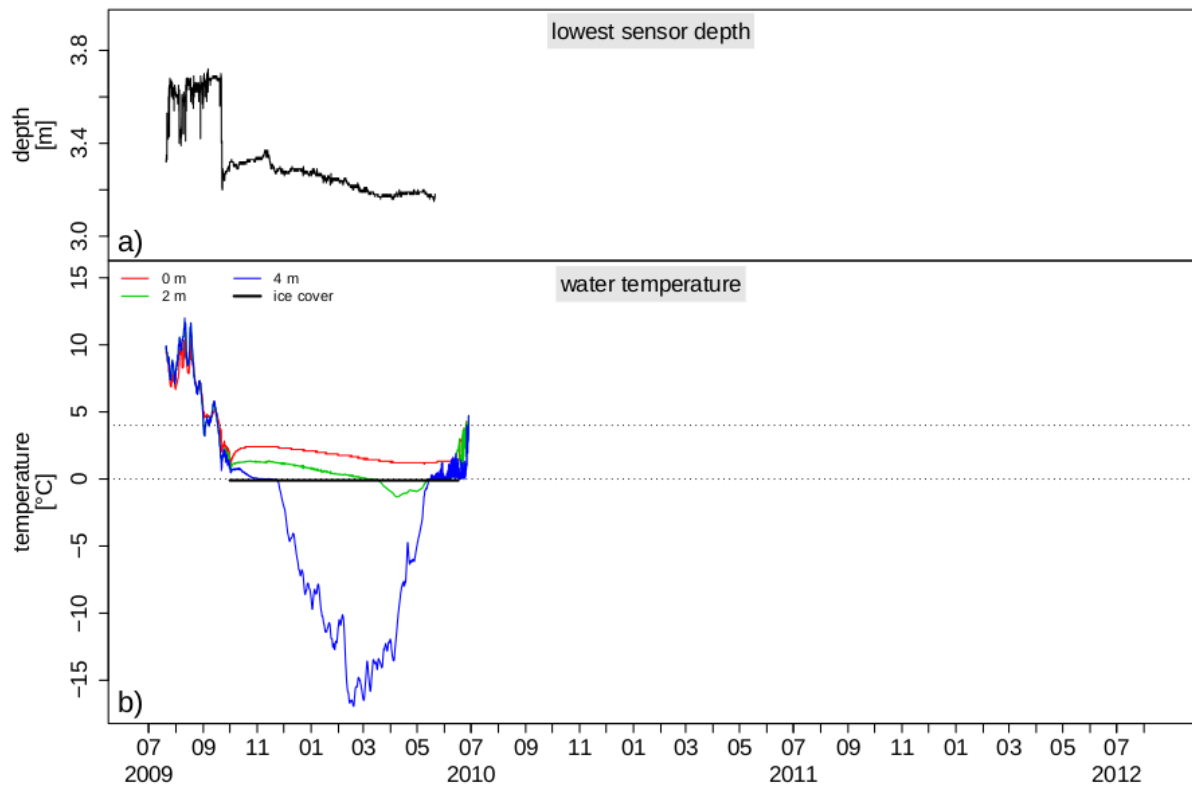
7



1

2 Figure A7. Hourly lake temperatures and lowest sensor depth (indicating water level changes)  
 3 for Sa\_Lake\_3, from July 2009 to August 2012. Thick black lines indicate ice covered  
 4 periods.

5



1

2 Figure A8. Hourly lake temperatures and lowest sensor depth (indicating water level changes)  
 3 for Ku\_Lake\_1, from July 2009 to August 2010. Thick black lines indicate ice covered  
 4 periods.

5



1

2 **Supplementary material: data and animations**

- 3 • Model data input (Samoylov); air temperature, air humidity, wind speed; radiation  
4 components

5 Samoylov\_2009\_2012.dat

6

- 7 • Model validation data: hourly lake temperatures and sensor depth (lake water level)  
8 data, where measured

9

10 Sa\_Lake\_1\_2009\_2012.dat

11 Sa\_Lake\_2\_2009\_2012.dat

12 Sa\_Lake\_3\_2009\_2012.dat

13 Sa\_Lake\_4\_2009\_2012.dat

14 Ku\_Lake\_1\_2009\_2010.dat

15 LenaRiver\_2009\_2010.dat

16

- 17 • Animation (movie) of temperatures in Sa\_Lake\_1 using daily average temperatures at  
18 depth and interpolated between depths using cubic interpolation. Daily temperature  
19 plots were added to produce the animation of temperatures

20 Sa\_Lake\_1\_2010-daily-color-.2s.gif

21

- 22 • Summary table of mean monthly air and bottom lake temperatures:  
23 meanlake\_air\_temp.txt

24

25